Spring 5-15-2017

Defining the Ontogeny and Functions of Macrophages in Pancreatic Ductal Adenocarcinoma

Yu Zhu
Washington University in St. Louis

WASHINGTON UNIVERSITY IN ST. LOUIS

Division of Biology and Biomedical Sciences
Molecular Cell Biology

Dissertation Examination Committee:
David G. DeNardo, Chair
Daniel C. Link
Jason C. Mills
Gwendalyn J. Randolph
Sheila A. Stewart

Defining the Ontogeny and Functions of Macrophages in Pancreatic Ductal Adenocarcinoma

by

Yu Zhu

A dissertation presented to
The Graduate School
of Washington University in
partial fulfillment of the
requirements for the degree
of Doctor of Philosophy

May 2017
St. Louis, Missouri

Table of Contents

List of Figures

List of Tables

Acknowledgements

First and foremost, I would like to thank my mentor, Dr. David DeNardo, for his guidance and mentorship during the past five and a half years. He introduced me to the fascinating field of cancer immunology, taught me how to approach and address scientific questions with rigor, gave me freedom and support to develop projects, and constantly sought ways to help improving my work. He always reminds me of asking myself "who cares" in pursuing scientific endeavors. I also want to particularly thank him for being genuinely invested in my career development, and for encouraging and challenging me to grow in all different aspects as a scientist. I could not have asked for a better mentor.

I would like to thank Drs. Daniel Link, Gwendalyn Randolph, Jason Mills, and Sheila Stewart, all of who have been serving on my thesis committee since my thesis proposal. Every adviser has given me a lot of valuable suggestions and help, both during and outside every single thesis update meeting. Dr. Daniel Link always gave me a lot of encouragement and inspirations, and always reminded me to step back and think of the significance of my research. I would also like to thank him for serving as the chair of my committee, and for providing valuable advice for my project and career. I am very grateful for his attention and genuine care for my growth. Dr. Gwendalyn Randolph provided a tremendous amount of help with my projects. She stimulated my passion for macrophage biology, taught me to be critical and creative, challenged me to pursue high standards of research, and led a great example of the kind of scientists that I desire to emulate. Dr. Sheila Stewart was the first professor I met during my graduate school interview at Washington University. The unforgettable conversations with her ignited my initial interest in studying cancer

microenvironment, and her contagious passion for science had a great impact on me. Dr. Jason Mills always provided very helpful advice on pancreas biology and always challenged me to look at the big picture. I also greatly benefitted from the encouraging words that he sent me after every single thesis committee meeting.

I would like to thank all members and alumni of the DeNardo Laboratory: Brett Knolhoff, John Herndon, Melissa Meyer, Audrey Bearden, Holly Medler, Chong Zuo, Hong Jiang, Samarth Hegde, John Baer, Roheena Panni, Larissa Belaygorod, Akash Mangalore, and Yuxiao Li. It has been an amazing experience to work and grow in this community. In particular, I want to thank Brett Knolhoff, who helped me with mouse colonies, tumor implantation, and various other big and little aspects of different experiments throughout the past six years. Without his huge amount of help, my PhD experience would have been much more challenging and less enjoyable. I also wanted to thank John Herndon, without whose efforts and expertise I could not have completed the most challenging experiment using various lineage tracing models. He also invested a lot of time and effort in characterizing the histology of mouse tumor tissues and in profiling human macrophages, which tremendously helped push the project forward. Without him I could not have completed the hard-fought manuscript revision process.

I would also like to thank all my collaborators at Washington University. Members from the laboratory of Dr. Gwendalyn Randolph helped me with various aspects of defining macrophage origin in pancreatic cancer. They provided reagents, mouse strains, and valuable suggestions. I would like to thank Ki-Wook Kim for numerous extremely helpful conversations. I would like to thank Dorothy Sojka and Li-Ping Yang from the laboratory of Dr. Wayne Yokoyama; they helped throughout the parabiosis experiments and patiently

taught me this awesome technique. I would also like to thank Dr. Kory Lavine for sharing mouse resources and his insights on macrophage ontogeny. I would like to thank members from the laboratory of Drs. David Linehan and William Hawkins for collaborations on the translational aspect of the dissertation. In particular, Darren Cullinan devoted a lot of time and efforts coordinating with the procurement of fresh human pancreatic tumor tissues, which really helped establishing the human relevance of our mouse studies. I would also like to thank Mark Lewis from the laboratory of Jason Mills for help with pancreatitis studies, which led to the opening up of a new direction for our research.

I would like to thank my friends for making the past seven years in St. Louis a wonderful experience that I will treasure forever.

Last but not least, I am eternally grateful for my family for their support and love. Any words here would be too pale to express what I want to say to them.

Yu Zhu

Washington University in St. Louis

May 2017

ABSTRACT OF THE DISSERTATION

A Thesis on the Ontogeny and Functions of Macrophages in Pancreatic Ductal Adenocarcinoma

by

Yu Zhu

Doctor of Philosophy in Biology and Biomedical Sciences

Molecular Cell Biology

Washington University in St. Louis, 2017

Professor David G. DeNardo, Chair

The immune system plays an essential role in protecting the host organisms against both foreign invaders and self-attacks arisen within the host, such as tumors. Instead of promoting the long-term fitness of the organism, the immune system is often suppressed or hijacked by tumor cells to accelerate the progression of malignancies. Among the key drivers of immune suppression, macrophages are one of the most abundant immune cells present in tumor tissues. High levels of macrophage infiltration in the malignant tissues correlate with negative patient outcome in many types of cancers, including pancreatic ductal adenocarcinoma (PDAC), one of the most lethal malignancies in human beings. Therefore, attempts have been directed towards targeting tumor-associated macrophages (TAMs) to improve the efficacy of cancer treatment.

We attempted to target TAM responses in murine PDAC models through inhibiting the colony stimulating factor-1 receptor (CSF1R) signaling pathway. CSF1R signal blockade not only depleted half of the TAMs within the tumor microenvironment, but also functionally reprogrammed the remaining TAM compartment to support anti-tumor T cell responses. More

importantly, CSF1R signal blockade sensitized the tumors to T cell checkpoint-based immunotherapies, which failed to achieve clinical efficacy as monotherapies. These findings revealed the potential benefits of targeting TAMs to improve treatment of PDAC patients.

However, TAM-targeting strategies have limitations. Optimal TAM-based therapeutic intervention requires in-depth understanding of the sources that supply macrophages to malignant tissues. Towards that end, we investigated the ontogeny of TAMs in murine PDAC models, and identified both inflammatory monocytes and tissue-resident macrophages as sources of TAMs. Unexpectedly, significant portions of pancreas-resident macrophages originate during embryonic development at the yolk sac stage. These cells undergo significant local expansion through *in situ* proliferation during tumor progression. While monocyte-derived TAMs play more potent roles in tumor antigen presentation, embryonically derived TAMs exhibit pro-fibrotic transcriptional profiles and *ex vivo* fibrotic activities, indicative of their role in producing and remodeling extracellular matrix molecules. Collectively, these findings uncovered the heterogeneity of TAM origin and functions, and could provide insights into therapeutically targeting different TAM subsets based on the different pathological features of the PDAC microenvironment.

Chapter 1: Introduction

1.1 Overview of Pancreatic Cancer

1.1.1 Pancreas and Pancreatic Cancer

Pancreas, named after the Greek words *pan* (all) and *kreas* (flesh), is a multi-modular glandular organ that lies in the retroperitoneal position of the abdomen behind the stomach. It is composed of exocrine glands and endocrine glands tightly organized together. Through these glands, pancreas functions as a critical component of both the digestive system and the endocrine system.

The pancreas predominantly consists of exocrine glands that play a central role in the conversion of consumed foodstuff into "usable fuels" for cells in the body. These exocrine glands accomplish their functions through the secretion of digestive enzymes and bicarbonate ions into the duodenum of the gastrointestinal tract. The key components of the exocrine pancreas are acinar cells and duct cells. The acinus, named after the Latin term meaning "berry in a cluster", are specialized in synthesizing, storing, and secreting digestive enzymes. The major types of pancreatic enzymes are proteolytic enzymes (involved in protein digestion), pancreatic amylase and chitinase (involved in carbohydarate digestion), and pancreatic lipase (involved in fat digestion). The three principal types of proteolytic enzymes are trypsinogen, chymotrypsinogen, and procarboxypeptide. These enzymes are stored in granules in inactive forms, known as zymogens, in the apical region of acinar cells. The apical surface of the cells also line up as microvilli, within which a filamentous actin network is organized to mediate the exocytosis of zymogen granules. Hormones and neurotransmitters that mediate the stimulation of enzyme secretion are mediated through receptors located in the basolateral membranes of these

cells. As the zymogens get secreted into the duodenum under hormonal regulation, they are cleaved into active forms through a cascade of proteolytic events initiated by enzymes secreted by cells lining the luminal border of the duodenum mucosa. Duct cells, on the other hand, are the main producers of bicarbonate ions. These ions are secreted to the duodenum to neutralize the acidity of chyme. This process creates a neutral or alkaline environment that is not only optimal for pancreatic enzymatic functions, but also minimizes acidic damages to duodenum mucosa.

On the other hand, the endocrine gland of the pancreas tightly regulates the digestive procedures by secreting hormones to control blood sugar levels. The major components are clusters of endocrine cells known as the islets of Langerhans, which are dispersed throughout the pancreas between the exocrine cells. Beta cells are the most abundant components of the islets of Langerhans, whose function is to produce and secrete insulin that regulates the blood glucose level. In addition, alpha cells, delta cells, PP cells are also integral part of the endocrine pancreas; these cells produce glucagon, somastatin, and pancreatic polypeptide respectively.

Given the importance of the pancreas in both the exocrine and the endocrine system, disorders in this organ can have significant impacts on the fitness of an entire organism. Common diseases in the pancreas include pancreatitis, type 1 diabetes mellitus, and pancreatic cancer. Pancreatitis is inflammation of the pancreas, which comes in acute or chronic forms. Type 1 diabetes mellitus results from the destruction of beta cells in the pancreas islets of Langerhans that leads to compromised abilities to produce insulin in response to high blood sugar levels. Pancreatic cancers are malignant tumors that arise within the organ. A small subset of pancreatic cancer arises from the pancreatic islet cells. These cancers are called pancreatic neuroendocrine tumors (PNETs) and account for 5% of pancreatic cancer cases. PNETs produce excessive amount of hormones, such as insulin, glucogan, and gastrin, which disrupt systemic

homeostasis. The vast majority of pancreatic cancers arise within the exocrine portion of the organ. These tumors are called pancreatic ductal adenocarcinoma (PDAC).

PDAC leads to a series of disruptions to organismal homeostasis. As a consequence of the destruction of acinar cells, the normal release of digestive enzymes is compromised. This leads to incomplete digestion of consumed molecules, malabsorption, diarrhea, and increased intestinal infections, among other consequences. Subgroups of patients develop uneven textures of fatty issue under the skin, due to the release of pancreatic enzymes that digest fat. Tumors in exocrine pancreas can also cause destruction or dysfunction of beta cells, leading to abnormal insulin secretion. Patients could experience irregular changes in blood sugar levels, or diabetes in some cases. Among all the abnormalities, liver dysfunction is most frequently observed. This often results from the obstruction of the bile duct by the tumor, which frequently localizes to the head of the pancreas close to the bile duct. Normally, the liver secretes bilirubin as part of the bile liquid, and bile goes through the bile duct into the intestine. As tumors block the bile duct, excessive amount of bilirubin builds up in the liver, causing liver dysfunction. In addition, liver is the most common site of metastasis. Presence of tumor cells in the liver will alter the tissue function. Moreover, increasing amount of evidence in mouse models suggests that before the dissemination of tumor cells, pre-metastatic livers undergo tissue remodeling and inflammation, which may well likely disrupt their functions.

PDAC is one the most lethal forms of solid cancers. Five-year survival rate of PDAC patients between 2006 and 2012 is 7.7% (https://seer.cancer.gov/). As a point of reference, the 5-year survival rate for breast cancer, prostate cancer, colorectal cancer, and skin melanoma patients are 89.7%, 98.9%, 65.1%, and 91.5% respectively. The median survival of pancreatic cancer patients is less than 6 months. Pancreatic cancer is the 4th most common cause of cancer-

related death, despite being the 12th most type of cancer in the United States. The dismal prognosis of pancreatic cancers is partially due to its late diagnosis, as the majority of pancreatic cancer patients have already developed metastasis at the time of diagnosis. Only 9% of patients demonstrate a confinement of the tumor at the primary site. An additional 29% of patients have cancers spread to regional lymph nodes. Even for the 9% patients with local diseases, the 5-year survival rate is only 29.3%, which contrasts with 98.8% in localized breast cancer patients.

Currently established treatment protocols do not confer significant clinical benefits in PDAC treatment. Treatment options are very limited. Surgical resection is applicable only in patients with local diseases. Traditional chemotherapies and radiation therapies are not effective in restraining tumor progression. Importantly, development of new treatment regimens has been very slow and relatively ineffective in comparison to other tumors. For example, the death rate for colorectal cancer patients was dropping by 2.7% annually between the years of 2004 and 2013, which is reflective of improved efficacies in targeted therapeutics; the rates for new colorectal cases have been dropping by 3.2% annually in the past decade as well. In comparison, the rates for new pancreatic cancer cases have been rising by 0.6% each year; five-year survival rate has been fluctuating between 3% and 7% since 1975 without significant improvement, all of which reflect a lack of improvement in treatment strategies. Newer treatment options, such as immune checkpoint-based therapies in particular, do not improve patient outcomes as monotherapies. In comparison, checkpoint immunotherapies demonstrated impressive response rates in many types of cancer, including metastatic diseases. Development of treatment strategies is desperately needed for PDAC patients, which requires in-depth understanding of pancreatic cancer biology.

PDAC is driven by mutations altering genetic programs that govern cellular activities. Oncogenic mutation in Kras is a signature of PDAC genetics, and is present in 90-95% of the patients. Kras is also the earliest detected mutations found in preneoplastic lesions, such as pancreatic intraepithelial neoplasia (PanINs). Tumor suppressor genes are also very frequently mutated, including p16/CDKN2A, p53, and SMAD4, whose functions are lost in approximately 90%, 75%, and 55% of cancers, respectively. Initial genetic abnormalities include not only oncogenic mutations, but also shortening of chromosomal ends, i.e. telomeres. Epigenetic regulation is also severely disrupted. Collectively, these cell autonomous aberrations lead to the transformation of PDAC cell of origin, causing disease to initiate and progress.

PDAC is believed to arise from a series of non-invasive precursor lesions. These include pancreatic intraepithelial neoplasia (PanIN), intraductal papillary mucinous neoplasm (IPMN), and mucinous cyctic neoplasm (MCN). The risk of patients with these lesions to develop pancreatic cancer is increased by more than 20-fold (Hruban et al., 2007). PanINs are the most common among these lesions. They harbor many of the same genetic mutations found in PDAC, even within the same patients. This adds strengths to the hypothesis that PDAC arises within these pre-neoplastic lesions.

The precise nature of cellular origin of PDAC is still under debate. PDAC obtained its name due to the ductal-like morphological features of the neoplastic cells. However, induction of oncogenic mutations in mature pancreatic ductal epithelial cells does not efficiently induce tumorigenesis. Instead, acinar cells are dramatically more prone to Kras-induced transformation (Kopp et al., 2012), suggesting the possibility that the cell of origin for PDAC may be acinar cells instead. Indeed, one of the early events during tumorigenesis in genetic mouse models is acinar-to-ductal metaplasia (ADM), an event where acinar cells change their identity to ductal

epithelial cells (Schmid, 2002). ADM is commonly observed in PanIN lesions, further suggesting the possibility that acinar cells may be the tumor-initiating cells. In addition to acinar cells and ductal epithelial cells, it also remains to be seen if there are pancreatic stem or progenitor cells in adults that could be the "tumor-initiating cells" for PDAC. Understanding the properties of cell of origin could help addressing sell-autonomous mechanisms by which PDAC evades cancer surveillance and therapeutic targeting.

Genetic mutations not only drive a series of cellular activities that govern proliferation, metabolism, and invasiveness, but also alter the way the cells shape their tissue microenvironment to promote tumor progression through non-sell-autonomous mechanisms. This will be discussed in the following sections.

1.1.2 Cancer and Cancer Microenvironment

Cancers are characterized by uncontrolled growth of transformed cells with genetic mutations. While encompassing a wide range of diseases covering almost all mammalian organs, cancers share some common features that help us understand the biology of these diseases. They acquire several biological traits that confer advantages of tumor cells at the expense of host fitness; these traits include self-sufficiency in growth signals, insensitivity to growth inhibition, resistance to programmed cell death, and unlimited replication potential.

First, cancer cells are self sufficient in growth signals. Normal cells require exogenous growth factors in order to exit a quiescent state and enter active proliferation. Such signals are transduced usually through transmembrane receptors, which trigger downstream signaling pathways that promote cell division. This way, cell division is orchestrated within a larger tissue context that enables optimal organ functions by meeting various cellular needs within different

tissue components. However, cancers generate their own growth signals independently of the extracellular milieu. Their altered oncogenic program takes over the proliferative system, usually making cells constitutively cycling, thereby reducing their dependence of stimulation from the external microenvironment.

On the other hand, multiple inhibitory signals are usually able to maintain tissue homeostasis by inhibiting cell proliferation within normal tissues. These signals could block the potential of the cells to proliferate, or force cells out of active division cycles back into quiescent states. Cancer cells can often disrupt the elements that mediate these negative regulatory pathways. This mechanism, coupled with growth signal autonomy, contributes to the hyper-proliferative features of neoplastic cells.

Fundamentally, tumor growth is the net result of cell production and cell loss. Abilities to proliferate autonomously and to evade growth inhibition are not sufficient to drive tumor growth, because higher rates of cell death can also compromise the ability of the cancer cell population to expand. Programmed cell death, or apoptosis, is essential to the homeostasis of most multicellular organisms due to its importance in eliminating unnecessary or harmful cells and cellular debris. Normal cells have sensors to detect apoptosis-inducing signals, either from intracellular molecules that indicate irreversible cellular damages, or from extracellular sources. However, cancer cells often develop strategies that render them resistant to programmed cell death, which is a hallmark of most types of tumors. They become resistant to apoptosis through several mechanisms, such as upregulating pro-survival effector molecules, downregulating "death receptors" that can engage apoptosis signals, and inhibiting the production or activities of pro-apoptotic effector molecules, such as caspases.

Moreover, cancer cells have limitless replication potential. Normal cells have limited life span, i.e. they could undergo a finite number of cell division cycles before entering a crisis state and undergo senescence. This phenomenon is termed “Hayflick limit”. Genetic mutations within cancer cells often allow them to evade the Hayflick limit. Under homeostatic conditions, normal cells undergo senescence often due to the shortening of telomeres, regions of repetitive nucleotides at the end of a chromosome. Cancer cells often utilize alternative programs to replicate their chromosome ends, such as upregulating telomerase that promotes telomere lengthening, which could dramatically or indefinitely delay the occurrence of senescence.

While a lot of initial attention in cancer research was directed towards the transformed cells themselves, in the past decade or so it has become well appreciated that tumors are not malignant cells growing in isolation. Instead, cancer cells are embedded within a very complex organ system that is composed of a wide range of cellular and non-cellular components. Fibroblasts, blood vessels, neurons, and immune cells are examples of key cellular components of the tumor microenvironment.

Fibroblasts are essential stromal components of the tumor microenvironment. One of the major functions of fibroblasts is to produce, deposit, and remodel the extracellular matrix (ECM), which in normal tissues ensures the integrity of the organ system. While cancer-associated fibroblasts (CAFs) carry out the same functions as their normal fibroblast counterparts, their activities are severely disrupted. Tumor cells recruit fibroblasts, promote fibroblast proliferation, and induce an activated myofibroblast phenotype. Activated fibroblasts in tumors could produce ECM molecules in an unrestrained fashion, therefore laying out excessive amount of ECM that leads to tissue fibrosis. The growth of fibrous part of the tissue, or desmoplasia, was originally considered to a protective mechanism by encapsulating, constraining, or even rejecting the tumor.

However, accumulating amount of evidence suggests a strong correlation between desmoplasia, tumor progression, and poor patient outcome. Excessive amount of ECM in the tissue activates cancer cell proliferation, suppresses apoptosis, and promotes the invasion and metastasis of tumor cells. Fibrosis also increases interstitial pressure and leads to poor tumor vascularization. These altogether lead to hypoxia and pose a barrier to effective therapy delivery. In parallel to ECM remodeling, CAFs can secrete a large amount of inflammatory cytokines that can further modulate the local environment through the recruitment of immune cells and modulation of tumor vasculature.

Blood vessels are also abundant in many kinds of tumor tissues. Despite their self-sufficiency in growth signals, tumor cells still require oxygen and nutrients to sustain their metabolic activities. As tumors reach the size of a few millimeters in diameter, tumors would experience low oxygen tension, known as hypoxia, and nutrient deprivation. To meet their metabolic needs, tumor cells would trigger vasculature generation and remodeling, a series of events collectively called “angiogenesis”. In addition to hypoxia, other events during tumor expansion, such as the buildup of extracellular matrix and inflammation, are also able to trigger angiogenesis. These players in the tumor stroma could trigger sprouting/branching of pre-existing blood vessels by promoting the protrusion of a selected endothelial cell. Alternatively, endothelial progenitor cells could be recruited from the circulation system to the tumor site, differentiate to new endothelial cells that line up blood vessels; this process is called “vasculogenesis”. Moreover, a subset of cancer cells could differentiate and adopt an endothelial cell-like phenotype and form *bona fide* blood vessels. Tumor cells can also line up blood vessels by mimicking, rather than differentiating into, endothelial cells. Tumor neo-vasculature is often morphologically and functionally distinct from normal vasculature. They appear disorganized

and tortuous. They are more leaky than normal blood vessels. Endothelial cells can demonstrate abnormal cell morphologies, such as aneuploidy, multiple chromosomes, and multi-centrosomes. The generation and remodeling of vasculature in the tumor not only allows the transport of oxygen and nutrients, but also produces or allows the supply of growth factors that further enhance tumor cell proliferation.

Nerves are also important components of the tumor stroma. Cancer cells can attract nearby nerves through the secretion of axon guiding molecules, thereby increasing the number and extensions of axons. Such process is called "axonogenesis", which is very similar to angiogenesis. Adrenergic signals from sympathetic nerve cells can directly stimulate cancer cells, rendering resistance to apoptosis, promoting invasive potential and migratory capacity. Neural activation of tumor cells can also lead to increased secretion of angiogenesis promoting cytokines. Cholinergic signals from parasympathetic nerve cells have also been shown to promote "cancer stem cell" properties. In addition, the nervous system can also act on other stromal components in the tumor, including vasculature and immune cells.

It is important to note that reorganization or disruption of the tissue microenvironment not only is a consequence of tumor development, but also occurs prior to malignant transformation and contributes to tumorigenesis. For example, while tumor cells secrete a wide range of inflammatory cytokines to recruit immune infiltration, chronic inflammation during premalignant stages can cause cell damages and facilitates tumorigenesis. Similarly, while tumor cells activate fibroblasts to promote fibrosis and inflammation, aberrant fibroblast activation can secrete factors that promote inflammation and facilitate cancer cell transformation. In addition, human beings that have chronic depression or have suffered traumatic life events are more likely to develop cancers, which suggests the possibility that neural deregulation may promote cancer

transformation. Indeed, adrenergic signaling in tumor stroma was shown to be essential for tumor initiation in murine transplantation models.

Taken together, tumors are malignant cells with aberrantly regulated proliferative programs that reside within a complex tissue microenvironment. Cancer cells remodel various aspects of the tissue environment, which in turn facilitate tumor progression. This dissertation is focused on understanding how tumors, in particular pancreatic ductal adenocarcinoma (PDAC), interact with the immune components of the stroma.

1.2 Overview of the Immune System

1.2.1 Overview of the Innate Immune System

The immune system plays an essential role in both defending organisms against pathogen invasion and protecting against abnormalities that rise within the host. It is a tightly regulated system composed of several lines of defense.

Anatomical barriers form the first line of defense that includes the skin, tears, and mucus. These are the initial sites of encounter as pathogens attempt to enter the body. Physical, biological, and chemical components exist in these sites to maintain barrier integrative in order to minimize the penetrance of pathogens into host organisms. For example, epidermal cells in the skin form a waterproof and airtight keratinized layer that is impermeable to most foreign organisms. Sweat glands in the skin also secrete bactericidal peptides such as dermicin to kill microbes. Cells in sebaceous glands also produce oily substances such as sebum to cover hair and the keratinized layer, preventing the cracking and drying of the barrier. Similarly, in other barriers, such as the digestive tract and the respiratory system, different components also function to deter ingested or inhaled pathogens.

External barriers are not perfect. As pathogens pass through and penetrate into the host organisms, innate immune system constitutes the second line of defense. The major functions of the innate immune cells are to (1) quickly recognize, contain, inactivate, and eliminate invaders, (2) remove debris, and (3) prepare the body for subsequent events that bring the organisms back to homeostatic conditions. Innate immunity can be further classified into cellular immune responses and humoral immunity, which are immune responses mediated by macromolecules present in the humors, or body fluid.

The major cellular components of the innate immunity are phagocytic cells, including macrophages, neutrophils, and dendritic cells. They recognize foreign materials by binding to pattern-associated molecular patterns (PAMP), which are molecules associated with pathogens but not host cells. Examples of PAMPs include lipopolysaccharides, double-stranded RNA, and unmethylated CpG motifs, all of which signal to the phagocytes the presence of "non-self". In addition, phagocytes can detect pathogens by sensing damage-associated molecular patterns (DAMP), which are host molecules expressed or released during inflammatory responses. Examples of DAMPs include heat shock proteins, extracellular matrix (ECM) proteins, DNA, and ATP, which signal cellular damages or cell death caused by infectious or non-infectious inflammation. PAMPs and DAMPs are recognized by pattern recognition receptors (PRRs), whose engagement on phagocytes lead to the activation of these cells. Upon activation, phagocytes could engulf pathogens or pathogen-infected cells, and subsequently eliminate pathogens through several mechanisms. For example, phagocytes would increase oxygen consumption upon phagocytosis, causing a respiratory burst, which produces reactive oxygen species that could effectively kill the microbes. Alternatively, phagocytes could eliminate pathogens through lysozymes, proteases, lactoferrins, among others, to destroy the key

components of the microbes. In addition, phagocytes could release chemicals such as nitric oxide to eliminate microbes in adjacent locations. Moreover, certain types of phagocytes, such as macrophages and dendritic cells, could transport specific fragments of the engulfed antigens to their cell surface, and present these molecules to lymphocytes, a key component of the adaptive immune system that could initiate specific defense reactions against pathogens of interest.

In addition to phagocytosis, certain innate immune cells could kill pathogens through other mechanisms. A class of innate immune cells called granulocytes (such as neutrophils, eosinophils, and basophils) and mast cells could undergo a process called degranulation, during which antimicrobial and cytotoxic molecules, such as myeloperoxidase, cathepsins, and histamines, are released to the extracellular space to combat infection. Neutrophils are also known for their abilities to secrete neutrophil extracellular traps (NETs), fibers composed of chromatin and proteases, that participate in the trapping and killing pathogens.

A third kind of innate immune cells are natural killer (NK) cells. Instead of directly killing the invading pathogens, NK cells target a type of infected cells that lack major histocompatibility complex (MHC) I, whose expression on the cell surface labels the cell as "self". NK cells kill by (1) natural killing, (2) antibody-dependent cellular cytotoxicity, (3) redirected lysis, and (4) lectin facilitated killing. They can also produce cytokines to amplify the immune responses by recruiting and/or activating other leukocytes.

In addition, a recently discovered class of immune cells, called innate lymphoid cells (ILCs), also constitute another key cellular component of the innate immune system (Klose and Artis, 2016). Unlike many other innate immune cells, ILCs lack pattern recognition receptors (Robinette et al., 2015). Instead, they sense cytokines and inflammatory mediators secreted by parenchymal cells or myeloid cells. Upon engagement, ILCs promote immune responses by

secreting soluble factors, such as classic T helper cytokines including IFNγ and TNF for type 1 ILCs (ILC1s), IL-5, IL-9, and IL-13 for ILC2s, and IL-17, IL-22, and GM-CSF for ILC3s. In addition, some previously unknown "ILC-specific" effector molecules are also secreted, such as amphiregulin (Monticelli et al., 2011; Robinette et al., 2015) and methionine-enkaphalin (Brestoff et al., 2015), which mediate epithelial cell repair and adipocyte beiging respectively.

In addition to the cellular components discussed above, the complement system is also a key component of innate immunity that, together with B lymphocytes of the adaptive immunity, forms the humoral immune system (Dunkelberger and Song, 2010). It is composed of more than 30 proteins circulating in the plasma that initiate a sequence of events on the surface of the pathogen to help eliminate the infection. The complement system can be engaged either upon identification of pathogen surface molecules, such as certain polysaccharides, or upon recognition of antibodies that bind to the pathogen surface. Upon activation, protein components will initiate a cascade of proteolytic cascades that eventually lead to the production of active opsonin and assembly of membrane attack complexes (MACs). Opsonins coat the pathogen surface, allowing either the phagocytosis of pathogens or membrane permeabilization by MACs that kill the invading bacteria. During the proteolytic events, a series of proinflammatory mediators are produced, leading to the amplification of immune responses by recruiting other effector cells.

Collectively, phagocytes, granulocytes, natural killer cells, and innate lymphoid cells altogether build up the cellular arm of the innate immune system. These innate immune cells, along with humoral components such as the complement system, initiate immediate responses against invading pathogens in order to maintain the fitness of host organisms.

The innate immune system is evolutionarily conserved from vertebrate animals to plants. It relies on germline-encoded receptors to recognize microbes bearing conserved surface molecules that are shared by many organisms. Therefore, the innate immune system does not require an extended phase to initiate responses and could elicit rapid responses to combat pathogens. However, the range of pathogens that can be recognized by the innate immune system is limited, due to the restricted diversity of recognition machinery. Moreover, the efficiency of the innate immune system to eliminate recognized pathogens is constrained because microbial organisms could evolve more rapidly than the infected hosts and develop strategies to evade these defense mechanisms. For example, many bacteria adopted strategies that allow them to hide pattern recognition molecules from being recognized by the immune system. To address the limitations of the innate immune system, vertebrates developed the adaptive immunity with higher levels of specificity and diversity.

1.2.2 Overview of the Adaptive Immune Responses

Similar to the innate immune system, the adaptive immune system is also composed of both cellular and humoral immunity. The major components of the cellular arm of adaptive immunity are T lymphocytes, whereas B lymphocytes are the central players of the humoral immune system. “T” designates “thymus”, named so based on the observation that T cells undergo the maturation process in the thymus. “B” stands for “bursa of Fabricius”, the site of B cells production in birds. Mammals do not have the organs equivalent of bursa of Fabricius; instead, B cells in mammals are produced in the bone marrow.

Unlike innate immune cells that can recognize a wide range of molecules commonly expressed by multiple pathogens, T and B lymphocytes recognize epitopes that are usually

unique to specific antigens. Both types of lymphocytes rely on their unique membrane receptors, termed T cell receptors (TCRs) and B cell receptors (BCRs) in the respective cell types, for this recognition. T cell receptors in most T cells are heterodimers of two chains designated alpha (α) and beta (β). Though a small fraction of T cells express TCR composed of gamma (γ) and delta (δ) chains. B cells express BCRs that are composed of cell surface-bound antibodies and signal transduction moieties. Each antibody is a Y-shaped molecule consisting of two identical polypeptide heavy chains and two identical light chains. Each heavy chain or light chain contains constant regions and variable regions. To generate TCRs and BCRs, a series of genetic recombination, known as V(D)J recombination, occurs in developing T cells and B cells respectively. The process involves somatic recombination events that occur at the locus of TCR genes and immunoglobulin genes, generating highly diverse products of TCRs and immunoglobulins that specifically recognize certain unique amino acid sequences. Therefore, both T and B cell responses are highly antigen-specific, which is one of the hallmarks of the adaptive immune system.

T cells are present in several categories and accomplish their defense responses through different mechanisms. Broadly speaking, T cells can be classified into effector T cells, regulatory T cells, and memory T cells. Effector T cells are activated cells that are relatively short-lived. These cells are responsible for eliminating pathogens upon activation by the innate immune responses. Memory T cells do not immediately become active, even though they are usually produced at the same time as effector T cells. Instead, they are long-lived, persist after the resolution of inflammation, and could mount quicker immune responses upon secondary exposure to the same antigen. On the other hand, the role of regulatory T cells (T_{reg}s) is to modulate and prevent excessive immune responses. T_{reg}s ensure the balance between effective

immunity that damages the invaders and immunopathology that damages the host, keeping other immune cells at bay so that effectors do not cause unnecessary tissue damages as they control or eliminate infections.

T cells activation is a tightly regulated process that requires multiple signals integrated together. First signal is initiated when TCRs recognize pathogen-specific peptides that are presented by MHC molecules on antigen presenting cells. It is important to note that T cells do not recognize free-floating antigens, but can only recognize peptide-MHC (pMHC) complex. This TCR-pMHC binding requires co-receptors that include at least CD3 along with either CD4 or CD8. In addition, T cell activation requires a second "co-stimulatory" signal, without which T cells would be rendered "anergic", or non-functional, by TCR-pMHC engagement alone. One of the best-characterized co-stimulatory molecules on T cells is CD28, which binds to CD80 or CD86 on antigen presenting cells and then triggers downstream signaling pathways to enable T cell expansion and differentiation. To ensure a proper T cell differentiation program that caters to the need of the pathogenic challenge, a third signal is triggered by inflammatory cytokines within the local environment. The cytokine milieu not only has a key influence on the kind of T cells being produced, but also determines if the first two signals lead to tolerance, effector T cell activities, or immune memory. The three signals are highly integrated to ensure proper T cell activation.

Effector T cells are predominantly composed of cytotoxic T cells and helper T cells. While other less abundant populations, including natural killer T cells, gamma delta T cells, and mucosal associated invariant T cells, are also subclasses of effector T cells. Cytotoxic T cells express CD8 molecules on their cell surface; they are activated by antigen presenting cells that

present antigens on surface MHC class I molecules (MHCI). Helper T cells express CD4 on their surface and are activated by peptides on MHC class II molecules (MHCII).

Cytotoxic T cells, or CD8+ T cells, kill pathogen-infected cells mainly through two mechanisms. When confronting infected cells, CD8+ T cells can release a series of cytotoxic granules including perforin, granzymes, and granulysin. Perforin and granulysin could form pores on the target cells, allowing granzymes, a family of serine proteases, to enter and initiate a cascade of apoptotic events. CD8+ T cells can also upregulate Fas ligand upon encounter with and recognition of infected cells. Fas ligand can bind to Fas molecule of the target cells and initiate receptor-mediated extrinsic apoptosis pathways.

T helper cells, or CD4+ T cells, do not directly kill pathogen-infected cells. Instead, their functions are mainly carried out through the release of cytokines that help the activities of other immune cells. These include mediating class switching in B cells, activating cytotoxic T cells, and modulating phagocytosis in macrophages. The type of cytokine milieu has a direct influence on what type of T helper cells are generated during CD4 activation, and different types of CD4+ T cells are able to produce different kinds of cytokines to respond to the challenges brought forth by various pathogens. The major classes of T helper cells are Th1 and Th2 cells. Th1 cells are mainly responsible for combatting against intracellular bacteria and protozoa. They are activated by IL-12 and IL-2 that trigger downstream signaling that converge to transcription factors STAT4 and T-bet. Th1 cells predominantly produce IFN-γ, which triggers macrophage phagocytosis and activates iNOS to produce bactericidal radicals. Th1 cells are also potent at activating CD8+ T cells to produce cytotoxic molecules to kill compromised cells. Th2 cells are responsible for defending against extracellular parasites, including helminthes. They are activated by IL-4, through STAT6 and GATA3, and produce IL-4, IL-5, IL-9, and IL-13 as

effector cytokines. These effectors activate eosinophils, basophils, and mast cells to attack parasites. IL-4 also stimulates B cell to produce immunoglobulin E (IgE) that further stimulates mast cells to produce inflammatory mediators. IL-4 also acts in an autocrine fashion to enhance Th2 responses. Th2 cells can also produce IL-10 that suppresses Th1 differentiation. In addition to Th1 and Th2 cells that make up the majority of the CD4+ effector T cell populations, there are also other T helper cell types. Th17 cells play a role in clearing extracellular bacteria and fungi mostly at the skin and mucosal surfaces. Th22 cells are involved in wound healing responses in the skin by acting on keratinocytes, myofibroblasts, and epithelial cells. Folicular helper T cells (T_{FH}) regulate the development of antigen-specific B cells in secondary lymphoid organs. There are also other less well-established helper T cells, such as Th9 cells, which may constitute their own distinct lineages.

Responses by effector T cells are tightly regulated to ensure that the system could discriminate between self and non-self and that the adaptive immune responses do not overshoot to cause autoimmunity. Regulatory T cells, or T_{reg}s, play a critical role in regulating effector T cell activities. These cells are characterized by high level of IL-2 receptor and glucocorticoid-induced TNFR family related gene (GITR) on their surface, and unique expression of the transcription factor FoxP3. T_{reg}s regulate or suppress effector T cells (and potentially other immune cells) through several possible mechanisms. First, T_{reg}s have high levels of IL-2 receptor expression on their cell surface, which could serve as a reservoir that deprives the other T cells of this activating cytokine. In addition, T_{reg}s are potent producers of transforming growth factor beta (TGFβ) and IL-10, which could either suppress the abilities of antigen presenting cells to activate effector T cells or downregulate T cell effector activities. Cell-cell contact-based mechanisms could also mediate T_{reg}-based immune suppression.

In addition to effector T cells and regulatory T cells, a third class of T cells constitute memory T cells, which are long lived T cells generated during primary immune responses and respond to cognate antigens during secondary encounters. Memory is the second hallmark of the adaptive immune system.

The principal function of B cells is to generate antibodies against soluble antigens. Unlike T cells that can only recognize peptides presented on MHC molecule, antibodies can recognize free-floating antigens. Antibody functions are several fold: first, antibodies can block and *neutralize* parts of the pathogen surface, rending the pathogen incapable of effective attacks. Second, antibodies can perform *agglutination*, a process in which invading cells are glued into clumps that are processed for phagocytosis. Similarly, antibodies can *precipitate* serum-soluble antigens out of solution, rendering them recognizable by phagocyte. In addition, antibodies that bind to foreign microbes can activate the complement system, allowing the formation of membrane attack complexes that lead to the lysis of the invaders. In a similar process, antibody-bound pathogen can also be recognized by cellular immune components, such as NK cells.

Like T cells, B cells are activated by several signals. First signal comes when BCRs bind to antigens. B cells then endocytose the antigen along with BCR, process the antigen that is then presented onto surface MHCII molecules, which subsequently act as antigen presenting cells and interact with cognate CD4+ T cells. These T cells would then provide the second signal to B cells for further activation. Upon activation, B cells would proliferate and form germinal centers in secondary lymphoid organs. In the germinal centers, activated B cells would differentiate into antibody-secreting plasma cells and memory B cells. Similar to the T cell counterpart, plasma cells would serve as immune effectors and carry out their functions by secreting antibodies, while memory B cells would persist for future infections.

In conclusion, T and B lymphocytes constitute the cellular and humoral aspects of the adaptive immune system. With unique features of antigen specificity and memory, adaptive immunity cooperates with innate immune players to form a tightly regulated defense system. This system not only plays a key role in defending the host organisms against foreign pathogens, but also protects the organisms against attacks arisen within the "self". Cancer is a classical example of such self-attacks.

1.2.3 Immune Responses in Cancer

The presence of immune cells in cancer was observed a long time ago, with the earliest known report by Rudolf Virchow in the 19th century. Ever since, the immune system was postulated to play a role in protecting organisms against malignant diseases. In the last two decades, these postulations were corroborated by experimental evidence in mouse models, as mice deficient in various aspects of the immune system are more prone to develop carcinogen- or oncogene-induced tumors or even spontaneous tumors. These pieces of evidence led to the generation of the "immune surveillance" theory, which proposes the protective role of the immune system. Indeed, mice deficient in the generation of functional T and B lymphocytes have higher chances of developing tumors upon induction (Shankaran et al., 2001). This is exacerbated when natural killer cells are also depleted, suggesting the involvement of innate immunity in cancer surveillance (O'Sullivan et al., 2012). Deficiencies of certain molecules in myeloid cells, as exemplified in CD80 and CD86 double knockout mice that lack co-stimulatory signals, are also more susceptible to carcinogen-induced sarcoma development (Loser et al., 2005), which further illustrates an integrated defense mechanism that involves interactions between innate and adaptive immune components. Cytokines likely play an important role

during this coordination, especially type I cytokines. Mice lack interferons (Dunn et al., 2005; Kaplan et al., 1998), interferon receptors (Kaplan et al., 1998), and certain type 1 interleukins, such as interleukin (IL)-12 and IL-23 (Langowski et al., 2006; Liu et al., 2004), are all prone to tumorigenesis. While being supported by a large number of mouse studies, the surveillance theory adopts a one-dimensional and static view of the role of the immune system. Later evidence suggested that the interactions between cancer and the immune system are rather dynamic. Therefore, a newer "immune editing" theory was developed, which adds the dimension that the immune system also sculpts the tumors. The immunoediting process is composed of three distinct phases: elimination, equilibrium, and escape. The elimination phase is evidenced by the experimental approaches that corroborate the "surveillance" mechanisms. Equilibrium phase occurs when the immune system fails to eliminate cancer cells but is able to suppress their outgrowth. This phase was mostly inferred from clinical observations, but later supported by a number of experimental animal models. The first piece of evidence came from a lose dose carcinogen treatment, where the majority of the mice do not develop tumors. However, if T cells were depleted after a prolonged tumor-free period after carcinogen treatment, mice would develop malignant diseases (Koebel et al., 2007). This suggests the capabilities of the immune system to suppress the outgrowth of tumor cells for an extended period of time. This equilibrium regulates both the primary tumor development and the occurrence of metastasis (Eyles et al., 2010). Unlike the elimination phase, in which both the innate and adaptive immune systems are important, equilibrium seems to rely mostly on adaptive immunity, which likely contains tumor cells in an antigen-specific manner. As tumors exit the equilibrium phase, they would escape immune regulation. Cancer patients present diseases that are in the "escape" phase.

Tumors escape immune attacks through both the suppression of anti-tumor immunity and the augmentation of pro-tumor immune responses. To negatively suppress inhibition by the immune system, tumor cells can suppress dendritic cell activities through the secretion of a series of cytokines and factors, such as adenosine (Novitskiy et al., 2008) and prostaglandin E2 (Lee et al., 2002). They can also evolve strategies that evade the recognition or phagocytosis by dendritic cells or macrophages. For example, multiple types of tumors have upregulated level of CD47, a molecule that delivers "do-not-eat-me" signals to phagocytes. These disruptions in myeloid cell activities lead to the prevention of antigen processing. As a consequence, antigen presentation becomes compromised in secondary lymphoid tissues. Therefore, anti-tumor T cells do not become activated or traffic to the tumor site. Even when confronting the activated and infiltrated T cells, tumor cells also have strategies to avoid attacks. They could downregulate MHCI molecules on their cell surface or alter their own antigen presentation machinery, both of which help hiding tumor antigens from T cell recognition. They can suppress lymphocyte activities through paracrine mechanisms, such as the upregulation of PD-L1 or shedding of NKG2D ligands, which renders anergy and suppress T cell/NK cell effector functions (Nausch and Cerwenka, 2008).

On the other hand, tumors often augment the myeloid compartment and the inhibitory arm of the adaptive immune system to allow immune escape. One of the hallmarks of many types of cancers is the extensive infiltration of immune cells. These include cells from both the myeloid lineage (such as macrophages, neutrophils, immature dendritic cells (DCs)) and the lymphoid lineages (such as regulatory T cells). Myeloid cells, including macrophages and neutrophils, have plastic phenotypes. Even though they could be equipped with cytotoxicity and anti-tumor activities, they are polarized in the tumor microenvironment to promote cancer

progression through various mechanisms. They do so by secreting growth factors that sustain the proliferation and survival of cancer cells, promoting angiogenesis, and metabolically inhibiting anti-tumor adaptive immune responses. Similarly, the dendritic cell compartment is reprogrammed. Conventional dendritic cells that are able to functionally activate CD8+ T cells are scarce in many tumors, due to a combination of defects in DC recruitment and tumor-induced DC apoptosis (Ma et al., 2013). Instead, tumors could recruit DCs with immature phenotype characterized by low MHC molecules and co-stimulatory molecules, such as CD80 and CD86, and inefficient motility (Kim et al., 2006; Mahnke et al., 2002; Palucka and Banchereau, 2012). Activation by these DCs lead to tolerogenic T cell activation, as evidenced by the induction of regulatory T cell responses (Jonuleit et al., 2000) instead of antigenic activation. Cancers often upregulate the infiltration of regulatory T cells to suppress the functions of CD8+ cytotoxic and Th1 T cells, thereby rendering the tumor cells tolerated by the immune system.

One of the corollaries of the immunoediting theory is that the immune system only attempts to sequester tumor initiation. While this may truly be the function of effector CD4+ and CD8+ T cells, other components of the immune system could promote the growth of nascent tumor cells instead. This is evidenced the demonstration of chronic inflammation as a significant risk factor for cancer (Hussain and Harris, 2007). During inflammation, tissue-infiltrating leukocytes could produce a large number of inflammatory mediators, such as reactive oxygen species, reactive nitrogen species, and cytokines, which could disrupt the environment that is suitable for the homeostasis of parenchymal cells. Possible disruptions include tissue damage, fibrosis, angiogenesis, and hypoxia (Mantovani et al., 2008; Multhoff et al., 2011). Inflammatory mediators, along with tissue disruptions caused by these factors, could promote genome instabilities and genetic alterations that lead to the initiation of tumorigenesis (Grivennikov and

Karin, 2010). In addition, epigenetic changes could be induced in premalignant cells. Stress could also disrupt proteostasis, by stimulating the over-production of heat shock proteins for example, that overwhelms the healthy cellular activities. While surveillance mechanisms exist to eliminate transforming cells, inflammation could supply pro-survival factors and nutrients that even overcome transformation-induced stress, such as oncogene-induced senescence. Moreover, a number of inflammatory cytokines could promote epithelial-to-mesenchymal transition, which upregulates the invasiveness and mobility of transformed or transforming cells.

In conclusion, the interactions between the tumor and the immune system are dynamic and complex. The immune system could restrain and eliminate nascent tumor cells, while chronic inflammation could participate in the promotion of tumorigenesis. Established tumors could evade immune recognition, while the immune system could also be utilized to target tumor cells. In order to better target the immune system to treat cancer, it is imperative to have a better understanding of how the immune system could function and how these processes could go awry in cancer-bearing organisms. This dissertation focuses on one of the most abundant innate immune cells in many types of tumors, macrophages.

1.3 Overview of Macrophage Biology

1.3.1 Macrophages in Pathogen Infection

Macrophages were originally discovered by Ellie Metchnikoff. Named after Greek words "*makro*" (large) and "*phagein*" (eat), these cells are known for their abilities to engulf and digest pathogens, cellular debris, and infected or transformed host cells. As a key component of the innate immune system, macrophages play important roles in the clearance of pathogen during infections by bacteria, viruses, fungi, and parasites.

Macrophages are present in almost all mammalian organs, including the sites that are susceptible to the initial attacks of invading pathogen. Because of their locations, tissue resident macrophages are often a key player in the initial phase of the combat against pathogens. However, tissue resident macrophages alone may not be sufficient to mount a sufficient defense. To ensure a sufficient number of defense effector cells, affected tissues would also send signals to recruit more inflammatory monocytes from circulation that differentiate into macrophages upon infiltration into affected tissues. In most infectious diseases, recruitment provides the major source of macrophages. The C-C motif chemokine ligand 2 (CCL2) and CCL2 receptor 2 (CCR2) signaling pathway is essential for monocyte recruitment (Pierce et al., 1990). Other cytokines and chemokines also demonstrated monocyte-attracting activities. These include macrophage colony-stimulating factor (M-CSF, also known as CSF-1), granulocyte-macrophage colony-stimulating factor (GM-CSF, or CSF-2), CCL3, CCL5, CCL8, vascular endothelial growth factor (VEGF), placental growth factor (PlGF), and CXC-motif ligand-12 (CXCL12) (Coffelt et al., 2009), although their relevance *in vivo* is less well established. Deficiency in monocyte recruitment compromises immune responses against bacteria including *Listeria monocytogenes*, *Toxoplasma gondii*, and *Mycobacterium tuberculosis*, viruses including influenza, and fungi infections (Serbina et al., 2008; Shi and Pamer, 2011; Zhang and Wang, 2014). On the contrary, during helminth infections, macrophages undergo proliferation at the site of infection independently of blood recruitment (Jenkins et al., 2011). However, in certain helminth infection models, such as *Schistosoma mansoni* infection, *in situ* proliferation occurs in monocyte-derived macrophages instead of tissue resident macrophages (Nascimento et al., 2014). These data suggest that recruitment and local proliferation may occur sequentially or

simultaneously to supply sufficient quantities of macrophages for defense against foreign pathogens.

At the infection site, macrophages become activated and contribute to the clearance of pathogens by a range of effector mechanisms. To recognize pathogens or pathogen-affected cells, macrophages are equipped with pattern recognition receptors (PRRs) to recognize pathogen-associated molecular patterns and damage-associated molecular patterns. These PRRs include membrane-bound toll-like receptors (TLRs) and C-type lectin receptors (CLR2), and cytoplasmic NOD (nucleotide-binding oligomerization domain)-like receptors (NLRs) and RIG (retinoid acid-inducible gene)-I-like receptors (RLRs) (Takeuchi and Akira, 2010). Altogether, these pattern recognition receptors recognize molecules associated with microbes (such as lipopolysaccharides, flagellin, and single-stranded or double-stranded RNA), and molecules associated with cellular damages that represent the "danger" signal (such as extracellular adenosine triphosphate (ATP) and high motility group box 1 protein, both of which are released by injured cells). Upon the engagement of PPRs, the intracellular signaling pathways triggered downstream will lead to transcriptional activation of inflammatory mediator genes followed by the production and secretion of these factors. In addition to PRRs, macrophages are also armed with a wide range of receptors for immunomodulatory cytokines. Engagement of different cytokine receptors could lead to differential activation of macrophages (Mosser and Edwards, 2008). An over-simplistic classification categorizes macrophage activation status into M1 and M2, corresponding to classically activated macrophages and alternatively activated macrophages. This nomenclature was proposed to parallel the classification of T cell differentiation into Th1 and Th2 cells. Cytokines such as interferon gamma (IFNγ) and tumor-necrosis factor (TNF) activate M1 macrophages, which then produce pro-inflammatory cytokines, promote Th1

responses, and cause extracellular matrix (ECM) destruction and apoptosis. Exposure to cytokines such as interleukin (IL)-4 leads to the activation of M2 macrophages, which promote Th2 responses, ECM construction, and wound healing. However, this simplistic scheme underestimates the variety of cytokines available in the tissue environment; macrophages are usually exposed to a large number of factors of different flavors at the infection sites. Indeed, increasing amount of data demonstrate a large spectrum of activation status that fits between and beyond the M1 and M2 dichotomy (Murray et al., 2014; Xue et al., 2014), which allows macrophages to carry out different functions tailored to the needs of specific pathogenic challenges.

To clear pathogens, activated macrophages perform phagocytosis, engulfing not only microbes but also microbe-infected cells. As discussed earlier, macrophages could initiate a series of microbicidal activities following phagocytosis, such as producing ROS during respiratory burst and synthesizing proteolytic enzymes to digest microbial components. Other than killing engulfed microbes, macrophages could kill extracellular pathogens or infected cells in proximity through the secretion of metabolites that have microbicidal activities. These metabolites include indoleamine-pyrrole 2,3 dioxygenase (IDO) and nitric oxide. Macrophages could also upregulate apoptosis-inducing molecules, such as Fas ligand, which gets rid of infected cells in a paracrine manner. In addition to direct microbicidal mechanisms, macrophages also secrete various proinflammatory cytokines and chemokines that recruit other effector leukocytes to the infection sites to clear pathogens. For example, CXC-motif ligand-10 (CXCL-10) and CXCL-11 secretion induces the infiltration of CD8+ T cells and Th1 cells to control virus and intracellular bacteria infections. Secretion of IL-17 could attract Th17 cells to fight

fungus infections at certain sites. IL-4 and IL-13 could attract granulocytes such as eosinophils to combat parasites.

During the clearance of infection, immune responses cause tissue damages due to the release of cytotoxic molecules and metabolites. A functional immune response dictates the inevitable consequence of immunopathology, compromising the short-term health of the host in exchange for long-term fitness of a pathogen-free organism. However, upon elimination of invading pathogens, uncontrolled inflammation needs to be avoided. Macrophages play a critical role in the resolution of immune responses against infections. They engulf effector immune cells that have accomplished their microbicidal functions. They adopt the "M2" activation state and secrete immunosuppressive cytokines that inhibit potentially excessive cytotoxic activities. They can also initiate the wound-healing process through actions on non-hematopoietic cells. For example, macrophages secrete factors such as transforming growth factor-beta (TGFβ) and metalloproteinases to activate fibroblast cells, which in turn lay out ECM molecules to serve as a scaffold for tissue repair (Ortega-Gomez et al., 2013).

1.3.2 Macrophages in Development and Homeostasis

In addition to defending the host against pathogen infections, another important function of macrophages is to maintain tissue integrity of an organism. First, they are necessary in embryonic and neonatal development, during which organs develop into functional units that perform designated activities of an organism. In adult organisms, macrophages are also involved in the maintenance of homeostasis.

The necessity of macrophages during development was manifested by a series of tissue abnormalities in mice that have a deficiency in macrophage colony-stimulating factor (MCSF,

also known as CSF1). Abnormalities cover a wide range of tissues, including the bone, mammary gland, kidney, and pancreas (Pollard, 2009). More dramatically, PU.1 deficient mice that lack macrophages are embryonically/neonatally lethal, which further suggests the importance of macrophages during development.

Macrophages regulate proper tissue development through several mechanisms. First, they provide factors that sustain the survival and proliferation of tissue parenchymal cells during development. This is best studied in brain development, where neuron viability relies on the presence of macrophages. In addition to supplying pro-survival factors, macrophages are also involved in fine-tuning and promoting the functions of parenchymal cells. Brain resident macrophages, called microglia, have also been indicated to modulate neuron activities, prune synapses during development, and maintain neural circuits and brain structure (Erblich et al., 2011). In addition to the regulation of terminally differentiated cells, microglia may also regulate neural stem cells during development (Nandi et al., 2012). Similarly, macrophages are also important in maintaining the viability and functions of mammary gland stem cells (Gyorki et al., 2009) during development.

In addition to its actions on parenchymal cells and/or tissue stem cells, macrophages are also important for remodeling the tissue structure. They do so through modifications of the extracellular matrix and vasculature. Moreover, processing cell death and cellular debris is another key mechanism by which macrophages oversees proper development. Development is accompanied by constant tissue remodeling, during which a lot of cells and structures that form temporarily will need to be recycled. These cells would receive signals to undergo apoptosis. Macrophages play a critical role at clearing apoptotic cells, both to avoid unnecessary or detrimental inflammation, and to clear space for further construction/reconstruction. A best-

known example is the disappearance of interdigital webs that formed during limb development, in which macrophages have been shown to actively scavenge the apoptotic cells (Gregory and Devitt, 2004). Not only are macrophages necessary for the recycling of apoptotic cellular debris, they are also active inducers of apoptosis. For example, during eye development, macrophages induce apoptosis through Wnt-dependent pathways in order to optimize the patterning of vasculature in the developing eye (Lobov et al., 2005).

Even though the vast majority of data defining the functions of macrophages were obtained from development and pathological conditions, these cells are also essential for the maintenance of organismal homeostasis. Homeostasis is not a static condition, but instead involves various events occurring in a very dynamic manner. Maintenance of hair is a great example, in which hair follicles undergo various phases to allow hair to grow. Hair follicle cycling not only happens in response to hair loss but is also involved during the homeostatic hair turnover. Macrophages can be activated to secrete factors that stimulate the active cycling of hair follicle stem cells to promote hair growth (Castellana et al., 2014). In the hematopoietic system, depletion of macrophages led to impaired generation of erythroblasts and caused peripheral blood anemia (Chow et al., 2013). This suggests that macrophages are important for the maintenance of the blood system that provides oxygenation to all organs, potentially through interactions between bone marrow resident macrophages and hematopoietic progenitor cells. In extramedullary hematopoietic sites, macrophages were shown to retain hematopoietic stem cells (HSCs) in the splenic niche, which is essential for maintaining HSC functions (Dutta et al., 2015). Macrophages have also been reported to interact with tissue stem cells in various organs, including the liver (Boulter et al., 2012), heart (Ben-Mordechai et al., 2013), mammary gland (Gyorki et al., 2009), colon (Pull et al., 2005), and intestine (Saha et al., 2016). More

experimental evidence is needed to define to what extent are these interactions involved in the regulation of tissue homeostasis needs.

In addition to activating cellular activities, macrophages can also participate in homeostasis by maintaining immune quiescence, i.e. inhibiting the activation of immune cells. A classic textbook example is the participation of macrophages in clearing out apoptotic cell products in a process called “efferocytosis”. Apoptotic cells undergo membrane flipping, where the inner leaflet of the cell membrane becomes exposed to the outside. Inner membrane phosphatidylserine was also translocated to the outer membrane, which is recognized by macrophages. Upon the receipt of this “eat me” signal, macrophages engulf apoptotic cells, which limits the non-discriminatory release of cellular materials that could trigger unnecessary inflammation (Arandjelovic and Ravichandran, 2015). Efferocytosis is essential for maintaining the non-phlogistic (not causing inflammation) nature of apoptosis, which is distinguished from necrosis. In a similar fashion, macrophages also get rid of senescent cells, as exemplified by the clearance of senescent red blood cells by splenic macrophages (Kohyama et al., 2009). In addition, macrophages can secrete other immune dampening factors, such as complement component 1q, resolven E1, protectin D1, and galectin, among others, to alleviate unnecessary immune responses (Pinto et al., 2014).

Moreover, macrophages are important for maintaining metabolic homeostasis in response to environmental changes, such as temperature decrease and caloric intake. Brown adipose tissue (BAT) is the primary thermogenic organ upon exposure to low temperature. BAT resident macrophages are required for metabolic adaptation to cold. Upon alternative “M2” activation, these macrophages secrete norepinephrine that stimulates sympathetic nerve cells to activate the thermogenic programs within the BAT (Nguyen et al., 2011). White adipose tissue is responsible

for long-term storage of nutrients and regulates systemic metabolic activities through hormone release. In lean animals, alternatively activated macrophages maintain insulin sensitivity in adipocytes, partially through the secretion of IL-10 (Odegaard and Chawla, 2013). As mice develop from lean into fat physique under the influence of high fat diet, classically activated macrophages infiltrate WATs and remodel these tissues during their enlargement (Lumeng et al., 2007). High fat diet also causes increased lipid storage in hepatocytes; liver resident macrophages, or Kupffer cells, participate in this process by regulating fatty acid oxidation in hepatocytes. Disruption in the alternative activation of Kupffer cells led to insulin resistance and steotosis (Kang et al., 2008). During the increased uptake of fatty acid mentioned above, macrophages act as lipid sensors and trigger the corresponding responses through the activation of peroxisome proliferator activator receptors (PPAR) (Jantsch et al., 2014). Similarly, macrophage activation is also altered to respond to changes glucose levels (de Souza et al., 2008).

Another critical aspect of homeostasis is the balance in body fluids. While kidney is the principal organ that regulates salt and water in an organism, the skin does not equilibrate readily with the plasma, and therefore is less susceptible to renal homeostatic control (Titze, 2014). Interestingly, macrophages infiltrate to hypertonic sites of the skin where sodium and chloride levels are above the normal threshold. These macrophages sense interstitial electrolytes, possibly through the engagement of pattern recognition receptors, which trigger inflammasome activation (Ip and Medzhitov, 2015). Consequently, nuclear factor of activated T-cells 5 (NFAT5) is activated to initiate essential transcription programs in response to the osmotic stress (Muller et al., 2013).

In conditions where homeostasis is disrupted, macrophages are important for restoring the normal functions of a tissue, in processes such as tissue regeneration. This is evidenced by

delayed tissue repair upon macrophage depletion. A key mechanism relies on the ability of macrophages to clear senescent cells and cellular debris through phagocytosis, which is believed to create an environment that is permissive to regeneration (Yun et al., 2015). For example, in a non-inflammatory lung injury model that mimics damages caused by respiratory stress, macrophages selectively deplete the dysfunctional type II lung epithelial cells, therefore alleviating the consequences of injury (Miyake et al., 2007). In addition, angiogenesis can also compensate for the lack of oxygenation at the injury site and facilitate tissue repair; macrophages have been shown to provide critical signals for angiogenesis. This has been shown in multiple pathophysiological processes, such as the repair during myocardial infarction (Aurora et al., 2014) and peripheral nerve damage (Cattin et al., 2015).

1.3.3 Macrophages in Malignant Diseases

Macrophages can promote the initiation of tumorigenesis by promoting chronic inflammation as discussed in Section 1.2.3. Chronic inflammation may cause DNA damages, lead to genome instabilities, and generate a hostile tissue environment. In addition, depletion of macrophages in pancreatic ductal adenocarcinoma correlated with significantly reduced number of cells with tumor-initiating properties, suggesting that macrophages could also promote tumor development through actions on "cancer stem cells" (Yang et al., 2013). Such activities could be executed through the activation of the signal transducer and activator of transcription 3 (STAT3) signaling pathway within the neoplastic compartment (Mitchem et al., 2013).

Beyond the inception of tumorigenesis, macrophages can also promote the progression of established tumors. They are highly abundant in tumor tissues in many types of cancers. High levels of macrophage infiltration in the tumor tissue, also called "tumor-associated macrophages"

(TAMs), correlate with worse patient outcome in most types of cancers. One exception is colorectal cancers, where contradictory roles of macrophages have been reported (Khorana et al., 2003; Lackner et al., 2004; van Netten et al., 1993). These inconsistencies could be due to variations in the timing of the disease progression and the location of macrophages that were examined in different studies. Other than colorectal cancer, TAMs tends to play pro-tumorigenic roles through various mechanisms that facilitate tumor progression.

First, TAMs can produce growth or survival factors that enhance the proliferation and viability of tumor cells. A classic example came from studies looking at the MMTV-PyMT breast cancer mouse model, in which macrophages recruited in a CSF1-dependent manner secrete epidermal growth factor (EGF) that stimulates the division of neoplastic cells. In this model, EGF also enhances the invasiveness of the cancer cell (Goswami et al., 2005; Patsialou et al., 2009).

Second, macrophages can remodel the stromal components that are normally present in the tissue to support organ functions, and skew their activities to facilitate tumor development. Two examples are blood vessels and fibroblast cells, whose activations by TAMs lead to angiogenesis and fibrosis respectively. The involvement of TAMs in promoting angiogenesis has been demonstrated in mice deficient in macrophage recruitment, which have reduced vasculature, increased hypoxia and reduced tumor growth and metastasis (De Palma et al., 2005; Pucci et al., 2009). TAMs secrete an extended list of cytokines, such as VEGF, CXCL12, which promote angiogenesis and vascularization through several mechanisms: they could trigger sprouting/branching of pre-existing blood vessels by promoting the protrusion of a selected endothelial cell. Alternatively, endothelial progenitor cells could be recruited from the circulation system to the tumor site and differentiate to new endothelial cells that line up blood

vessels; this process is called “vasculogenesis”. In a fashion similar to angiogenesis, TAMs can also remodel the lymphatic vessels through lymphangiogenesis, which will not be discussed here. As tumor vasculature is remodeled, basement membranes underlining the endothelial cells also need to be remodeled. TAMs can accomplish this remodeling function through the secretion of metalloproteinases (MMPs), such as MMP-9 (Coussens et al., 2002).

TAMs, especially the “M2” polarized macrophages, are well known for their abilities to promote fibrosis through the secretion of profibrotic cytokines that activate fibroblast cells. Quiescent fibroblasts would then become myofibroblasts and lay down extracellular matrix molecules. The best-studied cytokine involved in this process is TGFβ, which induces fibroblast proliferation and upregulates the transcription of profibrotic genes, including collagens and fibronectin (Border et al., 1990; Haberstroh et al., 1993), through the phosphorylation of Smad molecules (Meng et al., 2016). In addition to inducing the differentiation of fibroblasts into myofibroblasts, macrophages also play a role in sustaining myofibroblast survival through the stimulation of nuclear factor kappa B (NF-κB) activities (Pradere et al., 2013). In a similar mechanism, macrophages can produce factors that promote epithelial-to-mesenchymal transition, during which epithelial cells lose their identity and adopt a fibroblast phenotype and lay down ECMs (Usunier et al., 2014). Surprisingly, TAMs could also promote fibrosis by directly producing ECM molecules without involving the activation of fibroblasts. A recent proteomic study in colorectal cancer models demonstrated that TAMs produced a wide range of collagens, peoteoglycans, glycoproteins, and ECM modulators (Afik et al., 2016). It remains to be seen if TAMs in other cancers can also directly lay down ECM molecules. As a side note, though the angiogenic and pro-fibrotic functions of macrophages have been shown in multiple tissue contexts, it is not clear if all macrophages have the same potential to execute these activities, or

if only a subset of macrophages are capable of doing so. Characterization of angiogenic TAMs led to the identification that these cells represent a TIE2-expressing subset of macrophages (De Palma et al., 2005; Lewis et al., 2007). More recently, an atypical progenitor-like monocyte/macrophage population was identified to be necessary for fibrosis (Satoh et al., 2017). It remains to be seen to what extent in vivo are different macrophage subsets involved in these processes.

The third tumor-promoting mechanism involves the suppression of anti-tumor immune responses. Macrophages can secrete anti-inflammatory cytokines to inhibit the recruitment of CD8+ and Th1-biased CD4+ T cells. They can metabolically suppress the activities of anti-tumor T cells, by depleting the L-arginine in the environment that is necessary for T cell functions, through the secretion of L-arginine processing enzymes, nitric-oxide synthase and arginase I. TAMs could also chemically modify T cell receptors to inhibit their recognition of tumor antigens through molecules such as peroxynitrite. TAMs can also engage with T cells in a paracrine manner through surface markers such as co-stimulatory molecules. Upon engagement with macrophages, T cells could activate signaling pathways downstream of cytotoxic T lymphocyte antigen-4 (CTLA4) and programmed death-1 (PD1), which drive the cells towards an anergic or exhausted phenotype, rendering T cells non-functional. Macrophages also produce chemokines to recruit immunosuppressive regulatory T cells, through the secretion of CCL-17 and CCL-22 for example.

Through these integrated actions on tumor cells, fibroblasts, endothelial cells, and adaptive immune cells, macrophages create an environment that facilitates tumor growth and invasion but deters effective immune responses, thereby facilitating tumor progression.

Macrophages not only promote primary tumor growth but also accelerate metastasis. This could occur during both the intravasation process at the primary tumor site and the extravasation process at the metastatic/pre-metastatic site. TAMs at the primary tumor site promote the invasion of tumor cells through the secretion of factors such as EGF and vascular endothelial growth factor (VEGF) (Qian et al., 2011), thereby allowing tumor cells to enter circulation and home to distant organs. Metastasis-associated macrophages (MAMs) can capture circulating tumor cells and retain them at the pre-metastasis site, which extends the duration at which newly arrived tumor cells could interact with the pre-metastatic niche. This extended duration could allow further modifications to the tissue, and increases the possibilities of neoplastic cell extravasation to form a metastatic site (Kitamura et al., 2015). Similar to TAMs, MAMs can also produce growth factors to accelerate the expansion of tumor cells (DeNardo et al., 2009). In addition, even before the arrival or disseminated cells, macrophages can already contribute to the creation of a pre-metastatic niche, in part through the downregulation of dendritic cells and anti-tumor T cell infiltration (Sharma et al., 2015) and the induction of fibrosis at the pre-metastatic site (Nielsen et al., 2016).

Macrophages not only participate in the natural courses of tumor initiation and progression, but also affect how tumors respond to therapeutic interferences. This is usually accomplished through (1) secretion of pro-survival factors that blocks the apoptosis pathways induced by chemotherapies, (2) production of molecules involved in the metabolism of chemotherapeutic drugs, which are converted to a form that is less toxic to tumor cells, and (3) modulation of other stromal cells, such as dendritic cells (Ruffell et al., 2014), to suppress chemotherapy-induced activation of anti-tumor immune responses.

Taken together, macrophages infiltrating primary tumors and metastatic or pre-metastatic tissues promote tumor progression, metastasis, and therapy resistance through various mechanisms, therefore posing a significant barrier to effective anti-cancer treatments. Understanding the biology of TAMs and MAMs is essential for the development of trials that target these myeloid cells. While a lot of research has been done to elucidate the mechanisms by which macrophages regulate tumor growth, available strategies to target these cells are very limited, with the majority of the approaches focused on depleting these cells. Improving the clinical efficacy in these strategies requires in-depth understanding of the sources that supply macrophages to the tumor tissue. However, ontogeny of tumor-associated macrophages is not well defined.

1.3.4 New Paradigm of Macrophage Ontogeny

As part of the mononuclear phagocytes system (MPS), macrophages in tissues were considered to originate from the adult hematopoietic system. A four-decade-old dogma of macrophage ontogeny held that hematopoietic stem cells in the bone marrow give rise to monocytes through stepwise lineage specification; monocytes then enter circulation and further differentiate into macrophages upon extravasation into tissues. In other words, this paradigm proposed that monocytes in circulation constitute a mobile pool of intermediately differentiated progenitors that are on their way between their origin (bone marrow) and their destination (tissue). This dogma was proposed based on the initial observation that adoptively transferred monocytes differentiate into macrophages as they circulate into the inflamed peritoneum. It was later supported by a large number of similar observations in various tissues under different pathological conditions (Ginhoux and Guilliams, 2016).

This paradigm has been challenged in the past decade. As this model was based solely on observations under inflammatory conditions, several lines of evidence looking at the homeostasis of macrophages in non-pathological conditions raised discrepancies with the concept that the adult hematopoietic system provides the only source of tissue macrophages. For example, irradiation causes the ablation of the hematopoietic stem cells but does not wipe out tissue resident macrophages, which can be minimally affected, as is the case with skin Langerhans cells (Merad et al., 2002) and brain microglia (Ginhoux et al., 2010). Furthermore, patients who have severe monocytopenia could have normal numbers of macrophages in many tissues (Collin et al., 2006), a phenotype also recapitulated in mouse models. In addition, monocyte-derived cells tend to have a shorter life span and high turnover rate, which does not explain the long half-life of tissue resident macrophages. Moreover, the original MPS ontogeny paradigm views monocytes as a cell type with transition roles but little other functionality; differentiation in macrophages is their fate by default. This view has also been challenged. Monocytes were shown to be able to traffic out of the blood into multiple tissues constitutively without contributing to the macrophage pool. Instead these monocytes can sample antigens in a similar fashion as dendritic cells (Jakubzick et al., 2013). These observations led to the rewriting of the paradigm of MPS ontogeny.

An extensive list of parabiosis studies investigated the contribution of circulating Ly6C^{Hi} monocytes to the turnover of tissue resident macrophages. Some tissues, including the colon and intestine (Bain et al., 2014), dermis (Tamoutounour et al., 2013), and pancreatic islets (Calderon et al., 2015) rely on monocyte infiltration for macrophage maintenance. On the other hand, macrophages in a wide range of organs, including the lung, red pulp, pancreatic stroma, and brain, do not show significant exchange with the blood for even after up to 5 months of

parabiosis (Hashimoto et al., 2013). These data uncoupled the adult hematopoietic system with the maintenance of tissue resident macrophages in many organs, suggesting the existence of an alternative source that sustains these cells.

In addition to maintenance, the development of macrophages could also be independent of HSCs. One of the first pieces of evidence to uncouple the ontogeny of tissue resident macrophages with HSCs was based on the observation that macrophage development and hematopoiesis had differential transcriptional requirements. Hematopoietic stem cell differentiation requires the transcription factor c-Myb for proliferation and differentiation (Sandberg et al., 2005). However, subsets of tissue resident macrophages in a wide range of organs still develop in mice that lack this transcription factor (Schulz et al., 2012). This suggests that HSCs are not the only developmental source of macrophages. Moreover, Flt3-based lineage tracing experiments added further confirmation. Flt3 is a receptor tyrosine kinase that is expressed in multipotent hematopoietic progenitors. Its expression is activated during early stages of HSC differentiation (Boyer et al., 2011). Therefore, all hematopoietic cells in circulation are labeled by Cre recombinase. However, macrophages in a number of tissues, including epidermis Langerhans cells, liver Kupffer cells, spleen and kidney resident macrophages, and brain microglia, demonstrated low levels of recombination. These data suggested that an alternative hematopoietic source is responsible for the development of tissue resident macrophages.

A series of tamoxifen-inducible lineage tracing models provided crucial data that helped defining the origin of tissue resident macrophage: transgenic or knock-in mouse models that have the Cre recombinase genes driven by various promoters took advantage of the early expression of these promoter genes that precedes the emergence of HSC-initiated hematopoiesis,

also called “definitely hematopoiesis”. Before the appearance of HSCs and the occurrence of definitive hematopoiesis, the embryo undergoes several waves of blood production (Franklin and Li, 2016; Ginhoux and Guilliams, 2016). First wave is called “primitive hematopoiesis”, in which blood cells arise from the blood islands of extra-embryonic yolk sac. In mice this occurs around embryonic day 7.0. During primitive hematopoiesis, a progenitor population called “erythro-myeloid progenitors” (EMPs) arises around E7.25 and produces nucleated erythrocytes and macrophages, which respectively provide oxygenation and participate in tissue structuring. Following primitive hematopoiesis, a second wave of hematopoiesis occurs. During this period, a slightly larger variety of leukocytes could be produced. In addition to EMPs, a population of progenitors with lympho-myeloid potential is also produced. This wave of blood production occurs in the hemogenic endothelium of the yolk sac; therefore the EMPs produced during this wave are named “late EMPs” which distinguishes them from the EMPs that arise within the yolk sac blood islands. “Early” EMPs express CSF1R but is c-Myb independent, while the “late” EMPs appear to express c-Myb. Before the formation of the circulatory system, yolk sac serves as the primary site of blood production for the embryo. Concomitant with the emergence of late EMPs, a third wave starts within the hemogenic endothelium of the embryo proper around E8.25. Coinciding with this, the embryo develops a functioning circulation system by E8.5. During this wave of hematopoiesis, immature hematopoietic stem cells are generated within the para-aortic splanchnopleura (P-Sp) region. Subsequently, HSCs were observed in the aorta gonads and mesonephris (AGM) region at E10.5, and then in the fetal liver. Though still controversial, the immature HSCs observed in the P-Sp region were considered to be the progenitors of HSCs that later migrate to the AGM region and then ultimately settle in the fetal liver (Cumano and Godin, 2007). Fetal liver becomes the major site of hematopoiesis starting at E12.5 and peaks at E16.5

in mice, before bone marrow takes over the hematopoietic function at perinatal stages (Orkin and Zon, 2008).

Despite the agreement on the embryonic contribution to tissue resident macrophages, controversies still exist regarding the precise nature of the embryonic progenitors that give rise to these cells. This is partially due to differences in the mouse models used for lineage tracing and the labeling variations by promoters driven by different genes. Runx1-CreER took advantage of the early expression of Runx1 starting at E6.5. Tamoxifen pulse at E7.0 specifically labeled up to 30% of brain microglia while sparing hematopoietic stem cells (Ginhoux et al., 2010). CSF1R-CreER has also been used, whose expression comes later than Runx1, therefore allowing a longer time window for labeling. E8.5 tamoxifen treatment leads to the labeling of various tissue macrophages, including those in brain, epidermis, liver, and spleen (Schulz et al., 2012), and subsets of macrophages in the pancreas and heart (Calderon et al., 2015; Epelman et al., 2014; Gomez Perdiguero et al., 2015). These findings, along with the presence of these cells in Myb knockout mice, led to the model in which yolk sac EMPs differentiate into macrophages that persist into adulthood.

However, whether these data above supports this "yolk sac exclusive" ontogeny model is questionable. Persistence of macrophage populations in Myb knockout mice only suggests the *ability* of progenitors to contribute to these cells when HSC differentiation is deficient, but does not suggest that this is what actually happens in unperturbed situations. These observations could be the mechanisms by which "early" EMP differentiation compensates for the deficiencies of hematopoiesis induced by Myb-dependent "late" EMPs or HSCs. Along the same lines, depletion of yolk sac-derived macrophages, through the treatment of CSF1 receptor depleting antibodies on E6.5, did not lead to irreversible reductions in fetal macrophages in most organs.

The only tissue resident macrophages that were irreversibly depleted were macrophages. Indeed, kinetics studies using CSF1R- and Runx1-CreER fate mapping models demonstrated the replacement of yolk sac derived macrophages as hematopoiesis progresses to the fetal liver stage. In a novel S100A4-Cre model that specifically traces fetal monocytes, Cre labeling started to be observed at E12.5 in macrophages in lung, liver, spleen, and skin, and the labeling efficiency progressively increased to an average of 60% in neonates, which was maintained into adulthood. Going back to the Runx1-CreER model, tamoxifen treatment at a later time point (E8.5) led to the labeling of a myb-expressing EMP population that entered circulation and colonized the fetal liver. These "late" EMPs were distinct from the "early" EMPs, which lack Myb expression and differentiate into macrophages without going through the monocyte stage (Hoeffel et al., 2015). These data suggest that fetal liver progressively replace yolk sac derived cells, and led to the proposal of a new model in which late EMP-derived fetal liver monocytes are the major sources of most tissue resident macrophages, while early EMPs in the yolk sac provide the source for microglia.

In addition to early EMPs in the yolk sac and late EMPs in the fetal liver, fetal HSCs were also proposed to contribute to the generation of resident macrophages. This was based on the c-Kit-CreER model. In this model, E7.5 tamoxifen treatment led to significant amount of labeling in brain microglia but not in the resident macrophage populations from other major organs (Sheng et al., 2015). On the other hand, pulsing at later time points (E8.5 and E9.5) labeled macrophages that are resident in the liver, lung, spleen, kidney, dermis, and peritoneum. Because the kinetics of the labeling coincides with the occurrence of HSCs, these data led to the proposal of fetal HSCs as sources of resident macrophages other than microglia. Moreover, the labeling of other hematopoietic cells, including neutrophils and lymphocytes, led to the

hypothesis that c-Kit+ cells pulsed at E8.5 or E9.5 are HSCs. However, further confirmations of the identity of these cells are still needed to validate this model. Moreover, these data are still consistent with the EMP model.

In addition to embryonically derived populations, regardless of the precise nature of the progenitors, HSCs are also shown to be a significant contributor to many tissue resident macrophages shortly after birth. For example, infiltration of monocytes replenished macrophages in the colon during weaning. This was shown by the decrease of macrophages labeled on E8.5 by CSF1R-CreER concomitant with an increase in Flt3-Cre labeled cells (Bain et al., 2014). This replenishment was stimulated by microbiota in the neonates, suggesting that environmental stimuli could interact with the tissue to shape the ontogeny of local macrophages. While the contribution of perinatal hematopoiesis is best studied in organs that are exposed to the environment, such as the lung and colon, it can also happen in internal tissues, such as the arteries. Unlike the mouse models mentioned above, CX3CR1-CreER does not label significant amount of inflammatory monocytes, therefore allowing the investigation into the contribution of embryonic hematopoiesis to macrophages that do not express CX3CR1. E18.5 labeling in CX3CR1-CreER reporter mice led to the labeling of most macrophages in neonatal arteries. Interestingly, two weeks after birth, a significant portion of artery associated macrophages are replaced by unlabeled monocytes, suggesting the contribution of HSCs to cardiarc macrophages at the neonatal period (Ensan et al., 2016). Similarly, the MHCII+ macrophages in the peritoneum also develop within the first week after birth, in a CCR2-dependent manner, suggesting the perinatal contribution of HSCs to the development of this population (Kim et al., 2016).

Unlike the differentiation of macrophages from adult HSCs, embryonic macrophage differentiation before the formation of fetal liver HSCs does not appears to involve monocyte intermediates (Ajami et al., 2007). A question raised by this model is the mechanisms by which tissue macrophages generated their phenotypic and functional diversity across various organs. One possibility is that the diversity could be generated already upon differentiation at the hematopoietic sites. Variable "clones" of macrophages could be armed with differing repertoire of chemokine receptors that drive their unique migration pathways towards different organs or even different sites within an organ. This "pre-determinism" model resembles the generation of the homing of tissue resident memory T cells, which are activated uniquely in secondary lymphoid sites and home to unique tissues. An alternative but related possibility is that heterogeneous EMP populations give rise to different macrophages that home to their target organs. This model might be unlikely, because the generation of a diverse progenitor population may be costly. However, characterization of EMPs is relatively simplistic. We may underestimate the heterogeneity of the "primitive" progenitors that may exist. Moreover, in all lineage-tracing models mentioned above, the labeling of various mature macrophages populations by a single promoter does not mean they share the same progenitor. E8.5 tamoxifen pulse may label various CSF1R+ progenitors, each of which later gives rise to different resident populations. This "progenitor heterogeneity" model also implies the concept of pre-determined diversity and pre-determined destination.

Alternatively, progenitors such as EMPs could directly differentiate into macrophages, which then settle into embryonic organs or organ primordial, and quickly achieve organ-specific program upon the receipt of tissue specific niche signals. However, to accomplish this "fast maturation", macrophages may also need to develop unique receptors or signaling machineries

that allows them to respond to environmental signals. Another possibility involves the differentiation of embryonic progenitors into intermediate precursors, similar to monocytes in adult hematopoiesis, which then differentiate into macrophages and obtain organ-specific transcriptional program upon tissue entry. This "step-wise diversification" model was supported by the profiling of a $CD45^{+}cKit^{-}Lin^{-}F4/80^{-}$ population, whose surface markers and transcriptional profiles are intermediary between EMPs and mature macrophages (Mass et al., 2016). While these transition-state "pre-macrophages" could explain the generation of phenotypic diversity among tissue macrophages, further studies are needed to validate their existence and contribution to the macrophage ontogeny.

The contribution of multiple progenitors to macrophage ontogeny raised an important "nature vs. nurture" debate. Multiple studies demonstrated a wide range of diversity among various tissue macrophages. Macrophages resident in each tissue seem to demonstrate a distinct signature in terms of transcriptional activities (Gautier et al., 2012), enhancer landscape (Gosselin et al., 2014; Lavin et al., 2014), and chromosome modification profiles. A common theme of these studies is a focus on the importance of environment in the regulation of macrophage activities. To what extent does ontogeny contribute to the shaping of macrophage functionality? Answer to this question requires investigations into macrophages of different origins that co-exist within the same tissue. A number of studies used artificial systems by partially depleting the tissue resident population to induce their replacement by monocytes, followed by profiling the transcriptional signature of monocyte-derived macrophages and remaining tissue resident macrophages. In the lung and peritoneal cavity, macrophages derived from newly recruited monocytes acquired the majority of the majority of the gene signature of their endogenous counterparts. On the other hand, monocyte-derived liver macrophages differ

significantly from Kupffer cells in terms of enhancer signature (Lavin et al., 2014). Similarly, monocyte-derived microglia also had more than 2,000 differentially expressed genes compared from yolk sac-derived microglia (Bruttger et al., 2015). These studies suggest that ontogeny could be one of the determining factors that shape the functional properties of macrophages. However, these data should be taken with caution, because the depletion strategies involve genotoxic irradiation, which could cause alterations in the activities of the endogenous populations, even though tissue resident macrophages may be radiation-resistant. Indeed, several studies have made similar attempts to enforce the recruitment and differentiation of monocytes into tissue resident macrophages, either through shielded irradiation that protects the endogenous population, or through transgenic diphtheria toxin receptor-mediated depletion. In both the lung and the liver, monocyte-derived macrophages resemble their endogenous counterparts, with very little distinction in transcriptional activities that may suggest most overlapping functionalities between cells from different origins (Gibbings et al., 2015; Scott et al., 2016). These contrasted results in how monocyte-derived liver macrophages resembled endogenous Kupffer cells demonstrated how differences in experimental systems could lead to different conclusions, and remind us of interpreting these studies with caution. Another important note is that a lot of these studies looked at macrophages in the tissue as one homogeneous entity. However, each organ is an intricate system with a complicated anatomy; therefore, cells located in different parts of the tissue may behave differently. In the pancreas, monocyte-derived macrophages infiltrate the islets, while embryonically derived macrophages are enriched in the exocrine stroma. Moreover, various subsets of stromal macrophages, as distinguished by the expression of CD206, have different gene expression profile (Calderon et al., 2015). These data suggest the possibility that

ontogeny and signals from different environmental niches may interact with each other to shape the properties of resident macrophages.

It is important to note that the ontogeny of tissue resident macrophages is not static. While embryonically derived macrophages are abundantly populated in almost all organs at birth, many cell populations are replaced by monocyte at various rates. On one end of the spectrum, brain microglia are the first tissue macrophages derived from yolk sac progenitors, and they persist long-term with very minimal contribution from blood monocytes. On the other end of the spectrum, macrophages in the colon and intestine are short lived, and rely on constant replenishment from the blood. The life spans of epidermis Langerhans cells, lung alveolar macrophages, and liver Kupffer cells are more like that of the microglia; dermis MHCII+ macrophages are more like colon macrophages. Macrophages in other organs mostly fall into the middle of the spectrum, including pancreas and heart. How do various tissue resident macrophage populations possess different life span? How do those in the brain, lung alveoli, and liver self-maintain through adulthood and aging? These unanswered questions are also worth addressing.

Another important question is whether ontogeny plays a role in determining the fates of macrophages during various pathological conditions. Macrophages undergo extensive proliferation in Helminth infection, which implies the involvement of tissue resident macrophages in Th2 inflammatory responses against pathogens (Jenkins et al., 2011). Local proliferation also characterizes macrophages within visceral adipose tissues, suggesting that resident macrophages may play a role in the regulation of metabolic diseases (Amano et al., 2014). Not only can resident macrophages participate in the regulation of these pathological conditions, they can also interact with the blood system to promote the infiltration of monocytes

to expand the local macrophage pool. In a *Listeria monocytogenes* infection mode, Kupffer cells undergo necroptosis to recruit monocytes that later differentiate into macrophages (Bleriot et al., 2015). What is the fate of tissue resident macrophages during tumor development? How do they contribute to tumor progression and metastasis? These questions are poorly addressed. In a breast cancer model, mammary gland resident macrophages seemed to disappear while monocyte influx gave rise to tumor-associated macrophages (Franklin et al., 2014). On the other hand, microglia appeared to persist in glioblastoma (Chen et al., 2017) and brain metastasis (Bowman et al., 2016). The limited number of studies suggests that the involvement of tissue resident macrophages in tumor development may be organ- and tumor- specific. One organ of particular interest to us is the pancreas. Pancreatic cancers can arise within either the exocrine or the endocrine portions of the organ; meanwhile, stroma and pancreatic islets are infiltrated with macrophages derived from different sources. It would be interesting to see if different macrophage sources supply TAMs to different kinds of pancreatic cancers. In addition, cancer occurrence in the heart is rare. Since the heart is infiltrated with macrophages of different ontogeny, it is also worth asking if these cells contribute differently to cancer immunosurveillance in this organ.

1.4 Scope of This Dissertation

1.4.1 Outstanding Needs for Improvement of Immunotherapies

Our knowledge of cancer biology is growing at unprecedented speed. In particular, we are increasingly appreciative of the role that the tumor microenvironment plays in the regulation of cancer development and in the utilities of cancer treatment. In parallel, advancement in the development of therapeutics also demonstrates a promising future of cancer treatment by

targeting the tumor stroma. A lot of attention has been paid to the immune components of the cancer environment, with a focus on targeting the adaptive immune system. The advantage is that: (1) the adaptive immune system is capable of combatting cancer in an antigen specific manner, thereby allowing the minimization of side effects due to attacks on healthy cells in the organisms that are necessary for host fitness; (2) memory is the second hallmark of the adaptive immune system, which could build a long lasting anti-cancer arsenal that suppresses tumor reoccurrence. Immunotherapies that activate adaptive immune responses have demonstrated promising potential in multiple types of malignant diseases; in some cases these therapies even showed impressive efficacy at treating late-stage patients with metastasis.

However, these immunotherapies do not work in all types of cancer. For example, checkpoint therapies do not improve patient outcome in pancreatic ductal adenocarcinoma. Moreover, even in responsive cancers such as skin melanoma, large cohorts of patients still do not sufficiently benefit. Therefore, we need a much better understanding of the tumor microenvironment unique in different kinds of tumors and metastasis in order to expand treatment benefits to a much larger group of patients.

Activation of the adaptive immunity is reliant on the innate immune system, in particular myeloid cells. Myeloid cells compose the overwhelming majority of leukocytes and far outnumber the anti-tumor adaptive immune cells. However, tumor-infiltrating myeloid responses are heavily skewed in the tumor to adopt a suppressive phenotype that promotes tumor growth instead of inducing effective anti-tumor responses. Therefore, we need to change myeloid responses in order to optimize therapies that are targeted towards boosting the adaptive immune system. Targeting myeloid components of the tumor stroma is not a new concept in the development of cancer immunotherapies. The prevailing strategy is directed towards reducing

the amount of immune suppression by reducing the quantity of cells. However, such depleting strategies have their own limitations. First, lower *quantity* of suppressive myeloid cells does not equal higher *quality* of immune responses. Second, without understanding the sources of these myeloid cells, depletion of these cells from the tumor stroma could simply induce a positive feedback loop that further enhance their production and recruitment to the tumor site. Therefore, as we develop therapeutic strategies, we may need to change our thinking from *depleting* these cells to *reprogramming* these cells. In addition, we need to better understand the cellular origin that provides these myeloid cells to the tumor tissue, and cut the supply from the source. Furthermore, we can combine the knowledge in both aspects, and design an alternative strategy: first depleting pre-existing suppressive myeloid cells to create vacancies that can later be occupied by new comers, and then programing or conferring these new comers with anti-tumor functions.

1.4.2 Central Questions of This Dissertation

We choose pancreatic ductal adenocarcinoma (PDAC) as a cancer model due to the high lethality and the desperate need for effective immunotherapies. PDAC has a very rich stromal environment, which is very scarce in CD8+ T cells but very extensively infiltrated with myeloid cells that could be utilized for treatment. Our long-term goal is to understand how neoplastic cells in PDAC tissues interact with their microenvironment. The scope of this dissertation focuses on macrophages, one of the most abundant immune cells in PDAC tissue. The quantity and quality of macrophages in PDAC correlate with patient outcome; therefore we aim to develop strategies to reprogram macrophage functions to enable anti-tumor responses. Towards that end, we want to understand: (1) how tumor-associated macrophages (TAMs) polarize

toward pro-tumor or anti-tumor phenotypes, (2) what tumor-derived signals are responsible for programming TAM activities, (3) where do TAMs come from, and (4) how we can utilize the sources of TAMs to alter the myeloid compartment and the adaptive immune responses in PDAC.

Chapter 2: CSF1/CSF1R Blockade Reprograms Tumor-Infiltrating Macrophages and Improves Response to T Cell Checkpoint Immunotherapy in Pancreatic Cancer Models.

Reference:

Zhu Y, Knolhoff BL, Meyer MA, Nywening TM, West B, Luo J, Wang-Gillam A, Goedegebuure SP, Linehan DL, DeNardo DG. CSF1/CSF1R blockade reprograms tumor-infiltrating macrophages and improves responses to T cell checkpoint immunotherapy in pancreatic cancer. *Cancer Research*, 2014, 74 (18): 5057-5069. PMID: 25082815

2.1 Summary

Cancer immunotherapy generally offers limited clinical benefit without coordinated strategies to mitigate the immunosuppressive nature of the tumor microenvironment. Critical drivers of immune escape in the tumor microenvironment include tumor-associated macrophages (TAM) and myeloid-derived suppressor cells (MDSC), which not only mediate immune suppression but also promote metastatic dissemination and impart resistance to cytotoxic therapies. Thus, strategies to ablate the effects of these myeloid cell populations may offer great therapeutic potential. In this report, we demonstrate in a mouse model of pancreatic ductal adenocarcinoma (PDAC) that inhibiting signaling by the myeloid growth factor receptor CSF1R can functionally reprogram macrophage responses that enhance antigen presentation and productive anti-tumor T cell responses. Investigations of this response revealed that CSF1R blockade also upregulated T cell checkpoint molecules, including PDL1 and CTLA4, thereby restraining beneficial therapeutic effects. We found that PD1 and CTLA4 antagonists showed limited efficacy as single agents to restrain PDAC growth, but that that combining these agents with CSF1R blockade potently elicited tumor regressions, even in larger established tumors. Taken together, our findings provide a rationale to reprogram immunosuppressive myeloid cell populations in the tumor microenvironment under conditions that can significantly empower the therapeutic effects of checkpoint-based immunotherapeutics.

2.2 Introduction

Pancreatic ductal adenocarcinoma (PDAC) is one of the most lethal human malignancies. Current therapies are ineffective at treating late stage disease. The few durable responses to therapy seen in PDAC patients are often associated with significant cytotoxic lymphocyte (CTL) infiltration into tumor tissue, suggesting that effective immunotherapy would hold promise to improve patient outcome (1, 2). However, attempts to use immunotherapeutics as single agents have achieved only limited clinical success (3, 4). While multiple factors can contribute to the resistance of PDAC to immunotherapies, one dominant player is the presence of a suppressive immune microenvironment. Critical drivers of this immunosuppressive microenvironment include tumor-associated macrophages (TAMs), monocytic myeloid-derived suppressor cells (Mo-MDSCs), and granulocytic MDSCs (G-MDSCs). These leukocytes can also promote tumor cell proliferation, confer resistance to cytotoxic stress, and facilitate metastatic dissemination (5, 6). Therefore, high numbers of tumor-infiltrating myeloid cells often correlate with early local or metastatic relapse, leading to poor survival in pancreatic cancer patients (7-9). Therapeutics that can reprogram these myeloid responses might overcome immunosuppression to enhance responses to immunotherapy. Previous work by our group and others demonstrated that combining cytotoxic chemotherapy with the blockade of colony-stimulating factor 1 receptor (CSF1R), which is prominently expressed by monocytes, Mo-MDSCs, and macrophages, results in improved anti-tumor T cell responses (10-12). These data suggest that CSF1R blockade could be effective at alleviating local tumor-induced immune suppression and bolstering the response to immunotherapy.

In this report, we investigate the mechanisms by which inhibition CSF1R signaling alleviates immune suppression. We demonstrate that CSF1/CSF1R blockade not only decreases

the number of TAMs, but also reprograms remaining TAMs to support antigen presentation and bolster T cell activation within the tumor microenvironment. This in-turn leads to reduced immune suppression and elevated interferon responses, which restrain tumor progression. However, in response to reduced immune suppression programmed death 1 ligand 1 (PDL1) is up-regulated on tumor cells and cytotoxic T lymphocyte antigen 4 (CTLA4) on T cells. These checkpoint molecules limit the potential of CSF1R inhibition to stimulate anti-tumor immunity. While both programmed cell death protein 1 (PD1) and CTLA4 antagonists demonstrate limited ability to restrain PDAC growth in this mouse model, similar to reported efficacy as single agents in PDAC patients (3, 4). However, CSF1R blockade overcomes these limitations to achieve regression in even well-established tumors. These data suggest that reprogramming myeloid cell responses via CSF1/CSF1R blockade could improve the efficacy of checkpoint-based immunotherapeutics.

2.3 Methods and Materials

Pancreatic cancer tissue microarray cohort and analysis

Tissue microarray (TMA) studies were conducted on surgically resected PDAC specimens from 60 patients diagnosed in the Department of Pathology at Washington University. Patients underwent pancreaticoduodenectomy followed by adjuvant chemotherapy. Fifty-nine of the sixty patients did not receive neoadjuvant therapy. To assemble TMAs, clearly defined areas of tumor tissue were demarcated and two biopsies (1.0-mm diameter) were taken from each donor block. The Washington University School of Medicine ethics committee approved this study. Fully automated image acquisition was performed using an Aperio ScanScope XT Slide Scanner system with a 20× objective (Aperio Technologies) to capture whole-slide digital images. Fluorescent staining analysis was performed using MetaMorph software.

Immunohistochemistry (IHC)

Tissues were fixed in 10% formalin, embedded in paraffin, and dehydrated in 70% ethanol. Five-mm-thick sections were deparaffinized in xylene, rehydrated in graded ethanol, and subjected to antigen retrieval by steam heating in Citra™ antigen retrieval solution (BioGenex). CSF1 was stained with clone 2D10 at 1:100 (Thermo) and detected using indirect immunofluorescence.

Cell lines and constructs

KC cells were derived from PDAC tumor tissue obtained from p48-CRE/LSL-KRas/p53$^{flox/flox}$ mice (backcrossed C57/B6, n=6 by speed congenic) by our laboratory. Kras-INK (KI) cells were obtained from Dr. Hanahan's laboratory (Collisson et al., 2011; Roy et al., 2011). All cell lines

were negative for MAP and mycoplasma. Subsets of these cells were labeled with a polycistronic click beetle red luciferase-mCherry reporters.

Orthotopic model and preclinical animal cohorts

Syngeneic orthotopic PDAC tumors were established by surgical implantation, as previously described (Aaltonen et al., 2009). Briefly, we injected 200,000 cells in 50 µl Matrigel (BD-Biosciences) into each mouse's pancreas. Cohorts of mice were randomized into different treatment groups by either bioluminescence imaging on day 12 or gross palpation of the pancreas. Mice were treated with 50 mg/kg Gemcitabine (GEM; Hospira) by intravenous (i.v.) injection into the right retro-orbital sinus every 4–5 days. Preclinical studies were conducted with 10–15 10-week-old female mice per group. Tumor burden was measured by establishing gross wet weight of the pancreas/tumor and comparing it to that of five parallel mice sacrificed at the beginning of treatment. All studies involving animals were approved by the Washington University School of Medicine Institutional Animal Studies Committee.

CSF1R inhibitors, CSF1 neutralizing antibodies, and checkpoint antagonists

CSF1 neutralizing antibody (clone 5A1, BioXCell) was administered via intraperitoneal (i.p.) injection every 4–5 days, with the 1st injection containing 1 mg and subsequent injections 0.5 mg. CSF1R inhibitors (CSF1Ri) were provided by Plexxikon Inc. PLX3397 is a selective bispecific inhibitor for c-Fms and the c-Kit receptor tyrosine kinases (Artis et al., 2005; DeNardo et al., 2011; Tsai et al., 2008). GW2580 has been described in detail previously (Conway et al., 2005). Both GW2580 and PLX3397 were administered at 800 mg/kg in chow. CTLA4 and PD1

antagonists (clones UC10-4F10 and RMP1-14, BioXCell) were given every 4–5 days at 250 and 200 mg/dose, respectively.

Flow cytometry analysis

Single-cell suspensions were prepared from dissected pancreatic tumors by manual mincing using a scalpel, followed by enzymatic digestion with 3.0 mg/ml collagenase A (Roche) and DNase I (Sigma) for 30 min at 37°C with constant stirring. Digestion mixtures were quenched by 10% fetal bovine serum (FBS), and filtered through 40-μm nylon strainers (Fisher Scientific). Cells were incubated for 10 min at 4°C with rat anti-mouse CD16/CD32 mAb (eBiosciences) at 1:200 dilution. Cells were washed twice in PBS/BSA and incubated for 20 min with 100 μl of fluorophore-conjugated anti-mouse antibodies (CD3e (145-2C11), CD4 (6K1.5), CD8a (53-6.7), CD11b (M1/70), CD11c (N418), CD19 (MB19-1), Ly6C (HK1.4), CD45 (30-F11), CD115 (AFS98), F4/80 (BM8), MHCII (M5/114.15.2), FoxP3 (FJK-16s), CD44 (IM7), CD69 (H1.2F3), PD1 (J43), PDL1 (MIH5), PDL2 (122), CTLA4 (UC10-4B9), IgG2α/κ (eBR2a), (all from eBioscience) and/or Ly6G (1A8, BioLegend), and CD206 (MR5D3, AbDSerotec) using the manufacturers' recommended concentrations. Data acquisition was performed on the LSR-II system (BD Biosciences), and FlowJo software version 9.2 (Tree Star) was used for analysis.

Quantitative reverse transcription-polymerase chain reaction (RT-PCR)

Total tissue RNA was extracted from snap-frozen tumor tissue or lysed tissue culture cells using the E.Z.N.A. RNA Kit (Omega). cDNAs were synthesized using qScript cDNA SuperMix (QuantaBio). Quantitative real-time PCR Taqman primer probe sets specific for TBP, HPRT, GAPDH, CSF1R, CSF1, CCR2, CCL2, CCL5, CCL22, CXCL10, interferon (IFN)-α, IFNβ,

interleukin (IL)-1b, IL10, IL12p35, NOS2, ARG1, TGFβ, EGF, PDL1, PDL2, PD1, and CTLA4 (Applied Biosystems) were used, and the relative gene expression was determined on a StepOne Plus™ Real Time PCR System (Applied Biosystems) using Taqman Gene Expression Master Mix (Applied Biosystems). The comparative threshold cycle method was used to calculate fold changes in gene expression, which were normalized to the expression of TBP, HPRT and/or GAPDH as reference genes.

Flow cytometry analysis

Single-cell suspensions were prepared from dissected pancreatic tumors by manual mincing using a scalpel, followed by enzymatic digestion with 3.0 mg/ml collagenase A (Roche) and DNase I (Sigma) dissolved in Dulbecco's modified Eagle medium (DMEM; Gibco) for 40 min at 37°C with constant stirring. Digestion mixtures were quenched by adding DMEM containing 10% fetal bovine serum (FBS), and filtered through 40-µm nylon strainers (Fisher Scientific). Cells were incubated for 15 min at 4°C with rat anti-mouse CD16/CD32 mAb (eBiosciences) at 1:200 dilution in phosphate-buffered saline (PBS) containing 1.0% bovine serum albumin (BSA; Sigma) to prevent nonspecific antibody binding. Cells were washed twice in PBS/BSA and incubated for 20 min with 100 µl of fluorophore-conjugated anti-mouse antibodies (CD3e (145-2C11), CD4 (6K1.5), CD8a (53-6.7), CD11b (M1/70), CD11c (N418), CD19 (MB19-1), Ly6C (HK1.4), CD45 (30-F11), CD115 (AFS98), F4/80 (BM8), MHCII (M5/114.15.2), FoxP3 (FJK-16s), CD44 (IM7), CD69 (H1.2F3), PD1 (J43), PDL1 (MIH5), PDL2 (122), CTLA4 (UC10-4B9), IgG2α/κ (eBR2a), (all from eBioscience) and/or Ly6G (1A8, BioLegend), and CD206 (MR5D3, AbDSerotec) using the manufacturers' recommended concentrations. This was followed by two washes with PBS/BSA. Either 7-AAD (BD Biosciences) or Live/Dead Blue

(Invitrogen) was used to identify dead cells. Data acquisition was performed on the LSR-II system (BD Biosciences), and FlowJo software version 9.2 (Tree Star) was used for analysis.

Fluorescence-Activated Cell Sorting (FACS)

Cell suspension and antibody staining were prepared as described above. Sorting was performed using the FACSAria-II cell sorter (BD Biosciences) at the FACS Core of Washington University Department of Pathology and Immunology. For gene expression analysis, cells were directly sorted into the TRK lysis buffer (Omega). For all sorting experiments, post-sort analyses were performed to ensure >90% purity.

Gene Signature Survival Analysis

The full gene lists were matched for human-mouse ortholog by the provided gene symbols for human genome annotation (gene symbol and entrez ID); some genes are missing the annotation. The genes with human genome annotation were matched in the public datasets and their expression was matched with outcomes. We used GSE1501 for survival analysis. For each individual gene, the Kaplan-Meier survival curves on the binary gene expression (dichotomized by median as low/high) were generated with log-rank test p-values. Top significant individual genes log rank p-value included ZBP1, OAS3, PTPN6, SFPI1, IRF9, CDH13, SIGLEC1, STAT1, SLC11A1, SH2D2A etc. The up- regulated genes and the down-regulated genes were each centered by mean and scaled by standard deviation. The averaged expression of down-regulated genes (all available genes or the significant genes only from the previous individual gene analysis based on either log-rank test p or Wald test $P<0.05$) were separately calculated. Each sample was categorized into one of the two groups (low, high by median averaged gene

expression), then into one of the three groups (low, medium, high by the 33.33% and 66.67% quantile of the averaged gene expression). The resulting 2 groups and 3 groups classification was each associated with overall survival (OS).

2.4 Results

2.4.1 CSF1 is overexpressed by human PDAC cells.

Previously, we reported that inhibition of CSF1/CSF1R signaling could improve the efficacy of chemotherapy in murine PDAC models by enhancing chemotherapy-induced anti-tumor immunity (Mitchem et al., 2013). However, the mechanisms by which inhibition of CSF1/CSF1R signaling regulates anti-tumor immunity are not well understood. To determine the cellular sources of CSF1 and CSF1R in human pancreatic cancer patients, we analyzed TMAs constructed from 77 cases of invasive PDAC and 4 samples of normal pancreatic tissue. IHC staining showed that CSF1 is frequently, but not exclusively, expressed by malignant PDAC cells (**Figure 2.1A**). In addition, tumors frequently had elevated expression of CSF1 compared to normal tissue. PDAC cells in 70% of tumor specimens exhibited moderate to high levels of CSF1 expression (**Figures 2.1A–C**). By contrast, CSF1R was frequently detected in the tumor stroma, while only ~10% of the tumors examined had CSF1R expression in the epithelial compartment (**Figures 2.1A and D**). These observations are consistent with other reports (Jiao et al., 2012; Pyonteck et al., 2011) and suggest that PDAC tumor cells frequently produce high levels of CSF1.

2.4.2 Inhibition of CSF1R signaling reprograms the tumor microenvironment.

In order to understand the impact of CSF1R signaling on the tumor microenvironment, we compared the gene expression profile of PDAC tumor tissue following treatment with either CSF1R inhibitors (CSF1Ri) or vehicle. Towards this end, we orthotopically implanted KI PDAC tumor cells into syngeneic mice. This cell line produces high levels of CSF1 but does not express

CSF1R (Mitchem et al., 2013). Starting on day 14 post-implantation, we treated mice with either vehicle or the CSF1R tyrosine kinase inhibitor, PLX3397. Additional details on PLX3397 can be found in the Methods section and published elsewhere (Artis et al., 2005; Conway et al., 2005; Schubert et al., 2007; Tsai et al., 2008). Eight days of CSF1Ri treatment resulted in a significant reduction in the number of tumor-infiltrating $CD11b^{+}Ly6G^{-}Ly6C^{Lo}F4/80^{Hi}MHCII^{+}$ macrophages and $CD11b^{+}Ly6G^{-}Ly6C^{Hi}$ monocytes/ Mo-MDSCs, but not $CD11b^{+}Ly6G^{+}Ly6C^{+}MHCII^{Low}$ G-MDSCs (**Figure 2.2A, Figure 2.8**). Microarray analyses of whole tumor tissue mRNA expression revealed 204 downregulated and 158 upregulated genes following CSF1Ri treatment (**Figure 2.2B, Table S1)**. As expected, expression of genes indicative of macrophage infiltration, including *Cd68*, *Mrc1, Msr1,* and *Csf1r*, were decreased in CSF1Ri-treated tumors **(Figure 2.2D)**. The list of downregulated genes was enriched for molecules involved in "inflammatory responses, chemotaxis, myeloid leukocyte-mediated immunity, and proteolysis," consistent with the decreased number of infiltrating macrophages (**Figures 2.2C–D**). The list of upregulated genes was enriched for molecules involved in "antigen presentation, allograft rejection, interferon responses, and T_H1 immunity" (**Figure 2.2C**). This is consistent with the idea that CSF1R blockade can overcome immune suppression. Corresponding to these altered pathways, genes indicative of cytotoxic T lymphocyte (CTL) responses (*Ifng, Cd3e, Cd8a,* and *Prf1*), T cell recruitment (*Cxcl10, Ccl3,* and *Ccl4*), and interferon responses (e.g. *Ifng, Stat1, Irf1,* and *Irf9*) were upregulated (**Figure 2.2E**). Array results were also validated by quantitative real-time PCR (qRT-PCR) on a second set of samples (**Figure 2.2F**). To determine the impact of these alterations, we applied these gene lists to existing gene expression datasets from PDAC patients (Stratford et al., 2010) and found that the core elements of the downregulated gene list were indicative of poor clinical outcomes (**Figure**

2.2G). Taken together, these results suggest that: (1) inhibition of CSF1R signaling in the stromal compartment decreases myeloid responses and reprograms the tumor microenvironment to support T cell-mediated anti-tumor immunity and (2) these changes could improve patient outcomes.

2.4.3 CSF1/CSF1R signal blockade selectively kills CD206^{Hi} TAMs.

To determine how inhibition of CSF1/CSF1R signaling impacts myeloid responses, we treated tumor-bearing mice with CSF1 neutralizing antibodies for 6, 12, 24, or 48 hours or 8 days and analyzed tumor-infiltrating myeloid cell composition and cell death at these time points. Within the first 6 hours of aCSF1 treatment, total TAM numbers began to decrease. By 8 days, TAM numbers had decreased by ~60% **(Figure 2.3B)**. TAMs are a heterogeneous population of macrophages with diverse biological activities (Mantovani, 2008; Mantovani and Sica, 2010; Martinez et al., 2008; Movahedi et al., 2010; Qian et al.). While classical activation of macrophages can restrain cancer development, alternative activation often plays a pro-tumorigenic role (Martinez et al., 2009; Mosser and Edwards, 2008). Distinct surface markers have been used to distinguish between classically and alternatively activated macrophages. Murine PDAC tumors contain a distinct subset of CD206^{Hi} TAMs **(Figures 2.3A, 2.8)**, and their counterparts in human pancreatic cancer have been associated with poor clinical outcomes (Ino et al., 2013). Quantification of CD206^{Hi} and CD206^{Low} TAM subsets revealed that aCSF1 treatment for 8 days led to a >90% depletion of CD206^{Hi} TAMs, while CD206^{Low} TAMs decreased by only ~45% **(Figures 2.3C-D)**. Similar results were seen following CSF1Ri treatment (**Figure 2.3G**). The loss of CD206^{Hi} TAMs could result from either preferential killing of this TAM subset or altered CD206 expression. To distinguish between these possibilities, we

analyzed the kinetics of macrophage cell death. We found that in PDAC tumors, $CD206^{Hi}$ TAMs experienced significantly higher levels of cell death following aCSF1 treatment than $CD206^{Low}$ TAMs **(Figures 2.3C-E)**. These data suggest that $CD206^{Hi}$ TAMs are more sensitive to the CSF1R signal blockade. Consistent with this differential sensitivity, we found that $CD206^{Hi}$ TAMs express higher levels of CSF1R (**Figure 2.3F**). In addition, while total Mo-MDSCs ($CD11b^{+}/Ly6G^{-}/Ly6C^{+}$) did not demonstrate decreased infiltration until after 8 days of aCSF1 treatment, $CD206^{Hi}$ Mo-MDSCs were markedly reduced as early as 12 hours after CSF1 neutralization (**Figure 2.9A**). By contrast, the number of $CD206^{Low}$ Mo-MDSCs, $CD11b^{+}/Ly6G^{+}/Ly6C^{-}/MHCII^{+}$ mature granulocytes, and $CD11b^{+}/Ly6G^{+}/Ly6C^{+}$ G-MDSCs remained unaffected until after 8 days of CSF1/CSF1R blockade (**Figure 2.9B**). Taken together, these data suggest that the blockade of CSF1/CSF1R signaling preferentially, but not exclusively, depletes $CD206^{Hi}$ TAMs and $CD206^{Hi}$ Mo-MDSCs in pancreatic tumors.

2.4.4 CSF1/CSF1R signal blockade reprograms TAMs.

Despite extensive loss of macrophages and Mo-MDSCs, 40-50% of TAMs remain after αCSF1 or CSF1Ri treatment. To determine whether CSF1 blockade reprograms the remaining macrophages to support anti-tumor activities, we FACS sorted TAMs from 8-day vehicle or aCSF1-treated mice bearing established KI tumors and compared their gene expression profiles. TAMs from aCSF1-treated tumors displayed reduced expression of immunosuppressive molecules, including *Pdcd1lg2*, *Il10*, *Arg1*, *Tgfb1*and *Ccl22*. By contrast, anti-tumor immunity genes, such as *Il12a*, *Ifna, Ifnb1, Ifng, Cxcl10*, and *Nos2*, were upregulated (**Figure 2.3H**). We also observed markedly increased surface expression of MHCII after CSF1 or CSF1R inhibition

(**Figure 2.3I**). Taken together, these data suggest that the CSF1/CSF1R blockade reprograms remaining TAMs to support anti-tumor interferon responses and T cell activities.

2.4.5 CSF1/CSF1R signal blockade alters the function of TAMs and dendritic cells.

Based on the observed differences in cytokine profiles among TAMs, we predicted that CSF1/CSF1R blockade might also alter the ability of macrophages to suppress T cell functions. To address this hypothesis, we assessed the immunosuppressive activity and antigen presentation capacity of macrophages in PDAC tumors from mice following CSF1 blockade. Consistent with the reduced expression of immunosuppressive factors (**Figure 2.3H**), we found that fluorescence-activated cell sorted TAMs from 8-day aCSF1-treated mice had significantly reduced ability to block $CD8^+$ T cell activation in *ex vivo* assays (**Figure 2.4A**). These data suggest that the TAMs that remain after CSF1 blockade have reduced immunosuppressive activity.

We also analyzed how CSF1 blockade might impact the number and function of antigen presenting cells (APCs) in the tumor microenvironment. To identify potential APCs in PDAC tumors, we orthotopically implanted mCherry-labeled KI tumor cells. This model allowed us to identify potential APCs by their uptake of tumor antigens, based on their mCherry fluorescence (**Figure 2.4B**, (Engelhardt et al., 2012)). We were able to detect tumor-derived mCherry signal in granulocytes, monocytes, TAMs, and dendritic cells (DCs) (**Figure 2.4B**). The highest levels of mCherry uptake were observed in TAMs and a subset of $CD11b^{low/-}$/Ly6G/C^-/$CD19^-$/$CD11c^+$/$MHCII^+$ cells, presumably lymphoid-like DCs (LyDCs). CSF1/CSF1R blockade did not affect mCherry uptake. Interestingly, unlike in TAMs, CSF1/CSF1R blockade significantly increased the number of tumor-infiltrating LyDCs and their surface expression of MHCII

(**Figure 2.4C, and Figures 2.9C-E**). Because of the high level of tumor antigen uptake by TAMs and LyDCs, we tested the ability of these two cell types to present antigen to naïve $CD8^+$ T cells and stimulate their proliferation. We isolated TAMs and LyDCs from orthotopic KC tumors obtained from mice treated with either vehicle or aCSF1 for 8 days. These leukocytes were then loaded with SIINFEKL peptide and assessed for their ability to activate OT1 T cells. While macrophages and LyDCs isolated from vehicle-treated tumors had very limited ability to activate T cells, aCSF1 treatment significantly enhanced the capacity of these two cell types to induce $CD8^+$ T cell proliferation (**Figure 2.4D**). Taken together, these data suggest that CSF1 blockade alleviates immunosuppressive activities and enhances APC potential in both TAMs and tumor-infiltrating LyDCs.

2.4.6 CSF1/CSF1R blockade modestly increases anti-tumor T cell activity.

To further understand how the blockade of CSF1/CSF1R signaling might reprogram the tumor microenvironment to regulate tumor progression, we assessed alterations in tumor-infiltrating T lymphocytes and tumor growth following CSF1 or CSF1R blockade in established murine PDAC tumors. Mice bearing established (12 days, ~1cm) orthotropic KI or PAN02 tumors were treated with aCSF1 IgGs or CSF1Ri. Tumor progression was modestly reduced by aCSF1 or CSF1Ri treatment as a single agent (**Figures 2.5A–C**). This reduction in tumor growth correlated with increases in $CD3^+CD8^+$ CTLs and $CD3^+CD4^+$ effectors T cells, decreases in $CD4^+$ $Foxp3^+$ T regulatory cells (T_{Reg}s), and significantly improved effector-to-T_{Reg} ratios (**Figures 2.5D–E**). While the majority of tumor-infiltrating $CD8^+$ CTLs had a $CD69^+$, $CD44^+$, and $CD62L^-$ activated phenotype, CSF1R blockade led to a modest increase in both the number of $CD69^+$ $CD8^+$ T cells (65% to 76%) and the level of CD44 expression **(Figure 2.5F)**. The

observed increase in T cell numbers and enhancement of activation status correspond to our results from gene expression profiling in **Figure 1.2**.

2.4.7 CSF1/CSF1R signal blockade alters T cell checkpoint signaling.

Although the CSF1/CSF1R blockade enhanced T cell infiltration, we hypothesized that anti-tumor immunity might be limited via the engagement of T cell checkpoints. We found that approximately 70% of activated CTLs had a high level of PD1 expression, which was unaffected by CSF1R blockade. By contrast, CTLA4 expression on $CD8^+$ CTLs was significantly upregulated by CSF1R inhibition **(Figure 2.5F)**. Along these lines, our array analysis (**Figure 2.2**) showed that *Cd274* (PDL1) was significantly upregulated following CSF1R blockade. We verified these results using qRT-PCR, and found that both *Cd274* and *Ctla4*, but not *Pdcd1lg2* (PDL2), are upregulated in tumor tissues following CSF1 or CSF1R blockade (**Figures 2.6A–B**). These data suggest that while CSF1 blockade reprograms the tumor microenvironment to enhance effector T cell infiltration, engagement of T cell checkpoints is also enhanced.

To determine the cellular sources of these molecules, we analyzed PDL1, PDL2, and PD1 expression on tumor cells and tumor-infiltrating myeloid cells from vehicle- or CSF1Ri-treated mice. We found that TAMs expressed high levels of PD1, PDL1, and PDL2, but consistent with a decreased immunosuppressive capacity, tumor-infiltrating macrophages from CSF1Ri-treated mice had markedly decreased PDL2 and PD1 expression (**Figures 2.6C, 2.6F**). CSF1Ri treatment also decreased the total number of PD1- and PDL2-positive TAMs (**Figure 2.6D**). Similar effects were also seen with aCSF1 treatment (data not shown). Neither Mo-MDSCs nor G-MDSCs expressed significant levels of PDL2. While CSF1R blockade did not alter PD1 or

PDL1 expression in G-MDSCs, PDL1 expression was modestly elevated in Mo-MDSCs following CSF1Ri treatment.

Expression of PDL1, PD1, and PDL2 has been reported on human PDAC tumor cells, potentially allowing them to evade immune surveillance by suppressing T cell function. To determine if CSF1R blockade affects the expression of these molecules on PDAC cells, we used mCherry-expressing KI or KC cells to identify tumor cells *in vivo*. We found that both KI and KC cells express PDL1 at modest levels *in vivo*, but neither cell line expresses PDL2 or PD1 (**Figures 2.6C, 2.6F**, and not shown). However, following CSF1 or CSF1R blockade, the number of $PDL1^+$ tumor cells and overall expression level of PDL1 was markedly upregulated on PDAC tumor cells (**Figure 2.6C, 2.6E**). These observations correspond with the increased mRNA levels of *Cd274* identified by array analysis and qRT-PCR validation (**Figure 2.2, 2.6A)**. Taken together, these results suggest that while CSF1/CSF1R blockade reprograms macrophage responses to bolster CTL responses, this reprogramming also leads to upregulation of PDL1 on tumor cells and CTLA4 on T cells. These checkpoints will likely limit the efficacy of observed anti-tumor immune responses.

2.4.8 CSF1/CSF1R blockade enhances responses to checkpoint immunotherapy.

Based on the above data, we hypothesized that CSF1 or CSF1R blockade could enhance PDAC responses to PD1- and/or CTLA4-antagonist based immunotherapy. To assess this hypothesis, we treated mice bearing established KI tumors with aPD1 or aCTLA4 with or without CSF1Ri in combination with gemcitabine (GEM). PD1 and CTLA4 antagonists in combination with GEM had only limited efficacy at blunting the progression of established tumors (**Figures 2.7A–B**). By contrast, the combination of CSF1R blockade with either PD1 or

CTLA4 antagonists reduced tumor progression by more than 90%. Since combined PD1 and CTLA4 antagonist therapy is being tested clinically for the treatment of both melanoma and PDAC, we also tried this combined therapeutic approach. In the absence of chemotherapy, even combined aPD1/aCTLA4 treatment only limited tumor progression by ~50%. However, the addition of CSF1R blockade to aPD1/aCTLA4 treatment completely blocked tumor progression and even regressed established tumors by 15% (**Figure 2.7C**). When CSF1 blockade was combined with aPD1/aCTLA4 and GEM treatment, we observed complete tumor regression in 30% of animals and an average tumor regression of ~85% (**Figure 2.7D**). Similar results were seen in orthotopic KC tumors, and when the less potent CSF1R inhibitor, GW2850, was used (**Figures 2.7B, 2.10A-B**). Analysis of T cell responses following combined therapy with aCSF1 and aPD1/aCTLA4 antagonists demonstrated increased $CD8^+$ CTL and $CD4^+$ effector T cell infiltration and decreased $CD4^+$ $Foxp3^+$ T_{Reg} numbers (**Figure 2.7E**). In addition, the number of TAMs, Mo-MDSCs, and G-MDSCs decreased following this combined therapeutic regimen (**Figure 2.7F**).

To determine if alterations in tumor burden in CSF1Ri treatment mice were due to increased T cells responses we conducted CD4 and CD8 T depletion studies and found that CSF1R blockade no longer improved checkpoint-based therapy **(Figure 2.7G).** Taken together, these results suggest that CSF1/CSF1R blockade improve checkpoint immunotherapy by enhancing $CD4^+$ and $CD8^+$ T cell activities.

2.5 Discussion

In this report, we show that blockade of CSF1/CSF1R signaling in pancreatic tumors depletes $CD206^{Hi}$ TAMs and reprograms remaining macrophages to support anti-tumor immunity. The blockade alone modestly enhances anti-tumor interferon responses, promotes CTL infiltration, and slows tumor progression. However, the therapeutic effect is limited by the induction of T cell checkpoint molecules, including PDL1 on tumor cells and CTLA4 on T cells. Addition of the CSF1/CSF1R blockade markedly improved the efficacy of aPD1 and aCTLA4 checkpoint immunotherapy and led to the regression of even well-established PDAC tumors. These data suggest that CSF1/CSF1R signaling may be an effective therapeutic target to reprogram the immunosuppressive microenvironment of human PDAC tumors and enhance the efficacy of immunotherapy.

Recent data from several groups suggest that inhibition of CSF1R signaling alters the immunologic responses of tumor-infiltrating macrophages in several cancer types (DeNardo et al., 2011; Mitchem et al., 2013; Mok et al., 2013; Priceman et al., 2010; Pyonteck et al., 2013; Strachan et al., 2013). Mok *et al.* targeted CSF1R signaling using the compound PLX3397 in a murine melanoma model; PLX3397 treatment depleted >80% of TAMs, leaving behind a small population of $MHCII^{Hi}$ macrophages (Mok et al., 2013). These effects led to increased efficacy of adoptively transferred T cell based therapies. These data agree with our report here. In addition, recent work by Pyonteck *et al.* has shown that blockade of CSF1R signaling, using the small molecule inhibitor BLZ945, significantly blunts murine glioma tumor growth by reprogramming macrophage responses (Pyonteck et al., 2013). In contrast to pancreas, melanoma and breast models, macrophage numbers in these murine glioma studies were not reduced. Instead, TAM survival was sustained by tumor-derived factors. However, in glioma,

CSF1R blockade impairs the tumor-promoting functions of TAMs and regresses established tumors. Taken together, these results suggest that CSF1/CSF1R signaling can regulate both the number and the function of TAMs, but these activities may be highly dependent on tumor-type/tissue-specific factors.

One possible mechanism by which CSF1Ri reprograms the remaining TAMs is that CSF1R signaling may promote tumor-promoting macrophage phenotypes, while its blockade polarizes TAMs into the anti-tumor phenotype. In a study by Fleetwood *et al.* , macrophages cultured in CSF1 or CSF2 demonstrated different cytokine profiles and transcription activity(Fleetwood et al., 2007). For example, in response to lipopolysaccharide, CSF2-derived macrophages preferentially produce IL-6, IL-12, and TNFα, while CSF1-derived macrophages produce IL-10 and CCL-2, but not IL-12. These data suggest that the exact cytokine milieu differentially program macrophages to play diverse roles. Intriguingly PDAC tumors can also produce high levels of CSF2 (Bayne et al., 2012; Pylayeva-Gupta et al., 2012), which could reprogram TAMs toward DC-like phenotypes when unopposed by CSF1R signaling.

Alternative to TAMs being reprogrammed by CSF1Ri, another possible mechanism is that CSF1R signaling blockade selects for a subset of tumor-restraining macrophages that are insensitive to the CSF signal kills-off a subset of TAMs that have a pro-tumor phenotype. In many physiological and pathological settings, including cancers, macrophages are composed of heterogeneous subsets of populations with distinct functions (Movahedi et al., 2010). These subsets may depend on different factors for their survival, proliferation, and effector functions. Selection pressure due to CSF1 signal blockade may have enriched for subsets of anti-tumor macrophages in PDAC tissue that are less dependent on CSF1 signaling for their survival. Our analysis of cell death in $CD206^{Hi}MHCII^{Low}$ vs. $CD206^{Lo}MHCII^{Hi}$ TAM sensitivity to aCSF1 IgG

supports this hypothesis **(Figure 2.3B)**. While both $CD206^{Hi}$ and $CD206^{Low}$ TAM populations had detectable cell death upon CSF1 neutralization, the $CD206^{Hi}$ populations were preferentially depleted. The $CD206^{Hi}$ TAM subset had significantly higher CSF1R expression levels, suggesting that this population may be more dependent on the CSF1 signal. Taken together, the heterogeneity of macrophages within the tumor tissue suggests that subsets of TAMs can be targeted to modulate the tumor microenvironment and enhance tumor elimination.

CD206 is expressed in many subsets of myeloid cells other than macrophages, including immature dendritic cells and monocytes (Van Dyken and Locksley, 2013). Whether CD206 expression is correlated to differential activation status in these cell types is not known. Interestingly, $Tie2^{+}$ monocytes almost uniformly express CD206 (Pucci et al., 2009). It remains to be seen whether the loss of $CD206^{Hi}$ tumor-infiltrating monocytes upon αCSF1 treatment (**Figure 2.9A**) involves the $Tie2^{+}$ monocytes and/or affects tumor vasculature.

Although CSF1/CSF1R blockade enhances the anti-tumor activity of myeloid cells and T cell responses, its efficacy can be blunted by upregulation of immune checkpoint molecules, especially PDL1. While tumor intrinsic pathways have been reported to drive PDL1 expression in tumor cells (Le et al., 2013), multiple lines of evidence suggest that PDL1 expression by epithelial tumors is an adaptive response to interferon signaling from tumor stroma. Several groups have reported that IFNγ and IFNα directly lead to the upregulation of PDL1 (Chen et al., 2012; Rowe et al., 2012; Spranger et al., 2013; Terawaki et al., 2011). Consistent with these studies, *in vitro* treatment with recombinant IFNγ markedly upregulated PDL1 expression in our PDAC cell lines (not shown). Given the elevated expression of interferons and interferon response genes in CSF1Ri-treated PDAC tumor tissue, we reason that CSF1Ri-mediated

interferon production might drive the upregulation of PDL1 in PDAC cells, an inherent limitation of this therapy.

Even though T cell checkpoint inhibitors alone have achieved impressive clinical benefits in some other cancers, particularly melanoma (Hamid et al., 2013; Wolchok et al., 2013), their application in pancreatic cancer as single agents has had limited efficacy (Royal et al., 2010). This is potentially due to the immunosuppressive microenvironment of PDAC tissue, which could be alleviated by therapeutic strategies that reprogram dominant myeloid responses to allow for effective checkpoint therapy.

2.6 Figures

Figure 2.1

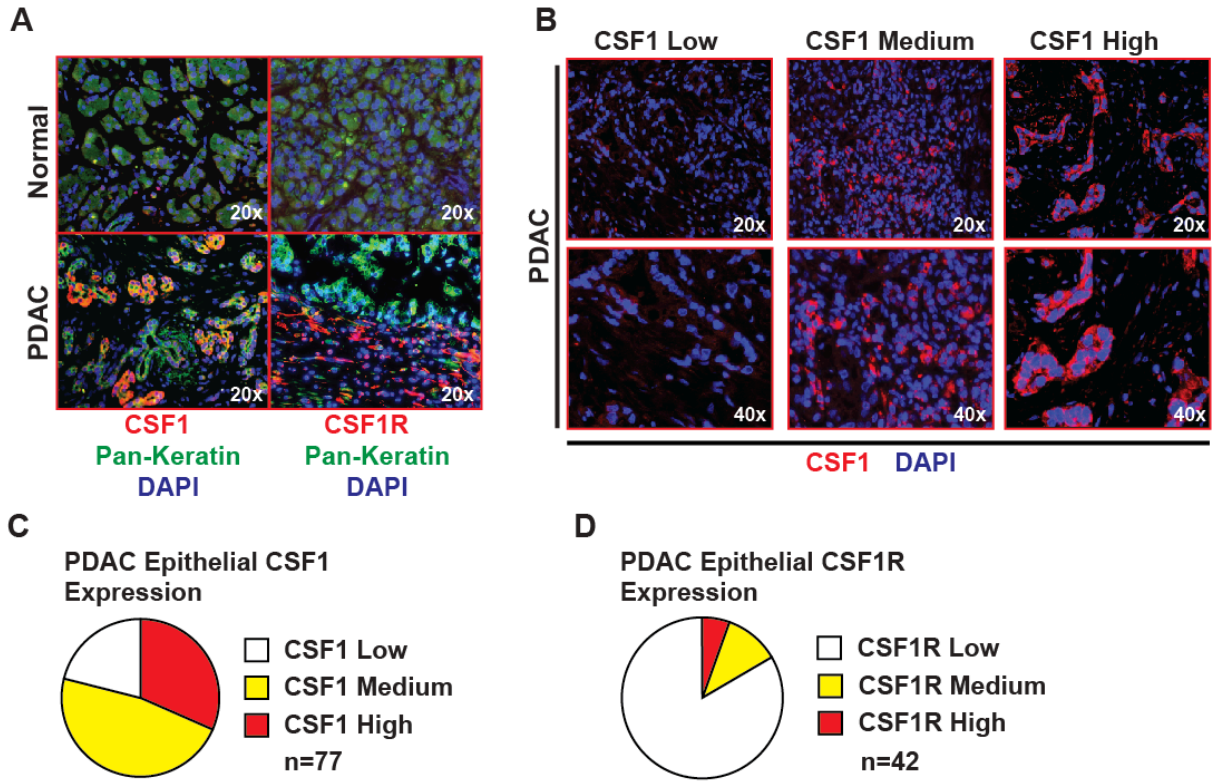

Figure 2.1. PDAC tumors overexpress CSF1.

A–B) Immunohistochemical analysis of CSF1 expression in normal pancreas and PDAC tissue. Representative immunofluorescent images are shown. **C–D**) Stratification of patient PDAC samples based on expression levels of CSF1 and CSF1R (n=4 normal and 77 PDAC).

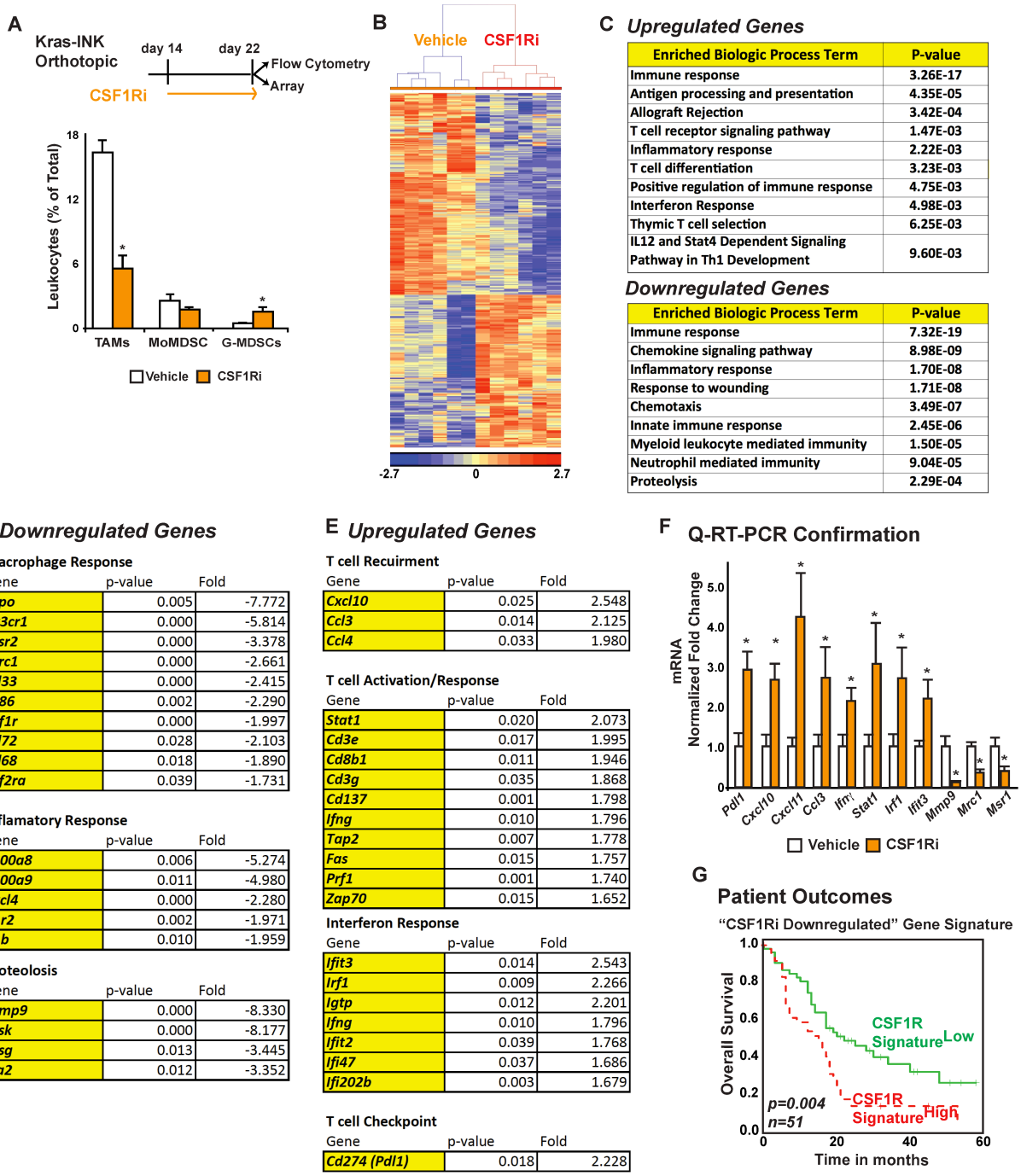

Figure 2.2. CSF1/CSF1R blockade reprograms the tumor immune microenvironment.

A) Leukocyte infiltration in KI tumors from mice treated with vehicle or CSF1Ri (PLX3397) for 8 days. The frequency of $CD11b^{+}CD3/19^{-}Ly6G^{-}Ly6C^{Lo}F4/80^{Hi}MHCII^{+}$ macrophages,

$CD11b^{+}Ly6G^{-}Ly6C^{Hi}$ Mo-MDSC, and $CD11b^{+}Ly6G^{Hi}Ly6C^{+}MHCII^{low/-}$ G-MDSC subsets is depicted as the mean percentage over total live cells.

B) Cluster analysis of differential gene expression (**Table S1**) in vehicle- and CSF1Ri-treated tumors.

C) Table of biologic processes enriched in "upregulated" or "downregulated" genes (DAVID analysis).

D–E) Selected gene sets are displayed with associated biological activities.

F) qRT-PCR analysis of orthotopic KI tumor tissue following treatment with vehicle or CSF1Ri for 8 days. Graph depicts mean fold change compared to vehicle.

G) Kaplan Meier analysis of patient cohorts stratified by expression level of genes down-regulated from the analysis in (B).

In all panels n=4-6 mice/group and * denotes $p<0.05$ (Mann-Whitney U-test), unless specified.

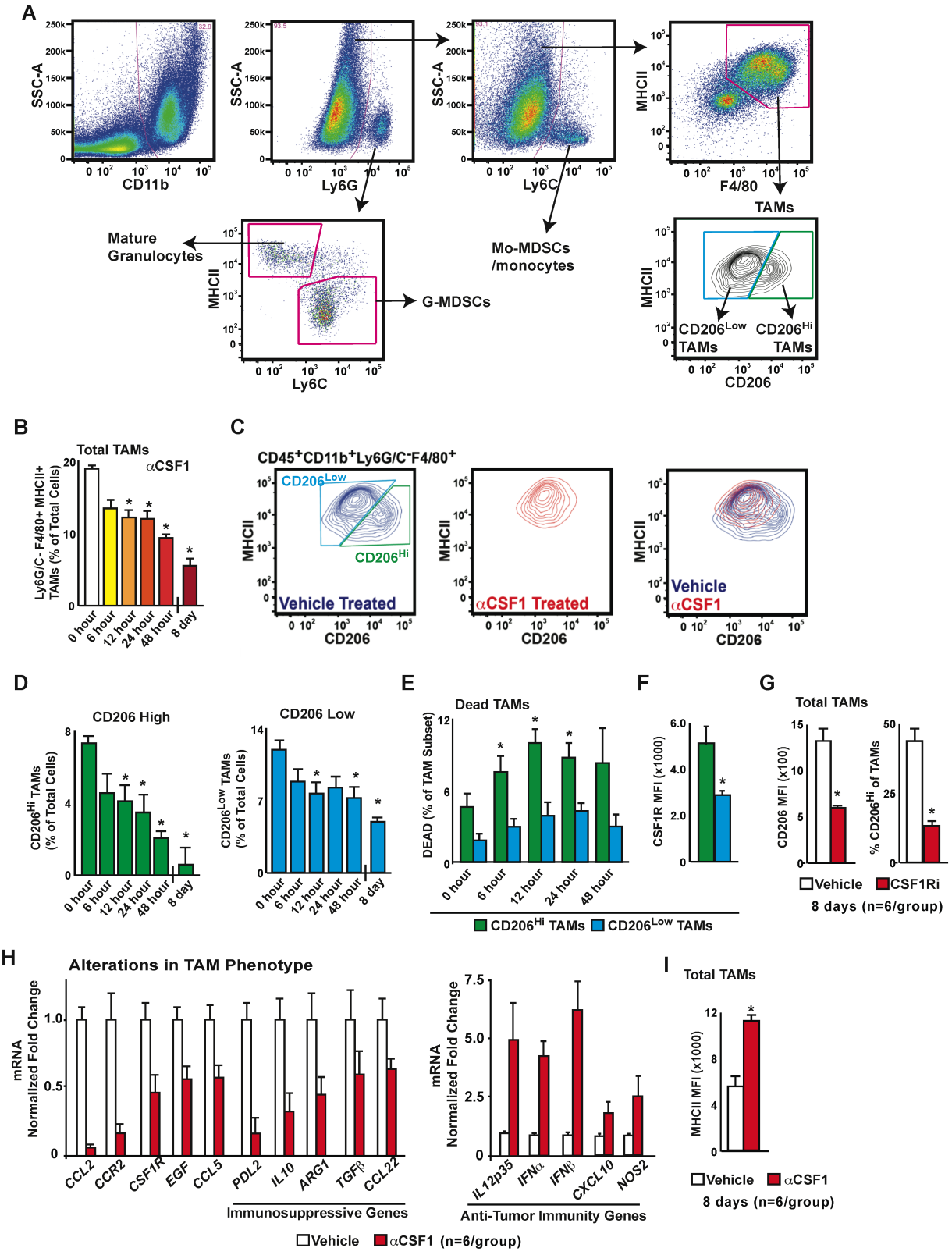
A
SSC-A
CD11b
Ly6G
Ly6C
MHCII
F4/80
TAMs
Mature Granulocytes
G-MDSCs
Mo-MDSCs /monocytes
CD206Low TAMs
CD206Hi TAMs
CD206
B
Total TAMs
αCSF1
Ly6G/C- F4/80+ MHCII+ TAMs (% of Total Cells)
0 hour
6 hour
12 hour
24 hour
48 hour
8 day
C
CD45+CD11b+Ly6G/C-F4/80+
CD206Low
CD206Hi
Vehicle Treated
αCSF1 Treated
Vehicle
αCSF1
D
CD206 High
CD206Hi TAMs (% of Total Cells)
CD206 Low
CD206Low TAMs (% of Total Cells)
E
Dead TAMs
DEAD (% of TAM Subset)
CD206Hi TAMs
CD206Low TAMs
F
CSF1R MFI (x1000)
G
Total TAMs
CD206 MFI (x100)
% CD206Hi of TAMs
Vehicle
CSF1Ri
8 days (n=6/group)
H
Alterations in TAM Phenotype
mRNA Normalized Fold Change
CCL2
CCR2
CSF1R
EGF
CCL5
PDL2
IL10
ARG1
TGFβ
CCL22
Immunosuppressive Genes
IL12p35
IFNα
IFNβ
CXCL10
NOS2
Anti-Tumor Immunity Genes
Vehicle
αCSF1 (n=6/group)
I
Total TAMs
MHCII MFI (x1000)
Vehicle
αCSF1
8 days (n=6/group)

Figure 2.3. CSF1/CSF1R signaling blockade reprograms TAM response.

A) Representative flow cytometry plots with gating strategy to identify mature granulocytes, G-MDSCs, Mo-MDSCs, and TAM subsets.

B-D) Frequency of total, $CD206^{Hi}$ and $CD206^{Low}$ TAMs in orthotopic KI tumors treated with aCSF1 for 6 hours–8 days. Mean percentage of macrophages over total cells is depicted.

C) Representative analysis of MHCII and CD206 expression in TAMs following 8-day treatment with vehicle or aCSF1.

E) Analysis of dead (live/dead blue dye^{+}) $CD206^{Hi}$ and $CD206^{Low}$ TAMs in PDAC tumors from (B).

F) CSF1R expression by MFI in $CD206^{Hi}$ and $CD206^{Low}$ TAMs in vehicle-treated mice from (B).

G) CD206 expression by MFI and $CD206^{Hi}$ TAM number following 8 days of aCSF1 treatment.

H) qRTPCR analysis on $CD11b^{+}Ly6G/C^{-}F4/80^{+}MHCII^{+}$ TAMs sorted from KI tumors following 8-day treatment with vehicle or aCSF1.

I) MHCII expression by MFI in TAMs from (H).

All graphs depict means values or normalized fold change +/-SEM, n=4-6 mice/group and * denotes $p<0.05$ by unpaired t-test or Mann-Whitney U-test.

Figure 2.4

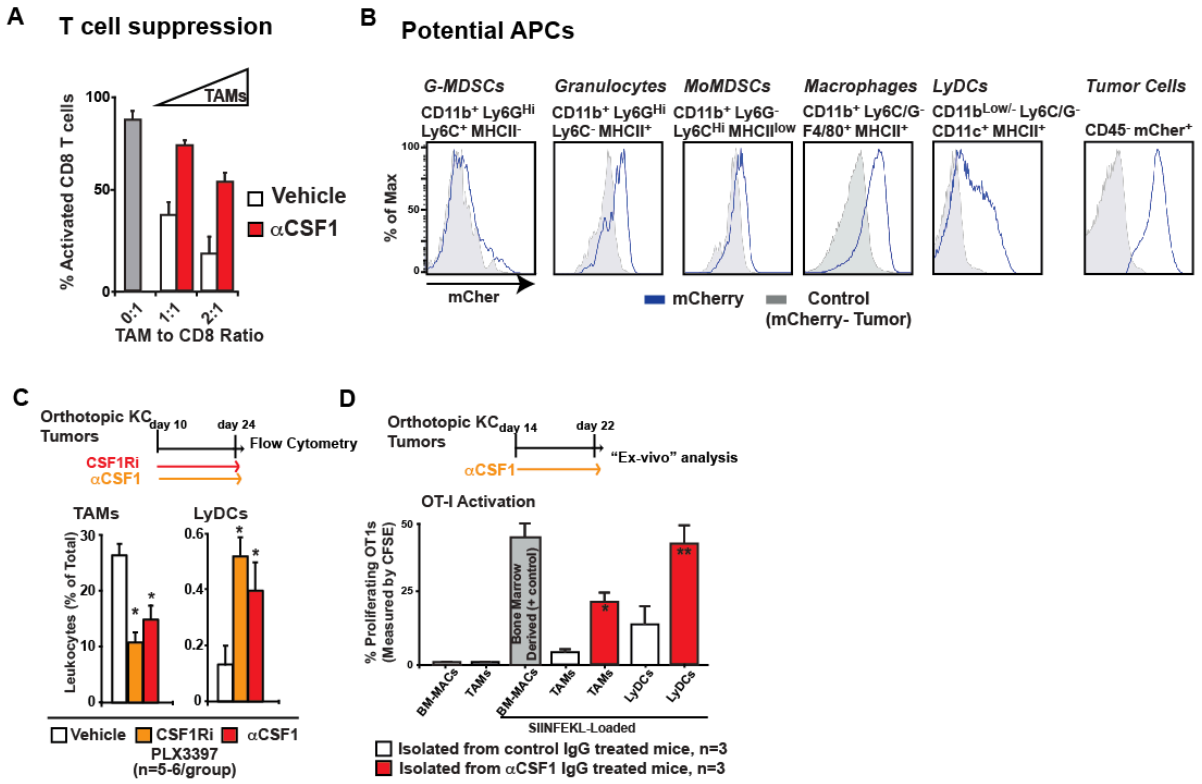

Figure 2.4. CSF1/CSF1R signaling blockade enhances TAM support for CTL responses.

A) Analysis of T cell suppression by TAMs from vehicle- or aCSF1-treated mice. TAMs were isolated by FACS and assayed for their ability to suppress splenic $CD8^+$ T cell proliferation following anti-CD3/CD28 stimulation. The mean number of proliferation cycles is depicted after 70 hours. Representative data from two replicate experiments (n=3 mice/group).

B) Flow cytometry analysis of tumor-derived mCherry fluorescence in tumor-infiltrating leukocytes. Representative plots from 5 mice are depicted.

C) Frequency of $CD11b^+/Ly6G^-/Ly6C^{Lo}/F4/80^{Hi}/MHCII^+$ TAMs and $CD11b^{Low/-}/Ly6GC^-/CD19^-/CD11c^+/MHCII^+$ Lymphoid DCs in orthotopic KI tumors after 8 days of aCSF1 or CSF1Ri treatment.

D) TAMs and LyDCs were isolated by FACS from mice in (C), loaded with SIINFEKL peptide, co-cultured with splenic OT1 cells for 18 hours. OT1 proliferation was measured by CFSE dilution. Results reflect two triplicate experiments using 3 mice/group.

All graphs depict mean values +/- SEM. * denotes $p<0.05$ by unpaired t-test.

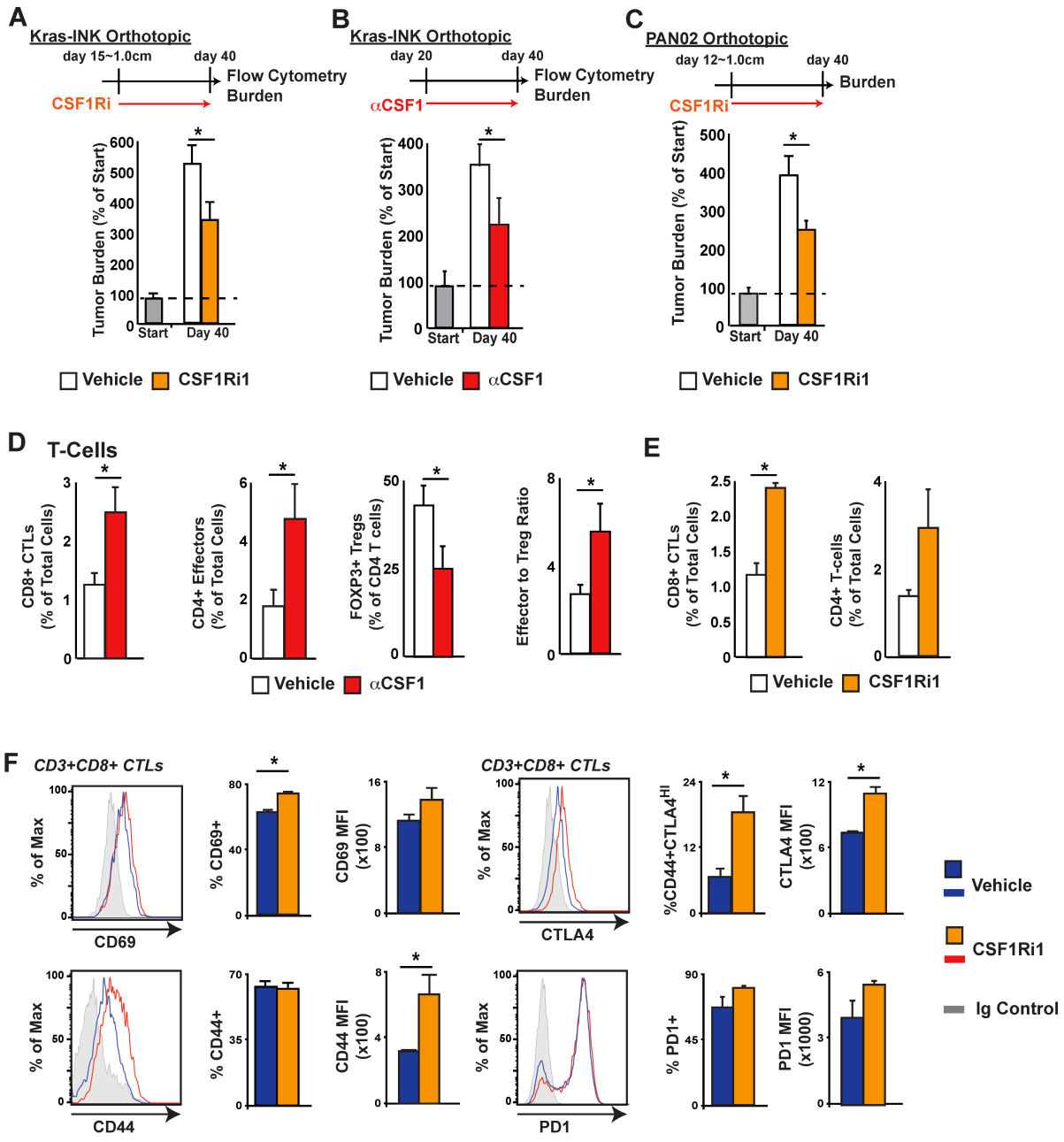

Figure 2.5. CSF1/CSF1R blockade bolsters T cell responses.

A–C) Mice bearing established orthotopic KI or PAN02 tumors were treated with vehicle, CSF1Ri, or aCSF1. Tumor burden is displayed as mean tumor weight (n=10–15 mice/group), normalized to five mice sacrificed at the start of treatment ("R_X Start").

D–E) Analysis of tumor-infiltrating $CD3^+CD8^+$CTLs, $CD3^+CD4^+Foxp3^-$ effector T cells, and $CD4^+Foxp3^+$ T_{reg} from mice in (A–B) is depicted as mean percentage over total live cells (n=6 mice/group). The mean effector (CTL + $CD4^+$ effector)-to- T_{Reg} ratio is also depicted.

F) CD69, CD44, CTLA4, and PD1 expression in $CD3^+CD8^+$CTLs from mice in (A) is depicted as both MFI and percentage of positive cells. Representative plots are depicted.

* denotes $p<0.05$ by Mann-Whitney and n=5-6 in all panels.

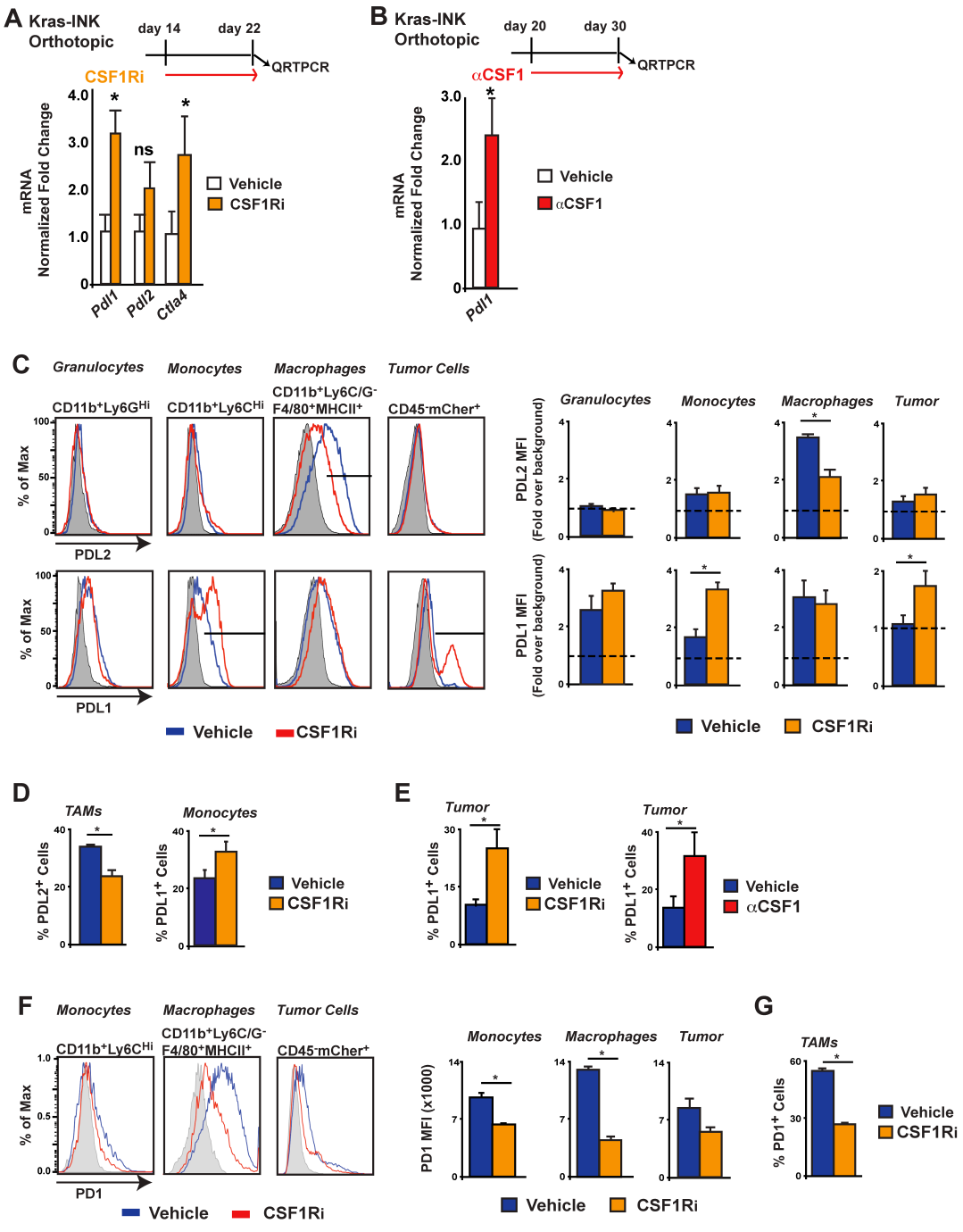

Figure 2.6. CSF1/CSF1R signaling blockade elevates PDL1 expression in tumor cells.

A–B) qRT-PCR analysis of KI tumors following 8-day treatment with vehicle, CSF1Ri or aCSF1. **C)** PDL1 and PDL2 expression in denoted tumor-infiltrating myeloid cells from orthotopic KI tumors treated with vehicle or CSF1Ri. Representative FACS plots and MFI are depicted.

D) Mean percentage of $PDL1^+$ and $PDL2^+$ TAMs and monocytes.

E) Mean percentage of $PDL1^+$ PDAC cells in orthotopic KI tumors from mice treated with vehicle, CSF1Ri, or aCSF1. PDAC cells were identified as $CD45^-$ $mCherry^+$.

F-G) PD1 expression in tumor-infiltrating myeloid cells following vehicle or CSF1Ri treatment. Representative expression plots, MFI and positive cells percentage data are depicted.

All graphs depict means values +/-SEM, n=3-7 mice/group. * denotes $p<0.05$ by unpaired t-test.

Figure 2.7

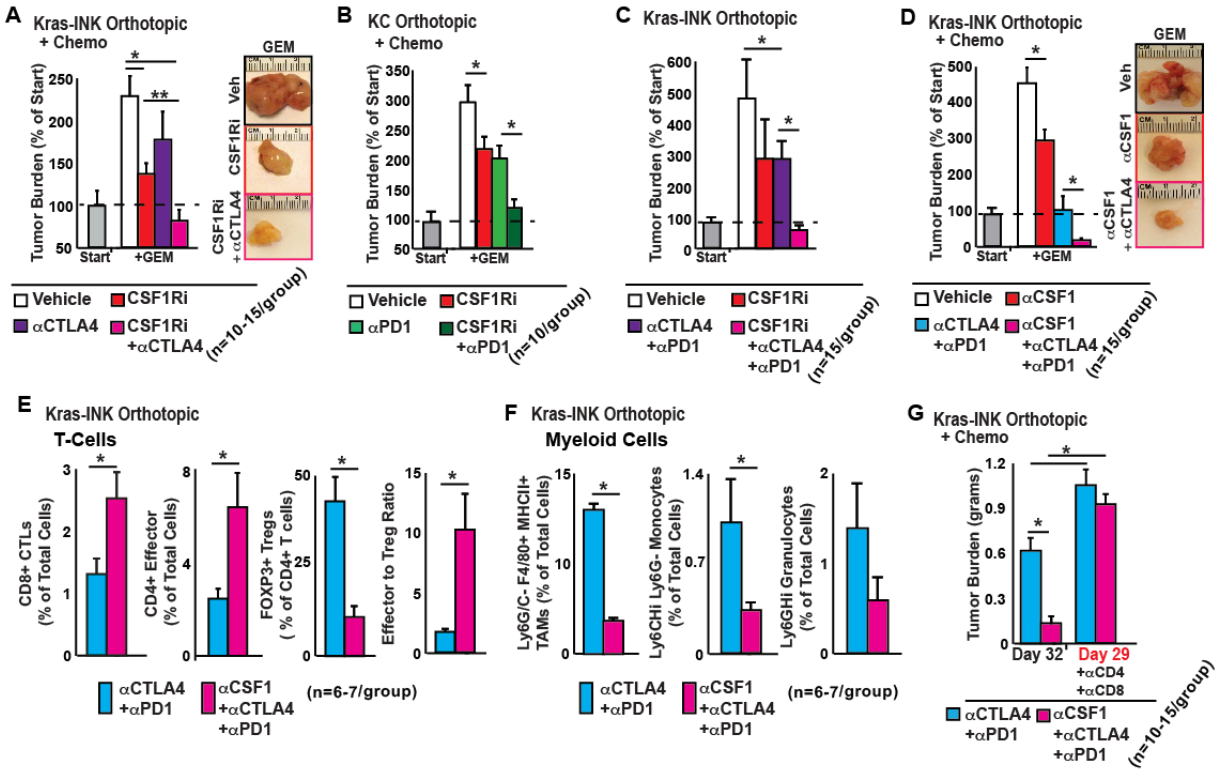

Figure 2.7. CSF1/CSF1R signaling blockade enhances T cell checkpoint immunotherapy.

A–D) Mice bearing orthotopic KI or KC tumors were treated with vehicle, CSF1Ri, or aCSF1, +/- GEM +/- aPD1, and +/-aCTLA4. The tumor burden is displayed as mean tumor weight (n=10–15 mice/group), normalized to five mice sacrificed at the start of treatment ("Start").

E) Frequency of tumor-infiltrating $CD3^+CD8^+$CTLs, $CD3^+CD4^+Foxp3^-$ T effectors, and $Foxp3^+$ $CD4^+$ T_{Reg}s from mice in (D) is depicted as mean percentage of total live cells (n=6 mice/group). Mean effector (CTL + $CD4^+$ effector) to T_{Reg} ratio is depicted.

F) Flow cytometric analysis of tumor-infiltrating $CD11b^+Ly6C/G^-F4/80^+MHCII^+$ TAMs, $CD11b^+Ly6C^+Ly6G^-$ Mo-MDSCs, and $CD11b^+$ $Ly6C^+Ly6G^+MHCII^-$ G-MDSCs from mice in (D) is depicted as mean percentage of total cells (n=6 mice/group).

G) Mice bearing orthotopic KI tumors were treated with GEM, aPD1, aCTLA4, vehicle or aCSF1, +/- aCD4 and aCD8. The tumor burden is displayed as mean tumor weight (n=10-15 mice/group).

All graphs depict mean values +/- SEM and * denotes $p<0.05$ by unpaired t-test and/or Mann-Whitney U-test.

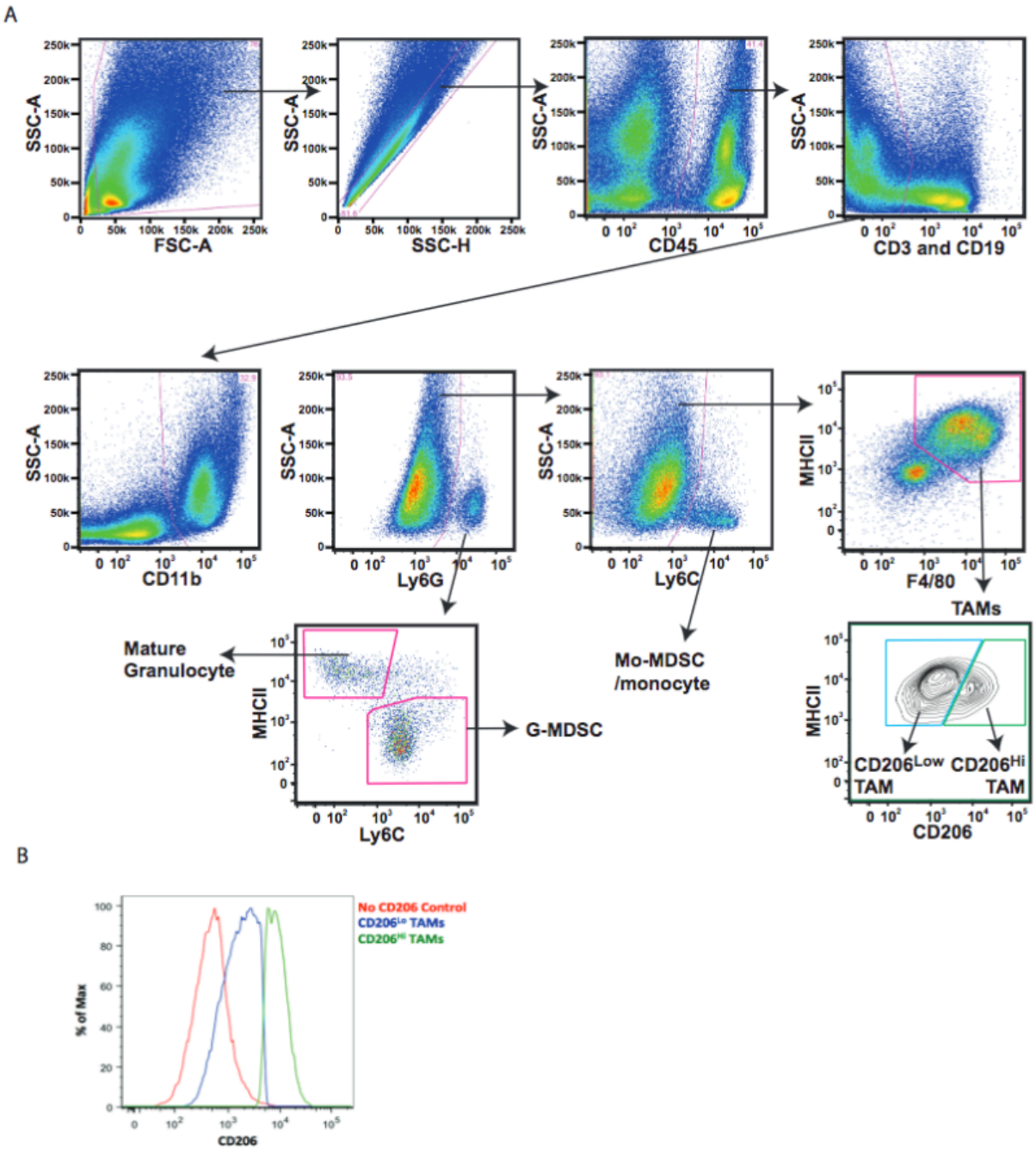

Figure 2.8. Flow cytometric analysis of leukocyte infiltration in orthotopic PDAC tumors.

A) Representative FACS plots with gating strategy to identify mature granulocytes ($CD11b^{+}Ly6G^{+}Ly6C^{-}MHCII^{+}$), G-MDSCs ($CD11b^{+}Ly6G^{+}Ly6C^{+}$), Mo-MDSCs ($CD11b^{+}Ly6G^{-}Ly6C^{+}$), and $CD206^{Lo}$ and $CD206^{Hi}$ TAMs ($CD11b^{+}Ly6G/C^{-}F4/80^{+}MHCII^{+}$).

B) CD206 expression in TAM subsets.

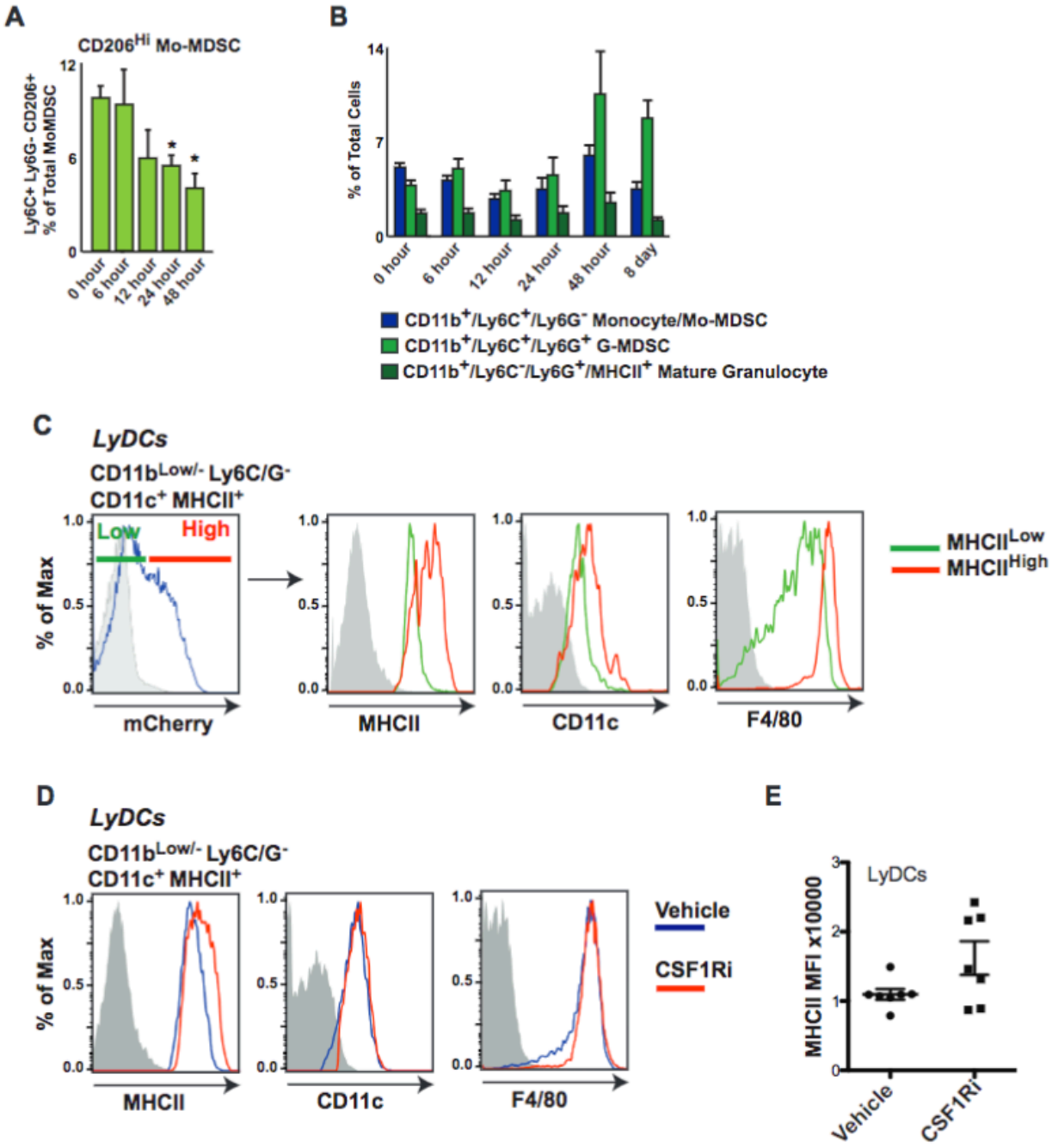

Figure 2.9. CSF1 blockade depletes CD206^{+} Mo-MDSCs and upregulates MHCII expression in Lymphoid DCs.

A) Frequency of CD206^{Hi} Mo-MDSCs in orthotopic KI tumors from mice treated with aCSF1 for 6 hours to 8 days.

B) Frequency of Mo-MDSCs, G-MDSCs, and mature granulocytes in KI tumors from (A).

C) Flow cytometry analyses of MHCII, CD11c, and F4/80 expression in $mCherry^{Low}$ and $mCherry^{Hi}$ tumor-infiltrating LyDCs from $mCherry^{+}$ KI tumor-bearing mice. Representative plots from 6 mice are depicted.

D) Flow cytometry analyses of MHCII, CD11c, and F4/80 expression in tumor-infiltrating LyDCs from orthotopic KI tumors following vehicle or CSF1Ri treatment.

E) MHCII expression in tumor-infiltrating LyDCs from mice in (D) is quantified as MFI.

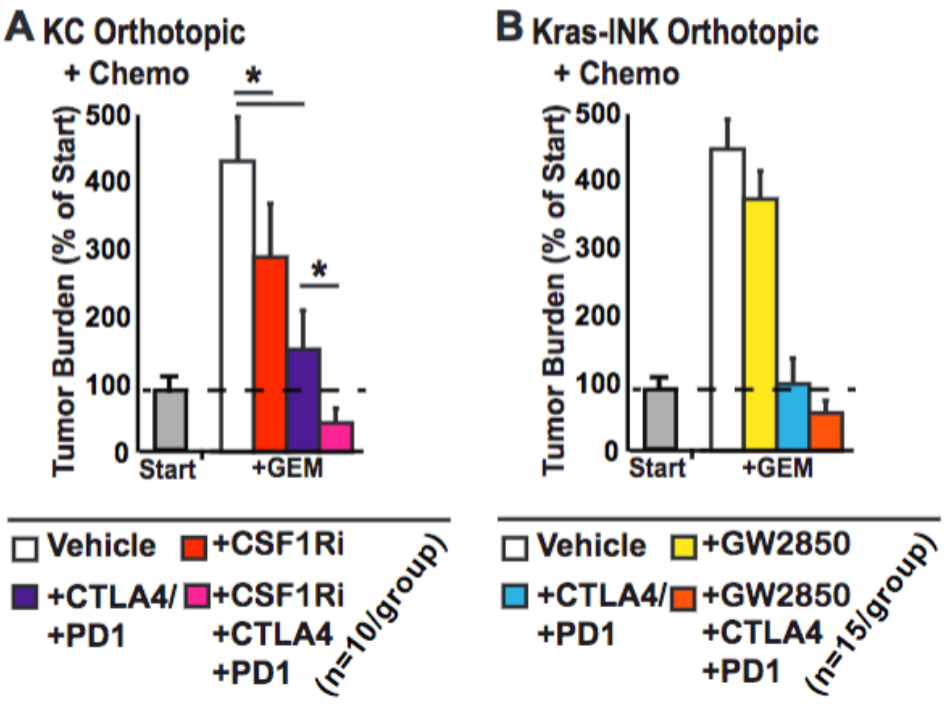

Figure 2.10. CSF1R signaling blockade enhances T cell checkpoint immunotherapy.

A-B) Mice bearing orthotopic KC (A) or KI (B) tumors were treated with vehicle, PLX3397, GW2850, +/- GEM +/- aPD1 and/or aCTLA4. The tumor burden is displayed as mean tumor weight (n=10-15) compared to that of 5 mice sacrificed at the start of treatment ("Start").

Chapter 3: Tissue Resident Macrophages in Pancreatic Ductal Adenocarcinoma Originate from Embryonic Hematopoiesis and Promote Tumor Progression

Reference:

Zhu Y, Herndon JM, Sojka DK, Kim KW, Knolhoff BL, Zuo C, Cullinan DR, Luo J, Bearden AR, Lavine KJ, Yokoyama WM, Hawkins WG, Fields YC, Randolph GJ, DeNardo DG. Pancreatic cancer-associated macrophage subsets have different origin and functions. *(Revision Submitted to Immunity)*

3.1 Summary

Tumor-associated macrophages (TAMs) are essential components of the cancer microenvironment and play critical roles in the regulation of tumor progression. Optimal therapeutic intervention requires in-depth understanding of the sources that sustain macrophages in malignant tissues. In this study, we investigated the ontogeny of TAMs in murine pancreatic ductal adenocarcinoma (PDAC) models. We identified both inflammatory monocytes and tissue-resident macrophages as sources of TAMs. Unexpectedly, significant portions of pancreas-resident macrophages originate during embryonic development and expand through *in situ* proliferation during tumor progression. While monocyte-derived TAMs play more potent roles in antigen presentation, embryonically derived TAMs exhibit a pro-fibrotic transcriptional profile, indicative of their role in producing and remodeling extracellular matrix molecules. Collectively, these findings uncover the heterogeneity of TAM origin and functions, and could provide therapeutic insight for PDAC treatment.

3.2 Introduction

Pancreatic ductal adenocarcinoma (PDAC) is one of the most lethal malignant diseases. Current therapeutic interventions are extremely ineffective in PDAC treatment, partly due to components in the microenvironment that promote tumor growth. Two hallmarks of the PDAC microenvironment are the dense fibrotic stroma and extensive infiltration of myeloid cells, including macrophages. Tumor-associated macrophages (TAMs) are one of the most abundant immune cells infiltrating PDAC. TAMs promote tumor growth by releasing growth factors, inhibiting anti-tumor adaptive immune responses, modifying angiogenesis, and promoting fibrosis, among other mechanisms (Biswas and Mantovani, 2010; Noy and Pollard, 2014; Ruffell and Coussens, 2015). Therefore, high numbers of TAMs correlate with poor patient outcome (Balaz et al., 2002; Ino et al., 2013; Kurahara et al., 2011). Consequently, TAMs are considered a highly desirable therapeutic target (Mantovani et al., 2014; Noy and Pollard, 2014).

Optimal therapeutic strategies targeting TAMs require an in-depth understanding of their ontogeny and the mechanisms governing their homeostasis. The traditional view holds that tissue macrophages are derived from circulating $Ly6C^{Hi}$ monocytes. In the last few years, an increasing amount of evidence suggests that various types of tissue-resident macrophages are established during embryonic development, persist into adulthood, and self-maintain independently of the adult hematopoietic system (Epelman et al., 2014; Ginhoux and Guilliams, 2016; Gomez Perdiguero et al., 2015; Hashimoto et al., 2013; Perdiguero and Geissmann, 2016; Schulz et al., 2012; Varol et al., 2015; Yona et al., 2013). Under homeostatic conditions, macrophages derived from different developmental origins co-exist in many organs. Two notable exceptions are brain microglia, the majority of which are generated during embryonic hematopoiesis at the yolk sac stage (Ginhoux et al., 2010; Hoeffel et al., 2015), and intestinal macrophages, which rely on

continuous replenishment by adult blood monocytes (Bain et al., 2014). Macrophages in many other organs, including the pancreas, have mixed origins (Calderon et al., 2015). A limited number of studies suggest that co-existing macrophages, derived from different developmental origins, have both overlapping and distinct functions within the same tissue (Epelman et al., 2014; Gibbings et al., 2015). However, more studies are needed to address the correlation between the ontogeny and functionality of different macrophage subsets.

Despite the growing body of knowledge of tissue-resident macrophages, monocytes are still often considered as the precursors of macrophages in tumors (Franklin and Li, 2016). Indeed, multiple studies in several tumor models have demonstrated the contribution of circulating monocytes to sustaining TAM numbers. (Franklin et al., 2014; Laoui et al., 2014; Movahedi et al., 2010). In addition to bone marrow, spleen was also shown to serve as an extramedullary hematopoietic site that supplies monocytes to replenish TAM pools (Cortez-Retamozo et al., 2013). However, the contribution of tissue-resident macrophages to TAMs has largely been understudied. Tissue-resident macrophages are known to proliferate *in situ* under pathological conditions (Amano et al., 2014; Jenkins et al., 2011). In addition, *in situ* proliferating macrophages have been observed in human cancers (Campbell et al., 2010). However, it is not known whether proliferation of tissue-resident macrophages contributes to TAM numbers in malignancies.

In this study, we document a previously unappreciated heterogeneity in the ontogeny of TAMs in pancreatic ductal adenocarcinoma. We identify both Ly6C^{Hi} monocytes and tissue-resident macrophages of embryonic origin as sources of TAMs. More importantly, TAMs derived from different origins demonstrate distinct phenotypes and transcriptional profiles, suggesting divergent functionality. While monocyte-derived TAMs are more potent at sampling

tumor antigens and regulating adaptive immune responses, embryonically derived TAMs have higher expression levels of pro-fibrotic genes that encode for extracellular matrix (ECM) and ECM remodeling molecules. These data reveal a potential novel function of embryonically derived macrophages, and suggest a previously unknown interaction between TAMs and the fibrotic PDAC stroma, which could serve as a therapeutic target for PDAC treatment.

3.3 Methods and Materials

Murine PDAC Models

KPC mice (p48-CRE/Lox-stop-Lox(LSL)-$Kras^{G12D}$/$p53^{flox/+}$) used in these studies have been previously described (Hingorani et al., 2005) and were backcrossed to C57BL/6 background and screened for C57BL/6 identity using congenic markers. KPC-1 cell line was derived from PDAC tissues of 2.2-month-old p48-CRE^{+}/LSL-Lox $Kras^{G12D}$/$p53^{flox/flox}$ (KPPC); the KPC-2 cell line was derived from tumors of 6-month-old p48-CRE^{+}/LSL-Lox $Kras^{G12D}$/$p53^{flox/+}$ (KPC) mice. Cells were grown on collagen-coated tissue culture flasks for <12 passages, and were tested for cytokeratin-19, smooth muscle actin, vimentin, and CD45 to verify their carcinoma identity and purity. To establish orthotopic KPC models, either 50,000 or 200,000 KPC-1 or KPC-2 cells in 50 μL of Cultrex (Trevigen) were injected into the pancreas of 6-12-week-old C57BL/6 mice according to published protocol (Kim et al., 2009). For mCherry analyses or bioluminescence imaging (BLI), KPC-1 or KPC-2 cells were infected with mCherry or click beetle red (CBR)-GFP vector respectively. $mCherry^{hi}$ or GFP^{hi} cells were selected by FACS prior to orthotopic implantation.

Other Mouse Models

The following mouse strains were purchased from Jackson Laboratories: $CCR2^{-/-}$, $Nur77^{-/-}$, Rosa26- LSL-eYFP, and Cx3cr1-CreERT2 (all on the C57BL/6 background). Csf1r-Mer-iCre-Mer mice were purchased from Jackson Laboratories, and were crossed to Rosa26-LSL-tdTomato mice, which were a kind gift from Dr. Gregory D. Longmore; both strains are on the FVB background. Flt3-Cre^{tg} mice were a kind gift from Dr. Thomas Boehm and were crossed to Rosa26-LSL-eYFP or –tdTomato mice, all under the C57BL/6 background. Mice were

maintained in the Laboratory for Animal Care barrier facility at Washington University School of Medicine. Washington University School of Medicine Institutional Animal Studies Committee approved all animal studies.

Labeling of Blood Ly6C^{hi} Monocytes

To selectively label Ly6C^{hi} monocytes, 250 uL of liposomes containing clodronate were injected intraveneously (i.v.), followed by i.v. injection of 250 uL of FITC-conjugated plain microspheres 16-18 hours later (1.0 um, 2.5% solids [wt/vol]; Polysciences, diluted 1:4 in PBS). Tissues were processed for flow cytometry analyses at indicated time points after bead injection.

Parabiosis

Parabiotic pairs were generated according to established protocols (Peng et al., 2013) from age- (3.5-month-old) and weight-matched female CD45.2^{+} (KPC or wild-type C57BL/6) and CD45.1^{+} (C57BL/6) mice. Mice were injected with Buprenex subcutaneously after surgery. Sulfatrim was continuously added in drinking water for 10 days post-surgery to minimize infections at surgical wounds. Mice were separated and perfused with phosphate buffered saline (PBS) containing 0.2% heparin. Single cell suspensions from tissues were stained with antibodies for flow cytometry analyses 2 or 6 weeks after the establishment of parabiosis.

Bone Marrow Transplantation

Three and a half-month-old C57BL/6 mice or KPC mice were exposed to γ-irradiation dosed at 1100 rads. Animals were subsequently injected with 2.5 x 10^6 bone marrow cells from CD45.1^{+}

C57BL/6 mice through i.v. injection (retro-orbital or tail vain). Leukocyte chimerism was analyzed 6 weeks later.

Macrophage Depletion

To deplete tissue resident macrophages, 8-16-week old C57BL/6 mice were treated with 3 doses of CSF1 neutralizing antibody (clone 5A1, BioXCell) (1 mg, 0.5 mg, 0.5 mg on Days -18, -14, and -11, **Figure 3**) and 3 doses of clodronate-containing liposome (200 uL/each on Days -17, -13, and -10). Control mice were treated with same doses/volume of IgG (clone HRPN, BioXCell) and liposome (or phosphate buffered saline as indicated). On Day 0, Mice were implanted orthotopically with 200,000 CBR^+ KPC-2 cells or 50,000 CBR^+ KPC-1 cells, and subjected to BLI on Days 3 and 7.

Similarly, KPC and KPPC mice were treated with 2 doses of αCSF1 (0.5 mg each, Day 1 and Day 5) and 2 doses of clodronate-loaded liposome (100 uL each, Day 3 and Day 7) starting at 2.5-month and 1-month of age, respectively. Tumor burden was analyzed when mice reached 4.5 months for KPC mice or 2.0 months for KPPC mice.

To deplete embryonically derived macrophages, C57BL/6 or Flt3-Cre^{YFP} mice were intraperitoneally injected with 3.0 mgs of CSF1R depleting antibody (AFS98 clone, BioXCell) on 13.5 dpc. Surviving mice were implanted with 50,000 CBR^+ KPC-1 at 6 weeks of age. Mice were sacrificed 12 days after tumor establishment for flow cytometry and tumor burden analyses.

Lineage Tracing of Embryonically Derived Macrophages

Timed breeding was set up by crossing Csf1r-Mer-iCre-Mer mice with Rosa26-LSL-tdTomato mice (both on the FVB background). Embryonic timeline was assessed based on vaginal plug

observation: 12pm on the day of plug formation was estimated to be 0.5 day post coitum (dpc). Pregnant mice were treated with tamoxifen (Sigma-Aldrich) (75 μg/g) combined with progesterone (Sigma-Aldrich) (37.5 μg/g) at one of the following time points: 8.5, 9.5, 10.5, or 13.5 dpc. To test the contribution of embryonically derived $CSF1R^{+}$ cells to monocytes or macrophages at homeostatic conditions, tumor-free F1 mice were sacrificed for fate mapping analyses as they reached 6 weeks of age. To test the contribution of embryonically derived $CSF1R^{+}$ cells to TAMs in PDAC tumors, 50,000 syngeneic Kras-INK cells were orthotopically implanted into F1 mice as they reached 6 weeks. Kras-INK cells were derived from p48-Cre/Lox-Stop-Lox (LSL)-$Kras^{G12D}$/Ink4a-$Arf^{lox/lox}$ mice on the FVB background as previously described. Mice were sacrificed approximately 12 days after tumor implantation for the analyses of tdTomato signal in different leukocyte populations.

To trace CX3CR1+ cells, Cx3cr1-CreERT2 mice were crossed with Rosa26-LSL-eFYP mice (both on the C57BL/6 background). Pregnant mice were treated with tamoxifen (75 μg/g) and progesterone (37.5 μg/g) on 13.5 dpc. F1 neonates were fostered by lactating female mice and then aged to 6 weeks for fate mapping analyses.

Mouse Tissue Isolation and Flow Cytometry

Mice were euthanized by intracardiac perfusion using 20 mL of PBS-heparin under isoflurane anesthesia. Tumor tissues and colon were manually minced and digested in 25 mL of Dulbecco's Modified Eagle Medium (DMEM) (Thermo Fisher) containing 2 mg/mL of collagenase A (Roche) and 1X DNase I (Sigma) for 30 minutes at 37˚C with constant stirring. Normal pancreas was digested in the same buffer for 15 minutes at 37˚C. Digestion was quenched in 5 mL of fetal bovine serum (FBS) (Atlanta Biologicals) and filtered through 40 μm Nylon mesh, pelleted

through centrifugation (2000 rpm for 5 min at 4˚C), and resuspended in staining buffer (PBS containing 1% BSA). Brain and spleen were minced and triturated through 40 μm filters.

Single cell suspensions were blocked with rat anti-mouse CD16/CD32 antibodies (eBioscience) (1/200) for 10 minutes, pelleted by centrifugation, and subsequently labeled with 100 uL of fluorophore-conjugated anti-mouse antibodies at recommended dilutions for 20 minutes on ice, and washed with staining buffer. For proliferation assays, mice were injected with 5-bromo-2'-deoxyuridine (BrdU, 1 mg) i.p. 3 hours prior to sacrifice. BD Bioscience Cytofix/cytoperm kit was used to stain for BrdU. eBioscience transcription factor staining buffer set was used to stain for Ki67. Data were acquired on LSR-II (BD Biosciences), and analyzed using FlowJo software (Tree Star). To quantify proliferating/cycling cells in Flt3-Cre^{YFP} mice, tumors were digested as described above, stained with fluorophore-conjugated antibodies for 20 minutes, fixed in 4% formaldehyde for 10 minutes on ice, permeabilized in ice-cold 70% ethanol for 3 hours, stained with Ki67 antibody diluted in staining buffer for 20 minutes on ice, pelleted and resuspended in staining buffer, and immediately processed for data acquisition on LSR-II. To assess hypoxia, Flt3-Cre^{YFP} mice were intraperitoneally injected with pimonidazole hydroxychloride (60 mg/kg) 1 hour prior to sacrifice (Hypoxyprobe). Single cell suspensions were stained with antibodies against pimonidazole adducts for 20 minutes at 4˚C without fixation or permeabilization prior to data acquisition.

To quantitate blood monocytes, 200 uL of blood was obtained by intracardiac puncture prior to perfusion, incubated in red blood cell lysis buffer (BioLegend) for 15 minutes on ice, and stained with fluorophore-conjugated antibodies for 20 minutes on ice**.** Stained cells were counted using LSR-II. For blood analysis that does not require numeration, blood was drawn via tail vein bleeding, followed by RBC lysis, antibody staining, and data acquisition.

Fluorescence-Activated Cell Sorting (FACS)

Normal or tumor-bearing mice (Flt3-Cre^{YFP}, KPC, or C57BL/6 control) were perfused with 20 mL of heparin-containing PBS. Tissues were digested in 25 mL of DMEM containing 2 mg/mL of collagenase A (Roche) and 1X DNase I (Sigma) for 30 minutes at 37˚C with constant stirring. CD45^{+} cells were enriched from single cell suspensions through MACS® magnetic selection using anti-mouse CD45 microbeads (Miltenyi). Elutes were blocked with rat anti-mouse CD16/CD32 antibodies (eBioscience) (1/200) for 10 minutes, pelleted by centrifugation, and labeled with fluorophore-conjugated anti-mouse antibodies at recommended dilutions for 20 minutes on ice. Cells were filtered through 40 μm Nylon mesh, and immediately sorted using Aria-II (BD Biosciences). For microarray analyses and gene expression analyses, cells were sorted directly into RNA lysis buffer (Omega Biotek); RNA was isolated using the EZNA kit (Omega Biotek) according to instructions by the manufacturer. For *ex vivo* assays, cells were sorted into DMEM containing 20% FBS before being pelleted and resuspended for subsequent treatments.

Human PDAC Tissues

Human PDAC tissues were obtained from surgically resected specimens from patients diagnosed in the Department of Pathology at Washington University (St. Louis, MO). Patients underwent pancreaticoduodenectomy followed by adjuvant chemotherapy. Patients did not receive neoadjuvant therapy. Tissues were embedded in paraffin blocks and processed into 6 μm-thick sections for immunofluorescence staining.

For gene expression profiling in PDAC patients, tissues were freshly obtained from 9 patients at pancreaticoduodenectomy, digested into single cell suspension using the protocol described above, stained with indicated antibodies **(Table 3.4)**, and processed for cell isolation using Aria-II (BD Biosciences). Cells were directly sorted into RNA lysis buffer (Omega Biotek). RNA was isolated using the EZNA kit (Omega Biotek) according to instructions by the manufacturer. cDNA was synthesized using the qScript Supermix (Quanta). cDNA targets were pre-amplified for 12 cycles, followed by QPCR analyses (Taqman®, Thermo Fisher). Four out of the nine patients have received neoadjuvant therapies, including FOLFIRINOX or ABRAXANE/gemcitabine prior to being scheduled for resection. All patients were off therapy for 21 days prior to surgery. All tissues were collected under informed consent from patients. Washington University Ethics committee approved the study under IRB protocol #201108117.

PDAC Patient Outcome Analysis

We used top 110 genes whose expressions were >10-fold higher in the mouse Flt3-Cre$^{\text{YFP-negative}}$ TAM subset than the Flt3-Cre$^{\text{YFP-positive}}$ subset. Mouse gene entrez IDs were mapped to human ortholog based on ENSEMBLE 87 annotation using Bioconductor package "biomaRt". Genes were queried in the cbioportal TCGA pancreatic RNA-seq data through the R package "cdgsr" on 178 primary PDAC tumors. For association analysis with survival outcomes, we considered the gene signature using the averaged gene expression across all mapped genes (after centering each by their median). The gene signature was dichotomized by associated median to divide patients into the two groups of over- and under-expression. The Kaplan-Meier method was used to estimate empirical survival probabilities and log rank test to compare survival difference

between patient groups. Hazard ratio from Cox proportional hazard model was reported with 95% confidence interval.

Sirius Red Staining and Immunofluorescence Staining

Tissues were isolated from perfused mice, fixed in 10% formalin overnight, incubated in graded ethanol, embedded in paraffin, and cut into 6 μm-thick sections. To analyze tumor fibrosis, tissue sections were deparaffinized in xylene, rehydrated in graded ethanol, and processed for Picro-Sirius Red staining according to instructions by the manufacturer (Sigma Aldrich). To visualize macrophages in mouse KPC and human PDAC tissues, paraffin sections were steam heated for antigen retrieval in citrate-based buffer (Biogenex), treated with 1% hydrogen peroxide (Invitrogen) for 20 minutes to quench endogenous peroxidase, incubated with blocking buffer (PBS containing 5% goat serum and 2.5% BSA) for 1 hour at room temperature (RT), blocked for biotin/avidin according to instructions by the manufacturer (Vector Labs), and stained with primary antibodies at recommended dilutions at 4˚C overnight (**Table 3.3**). Opal 4-color IHC kit was then used according to instructions by the manufacturer (PerkinElmer). When two antibodies were used for co-staining, FITC and Cy5 were used to minimize emission spectral overlap. To visualize YFP-positive macrophages in Flt3-Cre^{YFP} mice, orthotopic PDAC tissues were fixed in 4% formaldehyde at 4˚C overnight, incubated in PBS containing 30% sucrose and 0.1% sodium azide overnight at 4˚C, and embedded in OCT compound on dry ice. Frozen sections (6 μm-thick) were air-dried, treated with blocking buffer at RT for 1 hour, and stained with CD68 (1/200) (Abcam) overnight, followed by 1 hour incubation with goat anti-rabbit-Alexa594 (1/400) (Molecular Probes) at RT. All sections were washed in PBS containing 0.05%

Tween-20 between incubation steps, and mounted in DAPI-containing media (Vector Labs) for imaging on Nikon 80i microscope.

Statistical Analyses

Statistical analysis was performed using Unpaired Student's t-test, Mann-Whitney U test, Wilcoxon matched-pairs signed rank test, or ANOVA analysis as appropriate for the data set. Data in bar graphs are displayed as means ± SEM. Statistical significance is displayed as * $p<0.05$.

3.4 Results

3.4.1 Pancreatic Ductal Adenocarcinoma Tissues are Infiltrated with Macrophages

High levels of fibrosis and extensive inflammatory cell infiltration characterize the tumor microenvironment of human PDAC. Among the infiltrating cells, macrophages are frequently a dominant component. This can be readily observed by comparing the expression of pan-macrophage/myeloid cell markers CD68, CD163, and CD206 in paired human pancreatic tissue samples containing both PDAC lesions and adjacent normal tissue **(Figures 3.1A-B)**. This increase in macrophage number parallels the levels of tissue fibrosis. While tumor infiltration by macrophages is well characterized, the sources of these macrophages have not been elucidated completely.

To explore the ontogeny of TAMs in PDAC, we analyzed p48-Cre^{+}/LSL-$Kras^{G12D}$/$p53^{flox/+}$ (KPC) genetically engineered mouse models (GEMMs), which undergo stepwise progression through stages of pancreatic intraepithelial neoplasia (PanIN) and ultimately develop PDAC (Hingorani et al., 2005). The KPC model faithfully recapitulates many pathological features of the human disease, including progressive development of stromal fibrosis and extensive accumulation of macrophages **(Figure 3.1C)**. By flow cytometry, we identified $CD45^{+}CD11b^{+}CD3^{-}CD19^{-}Ly6G^{-}Ly6C^{Low/-}F4/80^{+}MHCII^{+}$ macrophages in normal pancreas, autochthonous tumors in KPC mice **(Figure 3.1D)**, and syngeneic orthotopic PDAC tumors established using KPC-derived cancer cell lines (KPC-1) **(Figure 3.8).** In all cases, we confirmed macrophage identity in our gating strategy based on the expression of CD68, MerTK, CD64 (Gautier et al., 2012), colony-stimulating factor-1 receptor (CSF1R), and CX3C chemokine receptor-1 (CX3CR1), but not Siglec-F **(Figur2s 3.1E, 3.8C)**. To confirm the exclusion of dendritic cells (DCs) in our macrophage gating, we established orthotopic tumors in

Zbtb46$^{gfp/+}$ reporter mice (Satpathy et al., 2012), and found minimal GFP signal in the macrophage population compared to DC specific gating strategies **(Figures 3.1E, 3.8D)**. Furthermore, the vast majority of DCs in both normal pancreas and orthotopic PDAC (identified by CD45^{+}Zbtb46-GFP^{+}) express considerably lower levels of macrophage markers, including MerTK, CD64, F4/80, and CX3CR1 **(Figure 3.8E)**, suggesting that pancreas-infiltrating macrophages are phenotypically distinct from DCs. Flow cytometry analyses of tissues from the KPC mouse model demonstrated a 24-fold increase in total number and 5-fold increase in density of macrophages in end-point PDAC compared to normal pancreas **(Figure 3.1F)**. Similarly, macrophage numbers expand in orthotopic PDAC tissues as the tumors progress **(Figure 3.1G)**. Taken together, the dramatic upregulation of the number and density of macrophages in KPC mouse models mimics that seen in human pancreatic cancer. However, the sources of these macrophages are not clearly defined.

3.4.2 Subsets of Macrophages in Pancreas and PDAC Tissues Are Maintained Independently of Blood Monocytes

To test the contribution of blood monocytes to macrophages in tumors, we first performed parabiosis by surgically joining the CD45.2-expressing KPC mice with congenic wild-type mice that express CD45.1. Parabiotic pairs were set up when KPC mice were 3.5 months of age. At this age, KPC mice have developed extensive PanIN lesions, with microscopic evidence of progression to full PDAC. To study the contribution of blood monocytes to macrophages in PDAC, we analyzed chimerism after 6 weeks (at 5 months of age), when disease in KPC mice would have progressed to late-stage PDAC. We also evaluated chimerism in a cohort of mice 2 weeks after the establishment of parabiosis to study the dynamics of

macrophage turnover. We observed 28% chimerism of Ly6C^{Hi} monocytes in the blood of KPC mice within the first 2 weeks, which did not increase further after 6 weeks of parabiosis **(Figures 3.2A-3.2B)**. This level of chimerism was mirrored by tissue-infiltrating Ly6C^{Hi} monocytes in both normal pancreas and KPC tumors **(Figures 3.9A-B)**. However, tissue macrophages in steady-state pancreas only achieved 2.5% chimerism after 6 weeks of parabiosis **(Figure 3.2B)**, suggesting that the majority of macrophages are maintained independently of circulating monocytes during this time period. This level of chimerism was close to what we observed in brain microglia (0.5%), which are known to be locally maintained (Ginhoux et al., 2010; Hoeffel et al., 2015). Interestingly, the chimerism of macrophages present in KPC tumors was only 8.8%, compared to 27% for Ly6C^{Hi} monocytes in the same tissue. These data suggest that while monocytes contribute to the expansion of macrophage numbers during PDAC progression, they might not be the sole source of macrophages in tumor tissues. Additionally, the level of chimerism observed in macrophages in PDAC tissues was comparable after 2 and 6 weeks, in spite of significant increases in macrophage numbers during this time period (**Figure 3.2B**). These data suggest that chimerism reached equilibrium within 2 weeks of parabiosis and that the expansion of TAMs was maintained with equal contributions from both monocytes and other sources.

It is well appreciated that macrophages in tumors exist in subsets with distinct pro-tumor activities. One approach to identity these TAM subsets is based on differential expression of major histocompatibility class (MHC) II (denoted MHCII^{Hi} and MHCII^{Low} here-in) (Movahedi et al., 2010; Zhu et al., 2014). To determine if monocytes replenish these subsets differentially, we analyzed the tumor tissue following parabiosis. We found that the MHCII^{Hi} subset constituted up

to 80% of the donor-derived TAMs, suggesting that monocytes preferentially, but not exclusively, replenish this population over the 6-week time course **(Figure 3.2C)**.

To complement these parabiosis studies, we established bone marrow chimeras by lethally irradiating wild-type CD45.2^{+} mice and adoptively transferring bone marrow cells from CD45.1^{+} wild-type mice. Six weeks after transfer, more than 99% of the immune cells in the blood and the bone marrow of KPC mice were CD45.1^{+} donor-derived **(Figure 3.2D)**. Strikingly, despite potential elimination of radio-sensitive tissue-resident macrophages and the influx of Ly6C^{Hi} monocytes induced by irradiation, 30% of macrophages in the pancreas were host-derived (CD45.2^{+}) **(Figure 3.2D).** In parallel, we lethally irradiated 3.5-month-old KPC mice at the PanIN stage, adoptively transferred bone marrow cells from CD45.1^{+} wild-type mice, and analyzed chimerism 6 weeks later in fully established PDAC. Similarly, a significant portion (>15%) of TAMs in KPC tumors were host-derived, which contrasts with the >99% chimerism detected in circulating monocytes **(Figure 3.2G)**. These data confirmed the existence of pancreas-resident TAMs that were not rapidly replaced by blood monocytes. Consistent with the results of the parabiosis studies, host-derived (CD45.2^{+}) macrophages were preferentially, but not exclusively, MHCII^{Low} in both normal pancreas and KPC tumor tissues **(Figures 3.2E-F, 3.2H)**.

To further assess the short-term contribution of blood monocytes to TAM maintenance, we used fluorescently labeled latex beads to selectively trace Ly6C^{Hi} blood monocytes in tumor-bearing mice, and observed the fluorescent signals in the TAM compartments at 12, 24, 48, and 72 hours after monocyte labeling **(Figure 3.9C**) (Tacke et al., 2006). While fluorescent beads labeled 25% of blood monocytes within 24 hours, which is the peak time for fluorescence detection in blood (Tacke et al., 2006), bead signal was observed in a negligible amount of

macrophages (<0.5%) in normal pancreas **(Figure 3.2I)**, suggesting that the turnover of pancreas-resident macrophages relies minimally on monocyte influx, at least short-term. In orthotopic PDAC, a significantly larger percentage (12%) of TAMs were fluorescently labeled **(Figure 3.2I)**, suggesting that tumors up-regulate the recruitment of circulating Ly6C^{Hi} monocytes to replenish a portion of TAMs. Consistent with BMT and parabiosis results, bead-labeled monocytes almost exclusively replenished the MHCII^{Hi} TAM subset **(Figures 3.2J-K)**, and this replenishment persisted through 72 hours after bead injection **(Figure 3.9D)**.

3.4.3 Impairment of Circulating Monocytes Alone Does Not Impact PDAC Progression

To determine the long-term contribution of blood monocytes to macrophages in the pancreas, we evaluated pancreas and PDAC macrophages in CCR2- and Nur77-defficient mice, which have impairments in circulating Ly6C^{Hi} and Ly6C^{Low} monocytes, respectively (Hanna et al., 2011; Serbina et al., 2008). Despite >95% reduction in the number of circulating Ly6C^{hi} monocytes **(Figures 3.3A and 3.10A)**, the frequency of macrophages in steady-state pancreas was not changed in CCR2-deficient mice **(Figure 3.10B)**. Additionally, while in PDAC tumor-bearing CCR2$^{-/-}$ mice, circulating Ly6C^{Hi} monocytes was still decreased by >95%, PDAC-infiltrating macrophages were decreased by only 50% **(Figures 3.3B and 3.10C)**. Consistent with the results of the monocyte labeling experiments, CCR2 deficiency decreased MHCII^{Hi} TAM frequency, while MHCII^{Low} TAMs were not affected **(Figure 3.3C)**. Surprisingly, while CCR2 deficiency did reduce macrophage numbers, this did not impact tumor growth in two independent PDAC models **(Figures 3.3D and 3.10D**). Similar to these syngeneic PDAC models, there were no changes in tumor burden in KPPC GEMMs treated with CCR2 inhibitors continuously for 45 days **(Figure 3.3K)**.

To address the possibility that Ly6C^{Low} monocytes might contribute to macrophages in PDAC tissues, we analyzed Nur77$^{-/-}$ mice. Similar to data from a previous reports (Hanna et al., 2011), we observed a 75% decrease in circulating Ly6C^{Low} monocyte numbers in Nur77$^{-/-}$ mice, compared to Nur77$^{+/-}$ littermates **(Figures 3.3E and 3.10A)**. However, neither macrophage numbers nor their MHCII-subset distribution was changed in either normal pancreas or orthotopic PDAC tissues **(Figures 3.3F-G).** Additionally, Nur77 deficiency did not impact PDAC tumor growth in three distinct orthotopic PDAC models **(Figures 3.3H and 3.10E**). Together, these data suggest that circulating Ly6C^{Hi} monocytes are important for sustaining MHCII^{Hi} macrophages, but dispensable for tumor progression.

3.4.4 Tissue-Resident Macrophages Promote PDAC Progression

To determine whether tissue-resident macrophages regulate tumor growth, we treated tumor-naïve mice with CSF1 neutralizing antibodies in combination with clodronate-loaded liposomes, followed by a 10-day chase period to allow mice to recover circulating monocyte numbers. Following the 10-day recovery, we found that circulating monocyte numbers in αCSF1/clodronate-treated animals were restored to control/untreated levels **(Figure 3.3I)**. By contrast, pancreas-resident macrophages were depleted as early as 12 hours after injection and remained depleted by 85-95% after 10 days of recovery **(Figures 3.3I and 3.10F)**. These data suggest that this regimen could allow us to test the impact of the loss of tissue-resident macrophages without decreasing circulating inflammatory monocyte numbers. To study how loss of resident macrophages affects tumor progression, we established orthotopic PDAC tumors 10 days after treatment with αCSF1/clodronate or IgG/PBS. We found that loss of resident macrophages prior to tumor implantation resulted in a 50% reduction in TAMs in established

tumors **(Figures 3.3I and 3.10F)**. These data suggest that loss of resident macrophages is not fully compensated for by monocyte-derived TAMs. In contrast to observations in CCR2-null mice, depletion of pancreas-resident macrophages led to a significant reduction in tumor burden, as measured by both bioluminescence imaging (BLI) and tumor wet-weights **(Figure 3.3J)**. These studies were repeated using two distinct KPC-derived PDAC models **(Figure 3.10G)**. To exclude the possibility that the impaired tumor progression was due to deficient tumor "seeding" upon implantation, we treated two genetic PDAC models (KPC and KPPC mice) with αCSF1/clodronate at the premalignant PanIN stage, and analyzed tumor burden after mice developed fully established PDAC. In both KPC and KPPC models, depletion of resident macrophages resulted in significant reduction in tumor burden **(Figures 3.3K)**. By contrast, continuous treatment of KPPC-mice with CCR2 inhibitors during the same time period, in spite of reducing monocyte numbers, did not impact tumor burden **(Figures 3.3K)**. More impressively, analysis of tumor pathology in KPPC mice showed that in addition to reducing overall tumor burden, depletion of resident macrophages dramatically reduced the development of high-grade invasive tumors, which correlated with reduced PDAC cell proliferation **(Figures 3.3L-M)**. Taken together, these data suggest that pancreas-resident macrophages are more critical, compared to monocyte-derived TAMs, in driving PDAC tumor progression.

3.4.5 Embryonically Derived Macrophages are Significant Components of Tissue-Resident Macrophages and Expand During Tumor Progression

To determine whether tissue-resident macrophages are derived from the adult hematopoietic system, we performed lineage tracing using Flt3-Cre^{+}/Lox-Stop-Lox (LSL)-YFP reporter mice (Flt3-Cre^{YFP}). Flt3 is upregulated at the multipotent progenitor stages of

hematopoietic stem cell (HSC) differentiation (Boyer et al., 2011). HSC-derived cells that have gone through the $Flt3^{+}$ stage become labeled as YFP-positive, whereas macrophages derived from embryonic progenitors outside HSCs are YFP-negative (Schulz et al., 2012). To validate this model, we analyzed circulating leukocytes and found that >95.5% of leukocytes in the blood, including both $Ly6C^{Hi}$ and $Ly6C^{Low}$ monocytes, were YFP-positive in both steady-state and tumor-bearing mice **(Figure 3.4A)**. As controls, we analyzed colon macrophages and brain microglia. Consistent with previous reports (Bain et al., 2014; Ginhoux et al., 2010), in adult mice (8-10 weeks old), 93% of the macrophages in the colon were YFP-positive and 98.8% of brain microglia were YFP-negative **(Figure 3.4B)**. In contrast, we observed heterogeneity of macrophage ontogeny in pancreatic tissues, with 32.4% of tissue macrophages labeled as YFP-negative. To determine if this heterogeneity is retained in aged mice, we analyzed 15-month-old Flt3-Cre^{YFP} reporter mice and found that 30% of the macrophages in the pancreas were still YFP-negative **(Figures 3.11A-B).** These data suggest that embryonically derived pancreas-resident macrophages persist with age.

To determine whether these YFP-negative macrophages persist during tumor progression, we established orthotopic KPC tumors in Flt3-Cre^{YFP} reporter mice. Surprisingly, despite the known contribution from circulating monocytes to the tumor macrophage pool, 35.4% of the macrophages in these KPC tumors remained YFP-negative, similar to the frequency in normal pancreas **(Figure 3.4C-D)**. Even more strikingly, the number of YFP-negative macrophages was elevated by >29-fold in tumors compared to normal pancreas **(Figure 3.4E)**. Immunofluorescence analysis also identified clear subsets of both YFP-positive and YFP-negative macrophages in normal pancreas and KPC-derived tumors **(Figure 3.4F)**. These data

suggest that a significant portion of TAMs in PDAC tumors are derived independently of the $Flt3^+$ progenitors, and that these TAMs expand rapidly in number during tumor progression.

The presence of large numbers of YFP-negative macrophages suggests that many TAMs could be derived during embryonic hematopoiesis. Alternatively, these cells could have originated from adult HSCs without going through extensive $Flt3^+$ stages. To distinguish between these two possibilities, we treated Flt3-Cre^{YFP} mice with one dose of a CSF1R antibody (αCSF1R) at 13.5 days post coitum (E13.5) (Hoeffel et al., 2015) to deplete macrophages derived from embryonic sources. We then quantified the abundance of YFP-negative macrophages in the pancreas of F1 progenies as they reached 6 weeks of age. Treatment with αCSF1R on embryonic day E13.5 resulted in 80% reduction in the density of YFP-negative macrophages in steady-state pancreas **(Figure 3.4G)**. To further confirm the contribution of embryonically derived macrophages to TAMs in PDAC, we orthotopically implanted KPC tumor cells in adult mice following αCSF1R treatment on E13.5. Embryonic αCSF1R treatment resulted in a 40-60% reduction in the number of macrophages in established tumors **(Figure 3.4H)**. Additionally, the loss of embryonically derived macrophages led to delayed tumor progression in two distinct syngeneic PDAC models (**Figure 3.4I**). Taken together these data suggest that embryonically derived macrophages facilitate PDAC progression.

To further assess the specific contribution of embryonic hematopoietic progenitors to PDAC TAMs, we administered one dose of tamoxifen in *Csf1r-mer-iCre-mer; Rosa26-LSL-tdTomato* mice at E8.5, E9.5, E10.5, E11.5, or E13.5 to span yolk sac and fetal liver stages. Using this model, we observed that HSC-derived circulating monocytes were labeled at all time points later than E9.5 (**Figures 3.12A-B**). Using E8.5 or E9.5 tamoxifen pulsing, we observed labeling in 4% and 10% of macrophages, respectively, in normal pancreas retained the label as

mice reached 6 weeks of age **(Figures 3.5A-B)**. To confirm this, we used Cx3cr1-CreERT2; Rosa26-LSL-eYFP reporter mice. After administration of tamoxifen on E13.5 at fetal liver stage, the majority of $Ly6C^{Hi}$ monocytes are not labeled (Yona et al., 2013), but we also observed significant labeling in pancreas tissue macrophages **(Figures 3.12C)**. To assess if the embryonically labeled macrophages would expand during tumor progression, we established orthotopic Kras-INK (KI)-derived PDAC tumors in *Csf1r-mer-iCre-mer/ LSL-tdTomato* mice. Consistent with results in Flt3-Cre reporter mice, $tdTomato^{+}$ macrophages labeled with a tamoxifen pulse at E8.5 or E9.5 expanded in number by 6.8- or 13.5-fold, respectively, during PDAC tumor progression **(Figures 3.5C)**. These data suggest that yolk sac-derived macrophages are a significant source of tissue-resident macrophages that undergo significant numerical expansion during tumor progression.

In both CSF1R- and CX3CR1-driven lineage-tracing models, we observed higher levels of labeling in the $MHCII^{Low}$ macrophage subset **(Figures 3.12D-E)**. Similarly, in the Flt3-Cre reporter mice, significantly larger portions of YFP-negative macrophages constitute the $MHCII^{Low}$ subset in both normal pancreas and PDAC tissues **(Figures 3.11C-D).** These results further confirm that embryonically derived macrophages are preferentially but not exclusively enriched in the $MHCII^{Low}$ macrophages. Interestingly, we found that in both HSC-derived and embryonically derived TAMs, the $MHCII^{Low}$ subset experiences higher levels of hypoxia. However, macrophage hypoxia level was independent of origin **(Figure 3.11E-F)**. These data suggest that macrophage origin might drive intrinsic differences in macrophage phenotype and function that can be further molded by conditions in the tumor microenvironment.

3.4.6 Embryonically Derived Macrophages Expand through *in situ* Proliferation

To determine if tissue-resident macrophages undergo expansion through local proliferation, we analyzed Ki67 expression and short-term 5-Bromo-2'-deoxyuridine (BrdU) incorporation in macrophages from normal pancreas and PDAC tissues. Analyses of normal pancreas demonstrated that <1% of macrophages incorporated BrdU following a 3-hour pulse and <3% were $Ki67^+$ **(Figure 3.6A-D)**. These data suggest that pancreas-resident macrophages in steady state are mostly quiescent. On the other hand, >15% of TAMs in either autochthonous KPC PDAC tissues or orthotopic KPC-1 tumors were $Ki67^+$, and 3.5-4% were labeled with BrdU within 3 hours **(Figures 3.6A-D)**. Of note, the 3-hour pulse resulted in no detectable BrdU signal in circulating monocytes **(Figure 3.13A)**, suggesting that BrdU signals in pancreatic macrophages reflect *in situ* proliferation. Confirming these data, immunofluorescence staining also identified a significant portion of $Ki67^+F4/80^+$ cells in autochthonous KPC PDAC tissues **(Figure 3.6C)**, but not in normal pancreas. Interestingly, the majority of these $Ki67^+F4/80^+$ cells localized to fibrotic tumor areas, whereas $F4/80^+$ cells in the tumor nests were mostly Ki67 negative **(Figures 3.6C and 3.13C)**. Consistent with this, macrophages cultured on high-density collagen I gels had higher proliferation rates compared to those cultured on low-density collagen (**Figure 3.13D**), suggesting that there may be cross talks between tumor fibrosis and proliferative expansion of macrophages. Microarray analysis of TAMs from autochthonous KPC tumors demonstrated distinct changes in cell cycle regulatory genes when compared to macrophages in normal pancreas **(Figure 3.6E)**. To assess if embryonically derived TAMs proliferate at higher rates than HSC-derived TAMs, we stained for Ki67 in tumor-bearing Flt3-Cre^{YFP} mice. Embryonically derived TAMs had a significantly higher frequency of Ki67 positivity than their HSC-derived counterparts **(Figure 3.6F)**. This increased level of Ki67 in embryonic TAMs was

independent of their MHCII status (**Figure 3.13B**). In addition, transcriptional profiling by Q-PCR also identified significantly reduced level of genes that negatively regulate cell cycle progression, such as *Mafb* and *c-Maf*, but higher levels of cell cycle promoting genes, such as *Jun* and *Ets2*, in the YFP-negative TAM subset **(Figure 3.6G**). These data suggest that macrophages in PDAC tissues up-regulate proliferative programs, perhaps in response to fibrosis, and that embryonically derived macrophages proliferate at high levels to keep pace with tumor progression.

We next sought to identity what signals sustain the survival of these TAM subsets in PDAC tissues. We took a targeted approach and treated orthotopic PDAC-bearing Flt3-Cre^{YFP} mice with neutralizing antibodies against CSF1 and CSF2, both of which have been implicated in macrophage survival in mouse models of cancer (Hoeffel et al., 2015; Zhu et al., 2014). Although CSF2 signal blockade did not change the number of TAMs, inhibition of CSF1 signaling led to a 48% reduction in the YFP-positive and a 75% reduction in the YFP-negative macrophages **(Figure 3.6H)**. These data suggest that CSF1 is important for the survival of both TAM subsets, but embryonically derived macrophages are more sensitive.

3.4.7 Embryonically Derived TAMs Have a Distinct Pro-fibrotic Phenotype.

Having identified both embryonically derived and HSC-derived monocytes as sources of TAMs in PDAC, we next asked whether distinct macrophage origins correlated with phenotypic differences. Towards that end, we first performed flow cytometry analyses to compare the expression of a panel of cell surface markers in TAM subsets using the Flt3-Cre^{YFP} mice. Both subsets expressed similar levels of macrophage identity markers, including CD64, CD115, and F4/80, whereas YFP-negative TAMs expressed lower levels of CD11b **(Figures 3.7A and**

3.14A), consistent with previous reports of CD11b level in embryonically derived macrophages under homeostatic conditions (Schulz et al., 2012). YFP-negative TAMs also expressed significantly lower levels of MHCI and MHCII **(Figure 3.7A)**. Similar differences were also seen between the two macrophage subsets in normal pancreas **(Figure 3.14B)**, which suggests possibly inherent differences in antigen presentation activities. By contrast, co-stimulatory molecules (CD80, CD86), T cell-activating molecules (CD40), and immune checkpoint molecules (PDL1, PDL2, PD1) were expressed at comparable levels **(Figure 3.7A)**. Embryonically derived TAMs also expressed significantly higher levels of CX3CR1 and lower levels of CD11a and CD49d **(Figures 3.7A and 3.14C)**. Interestingly, despite the lack of CXCR4 expression in either macrophage subset in the normal pancreas, CXCR4 was significantly upregulated in TAMs, but only in the YFP-negative population **(Figure 3.7A and 3.14B)**. Taken together, these data suggest that TAMs derived from different origins are phenotypically distinct.

To gain further insight into potential functional differences between embryonically derived and HSC-derived macrophages, we performed transcriptional profiling on macrophages sorted from Flt3-Cre^{YFP} mice **(Figures 3.7B and 3.14D)**. Only a modest number of genes were expressed differentially between the YFP-positive and YFP-negative macrophages in steady-state pancreas tissue. However, 660 genes were differentially expressed (>1.5 fold, $p<0.05$) between the two subsets in orthotopic KPC tumors, suggesting that TAMs of different origins may have distinct functions in PDAC tumors. Using gene set enrichment analysis, we found that the genes enriched in embryonic-derived macrophages showed a strong trend toward poor survival when mapped to data sets from human PDAC patients (**Figure 3.14E**). Analysis of gene ontogeny demonstrated that embryonically derived macrophages had a higher expression of

molecules involved in extracellular matrix (ECM) deposition and/or remodeling **(Figure 3.7C)**. Indeed, molecules on top of the list of genes that were expressed at higher levels in embryonically derived TAMs were mostly involved in ECM organization (**Table 3.1**). This included genes encoding for ECM molecules (collagen isoforms, nidogen, tenascin C, and elastin), ECM-producing enzymes (hyaluronan synthases 2 and 3), and ECM-remodeling molecules (lysyl oxidase), which we validated using Q-PCR analyses in two independent experiments **(Figures 3.7D and 3.14F)**. To test if the expression of pro-fibrotic genes is related to functional differences in ECM production, we isolated YFP-positive and YFP-negative TAMs from Flt3-Cre^{YFP} mice and tested their ability to produce collagen *ex vivo*. Correlating with their differential expression profiles, we found that embryonically derived TAMs could produce significantly more Collagen I and IV (**Figure 3.7F**). To correlate these *ex vivo* results to *in vivo* impact, we analyzed collagen density in PDAC tissue from mice treated on E13.5 with αCSF1R or control IgGs and compared these results to CCR2-deficient mice. We found embryonic macrophage depletion led to reduced collagen deposition. By contrast, CCR2-deficient mice had slightly elevated collagen levels compared to control mice (**Figure 3.14G**). These data suggest that macrophages of different origins have differential impacts on fibrosis.

To rule out the possibility that the identified YFP-negative cells contained fibroblasts instead of macrophages, we compared cancer-associated fibroblasts (CAFs) to YFP-negative TAMs. We found that CAFs expressed platelet-derived growth factor receptor-a (PDGFRa), but not CD45, F4/80, or CD11b, whereas YFP-negative TAMs demonstrated the opposite pattern **(Figure 3.14H)**. Similarly, the mRNA expression levels of macrophage/myeloid identity genes (*Emr1*, *Itgam*, *Csf1r*, *Csf2r*, and *Cx3cr1*) were comparable in both YFP-positive and YFP-negative TAMs, as determined by Q-PCR analysis, and were 10- to 1000-fold higher in both

subsets of TAMs as compared to CAFs **(Figure 3.14I**). These data confirm that the YFP-negative cells were not fibroblasts but were a macrophage subset with a unique pro-fibrotic phenotype. To evaluate how the pro-fibrotic gene signature in embryonically derived TAMs differed from that in CAFs, we compared selected fibrosis genes by Q-PCR. As expected, CAFs were the dominant producers of several isoforms of collagens (such as *Col1a2* and *Col3a1*), *Elastin*, and *Sparc* **(Figure 3.14J)**. However, mRNA for other ECM molecules, such as *Col6a1*, *Nidogen*, and *Adamts12*, were expressed at comparable levels. In contrast, embryonically derived TAMs were the more dominant expressers of *Col4a4*, *Col10a1*, *Col17a1*, *Col18a1, and Has3* **(Figure 3.14J)**. Taken together, these data suggest that embryonically derived TAMs may be more involved in "fine-tuning" fibrotic responses in PDAC tumors.

In contrast to pro-fibrotic genes, the levels of mRNA involved in class I and class II antigen presentations (*Erap1*, *Psme1,* and *Ciita*) were higher in HSC-derived TAMs **(Figure 3.7E)**. To test the antigen uptake capacity in TAMs subsets *in vivo*, we orthotopically implanted $mCherry^+$ KPC-1 PDAC cells and determined the mCherry positivity in TAMs. Although both TAM subsets demonstrated potent capacity to uptake tumor antigen, the amount of antigen uptake was >2-fold higher in HSC-derived TAMs compared to their embryonic counterparts **(Figure 3.7G)**. We next tested the ability of each TAM subset to present antigen (ovalbumin) to $OT1^+$ $CD8^+$ T cells and found that HSC-derived (YFP+) TAMs were far more potent at antigen presentation compared to their embryonically derived (YFP-) counterparts. In addition, HSC-derived TAMs expressed significantly higher levels of *Il12a*, *Il4*, *Ccl17*, and *Ifnb1* compared to their embryonic counterparts **(Figure 3.7E)**. Taken together, these data suggest that TAMs derived from HSCs and embryonic sources likely play more potent roles in regulating adaptive immunity and/or driving immune tolerance. This is consistent with previous reports showing that

monocyte-derived TAMs regulate immunosuppression in PDAC models (Beatty et al., 2015; Mitchem et al., 2013; Sanford et al., 2013) and in early phase clinical trials (Nywening et al., 2016).

3.4.8 Subsets of TAMs in Human PDAC Tissue Resemble Murine Embryonically Derived TAMs

To address whether the identification and characterization of embryonic TAMs in murine PDAC models is relevant for human cancer, we took advantage of the observation that CXCR4 was almost exclusively upregulated in murine embryonic TAMs (**Figure 3.7A**). We first evaluated human PDAC tissues for $CXCR4^+$ TAMs and found that 10-40% of TAMs expressed high levels of CXCR4 (**Figure 3.7I**). We also noted that these $CXCR4^+$ TAMs expressed lower levels of HLA-DR in eight out of nine patients evaluated (**Figure 3.7J**). These results are consistent with our observation that $CXCR4^+$ TAMs of embryonic origin expressed lower levels of MHCII in murine PDAC models. To determine if this subset of human PDAC TAMs shared the pro-fibrotic gene expression profile we identified in mice, we isolated CXCR4-positive and negative TAMs from PDAC tissues from three untreated surgical patients and performed Q-PCR analyses. Consistent with our animal model data, we found that $CXCR4^+$ TAMs expressed significantly higher levels of Collagens and ECM-modulating molecules compared to their CXCR4-negative counterparts **(Figure 3.7K)**. Collectively, these data suggest that $CXCR4^+$ TAMs in human PDAC resemble the ECM regulatory phenotype of murine embryonically derived PDAC TAMs.

3.5 Discussion

Ontological origins of tissue macrophages vary among different tissues under steady state. With the exception of brain and intestine, many other organs contain macrophages of different origins co-existing within the tissue context. Consistent with previous reports (Calderon et al., 2015), our study demonstrated that pancreas-associated macrophages contain cells derived from both adult HSCs and embryonic hematopoietic sources. The precise nature of embryonic hematopoietic progenitors that gave rise to these macrophages needs to be defined; likely sources include yolk sac-derived erythro-myeloid progenitors (EMPs) (Gomez Perdiguero et al., 2015) and EMP-derived fetal monocytes (Hoeffel et al., 2015). The origin of HSC-derived macrophages in normal pancreas is also unclear; possible sources include fetal liver HSCs and bone marrow HSC-derived monocytes that may populate the pancreas perinatally. Regardless of developmental origin, significant portions of macrophages in the pancreatic stroma are likely resident in the tissue without rapid replenishment from circulating monocytes. The majority of pancreas-resident macrophages are quiescent under steady state, suggesting that these cells may self-maintain through longevity. It is also important to note that the ontogeny of tissue-resident macrophages is not static. Embryonically derived macrophages in multiple organs have shown various degrees of replacement by monocytes with different kinetics (Bain et al., 2016; Ginhoux and Guilliams, 2016; Molawi et al., 2014). Our study using aged mice demonstrated that embryonically derived macrophages could persist long-term in the pancreas, despite potential slow replacement by blood monocytes that we cannot rule out. It remains to be seen if and to what extent could embryonically derived macrophages persist in aged human patients.

Fates of tissue-resident macrophages vary under different pathological conditions. For example, liver resident Kupffer cells undergo necroptosis during *Listeria monocytogenes*

infection, which recruits monocytes to replenish macrophages (Bleriot et al., 2015). On the other hand, tissue macrophages undergo *in situ* proliferation during helminth infections (Jenkins et al., 2011). Very few studies have looked at the fate of tissue-resident macrophages during cancer progression. One report documented a loss of resident macrophages concomitant with the increase in monocyte-derived TAMs in a breast cancer model (Franklin et al., 2014). On the other hand, microglia were shown to be present in brain tumor models (Bowman et al., 2016; Hambardzumyan et al., 2016). Here, we demonstrated that in PDAC, embryonically derived tissue-resident macrophages not only persisted in the tissue, but also underwent significant proliferative expansion to keep pace with tumor progression. TAMs in the PDAC tissues adopted a transcriptional program to enhance proliferation, and embryonically derived tissue-resident macrophages further enhanced their proliferative programs compared to the monocyte-derived counterparts. Of note, PDAC also upregulated the proliferation of monocyte-derived macrophages, similar to what is seen in other cancers and tissue repair (Franklin et al., 2014; Wang and Kubes, 2016); though their proliferative activities were less robust than those in the embryonically derived macrophages. Factors that sustain and promote *in situ* proliferation in different TAM subsets, as well as the cellular sources of these factors, have yet to be identified. It also remains to been seen to what extent would these observations hold true in other tumors or if this feature is enriched in PDAC due to its uniquely fibrotic nature. One tumor type of interest is pancreatic neuroendocrine tumors (PNET), which originate from the islets of Langerhans. Under steady state, macrophages in the pancreatic islets are maintained by blood monocytes, whereas stromal macrophages are embryonically derived and locally maintained (Calderon et al., 2015). It would be interestingly to see whether PNET contrasts with PDAC and relies on circulating monocytes to sustain TAMs in-spite of residing in the same tissue. Answers to these

questions could provide insights into how we can therapeutically target TAM subset-specific pathways in order to restrain the progression of different types of tumors even within the same organ.

A highly debated question regarding macrophage ontogeny is the functional differences between macrophages derived from distinct origins that are located within the same tissue context. This question remains largely unsolved. A limited number of transcriptional studies suggest that macrophages of different ontogeny demonstrate mostly overlapping transcriptional profiles within the same tissue, at least in non-disease settings (Gibbings et al., 2015; Gundra et al., 2014; van de Laar et al., 2016). Upon engraftment, circulating monocytes could also replenish the resident macrophage pool and adopt a transcriptional profile similar to their embryonically derived counterparts (Scott et al., 2016). These studies led to the assumption that tissue environment, as opposed to ontogeny, is the main driver of macrophage functions. Indeed, macrophages resident in different organs or at different niches within the same organ have distinct transcriptional profiles, supporting the concept that tissue environment could educate macrophages to adopt distinct functionalities (Gautier et al., 2012; Mass et al., 2016; Movahedi et al., 2010; Ojalvo et al., 2009). However, our microarray data demonstrated that although gene expression profiles of embryonically derived and HSC-derived macrophages are fairly similar in the normal pancreatic tissue, their expression profiles and *ex vivo* functions are very distinct in PDAC tissues. As a harbinger of this dynamic, CXCR4 is largely not expressed in macrophages of either origin in the normal pancreas, but specifically upregulated in PDAC TAMs of embryonic origin. These data suggest that origin may epigenetically poise macrophages to differentially respond to inflammatory insults with distinct bioactivities, such as ECM modulation or antigen processing/presentation. Future experiments are needed to determine

which lineage commitment factors poise macrophages for differing functional responses during tumor progression.

Our studies also demonstrate unique fibrosis-modulating functions in embryonically derived TAMs. Macrophages are well known for their ability to promote fibrosis in multiple physiological and pathological conditions, such as wound healing and cancer (Wynn and Vannella, 2016). However, such activities are thought to be indirectly executed by activating fibroblasts to lay down and remodel ECM. Here, our data suggest that subsets of macrophages may fine-tune fibrosis by directly depositing and/or remodeling the ECM. Fibrosis is a hallmark of PDAC, which imposes a major physical barrier that not only inhibits endogenous anti-tumor immune responses but also deters effective delivery of chemo- and immune-therapies (Beatty et al., 2011; Jiang et al., 2016). Although it has been demonstrated that tumor-derived factors promote macrophage expansion and fibrosis, the initiation of these two pathological features were considered to be independent of each other. Our data suggest these responses may be more integrated. Corresponding with this idea, a recent report demonstrated that TAMs directly construct ECM in colon cancer (Afik et al., 2016). Interestingly, such activities were carried out by monocyte-derived TAMs in their model.

Strikingly, depletion of macrophage subsets had different impacts on tumor progression in PDAC models. Loss of monocyte-derived macrophages had limited effects on tumor progression, whereas depletion of tissue-resident macrophages significantly reduced tumor growth and aggressivity/grade. These observations form a nice comparison to several other tumor models, where the depletion of monocyte-derived macrophages inhibits tumor growth and metastasis (Afik et al., 2016; Franklin et al., 2014; Qian et al., 2011). Although we cannot rule

out the importance of monocyte-derived TAMs in the regulation of PDAC development, our data suggest that tissue-resident macrophages are important in PDAC progression.

In summary, our study demonstrates that PDAC contains macrophages with heterogeneous ontological origins. In addition to Ly6C^{Hi} monocytes, tissue-resident macrophages derived from embryonic origin are also a major source of TAMs in murine models. Embryonically derived macrophages expand in PDAC tissues through *in situ* proliferation and exhibit a pro-fibrotic transcriptional profile, suggesting a potential role in fine-tuning fibrosis in PDAC. We provide a new paradigm of macrophage heterogeneity under the tumor setting, which may facilitate future investigations that ultimately improve therapeutics to target the "fibro-inflammatory" microenvironment of PDAC and potentially other cancers.

3.6 Figures and Tables

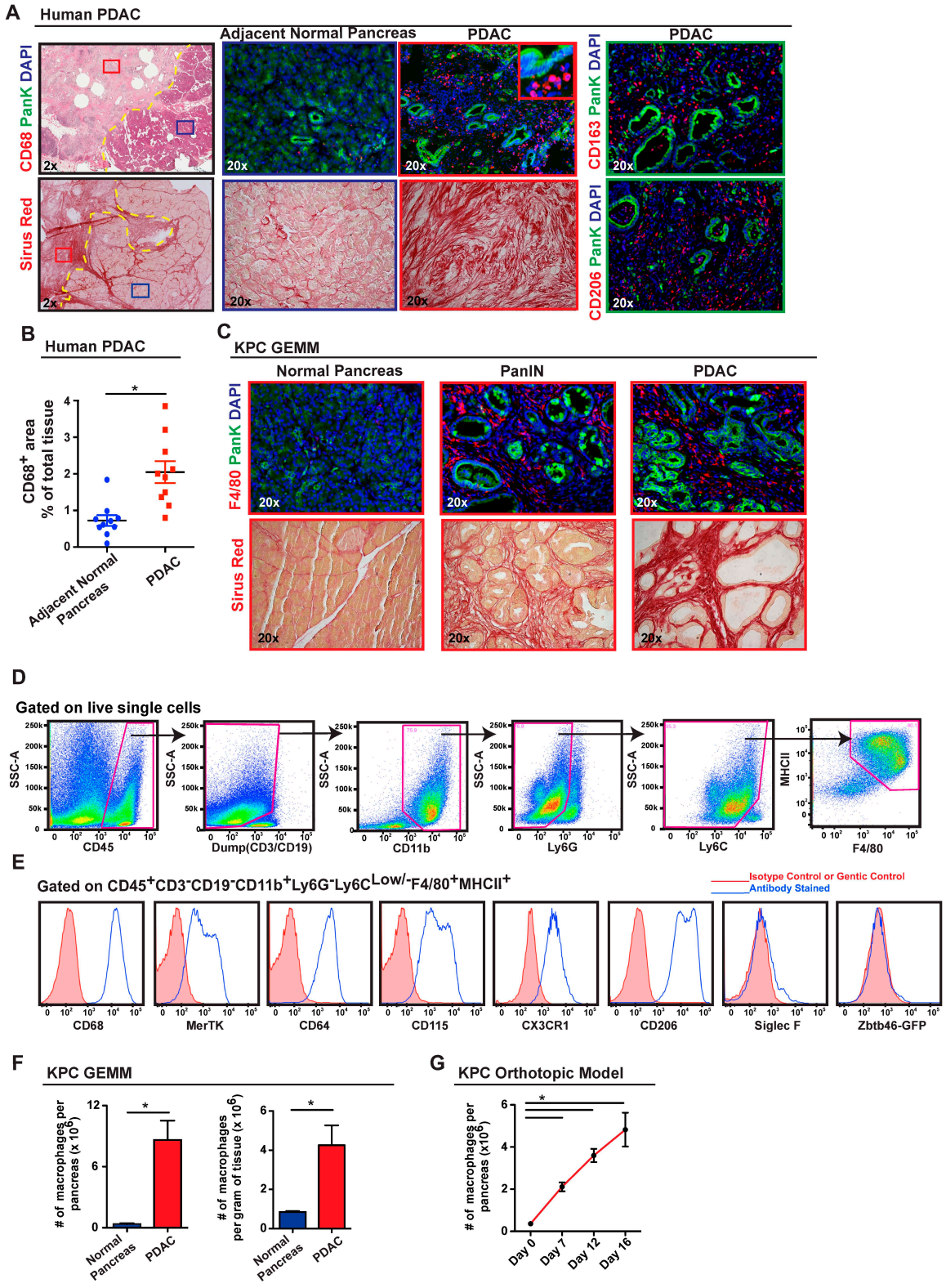

Figure 3.1. Pancreatic Ductal Adenocarcinomas Are Highly Infiltrated with Macrophages.

(A) Representative images of human PDAC and adjacent normal pancreatic tissues assessed for macrophage density (CD68, CD206, or CD163) and fibrosis (Sirius Red). Epithelial cells were stained by pan-Keratin (PanK).

(B) Quantitation of $CD68^{+}$ cells in human PDAC tissue vs. normal adjacent tissue from the same surgical sample.

(C) Representative images of pancreas tissue from the p48-CRE/$Kras^{G12D}$/$p53^{flox/+}$ (KPC) mouse model assessing macrophage infiltration (F4/80) and collagen density (Sirius Red).

(D) Representative flow cytometry plots showing gating strategy to identify macrophages in autochthonous KPC tumors.

(E) Measurement of listed cell surface markers analyzed by flow cytometry and pre-gated on macrophages as shown in (D).

(F) Quantification of macrophages by flow cytometry in normal pancreas tissues and advanced KPC PDAC tissues (n=4-8/group).

(G) Kinetics of macrophage numbers assessed by flow cytometry in syngeneic orthotopic KPC-1 tumors. (n=4/group)

Data are shown as mean ± SEM and * denotes $p<0.05$ by t-test or Mann-Whitney test.

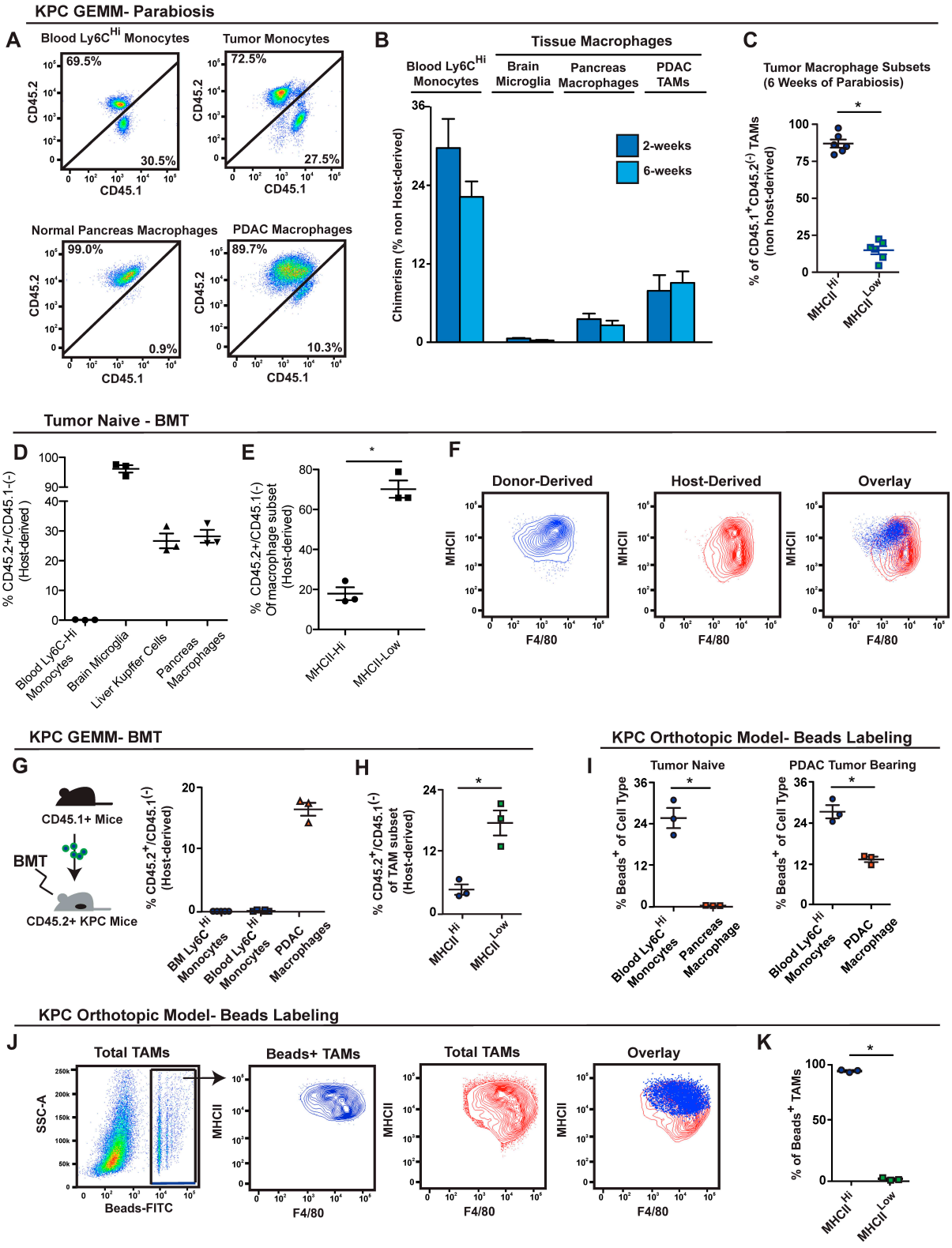
KPC GEMM- Parabiosis
A
Blood Ly6C^Hi Monocytes
Tumor Monocytes
Normal Pancreas Macrophages
PDAC Macrophages
CD45.2
CD45.1
69.5%
30.5%
72.5%
27.5%
99.0%
0.9%
89.7%
10.3%
B
Tissue Macrophages
Blood Ly6C^Hi Monocytes
Brain Microglia
Pancreas Macrophages
PDAC TAMs
Chimerism (% non Host-derived)
2-weeks
6-weeks
C
Tumor Macrophage Subsets (6 Weeks of Parabiosis)
% of CD45.1+CD45.2(-) TAMs (non host-derived)
MHCII^Hi
MHCII^Low
Tumor Naive - BMT
D
% CD45.2+/CD45.1-(-) (Host-derived)
Blood Ly6C-Hi Monocytes
Brain Microglia
Liver Kupffer Cells
Pancreas Macrophages
E
% CD45.2+/CD45.1(-) Of macrophage subset (Host-derived)
MHCII-Hi
MHCII-Low
F
Donor-Derived
Host-Derived
Overlay
MHCII
F4/80
KPC GEMM- BMT
G
CD45.1+ Mice
BMT
CD45.2+ KPC Mice
% CD45.2+/CD45.1(-) (Host-derived)
BM Ly6C^Hi Monocytes
Blood Ly6C^Hi Monocytes
PDAC Macrophages
H
% CD45.2+/CD45.1(-) of TAM subset (Host-derived)
MHCII^Hi
MHCII^Low
KPC Orthotopic Model- Beads Labeling
I
Tumor Naive
PDAC Tumor Bearing
% Beads+ of Cell Type
Blood Ly6C^Hi Monocytes
Pancreas Macrophage
PDAC Macrophage
KPC Orthotopic Model- Beads Labeling
J
Total TAMs
Beads+ TAMs
Overlay
SSC-A
Beads-FITC
MHCII
F4/80
K
% of Beads+ TAMs
MHCII^Hi
MHCII^Low

Figure 3.2. Substantial Portions of Macrophages in Steady-State Pancreas and PDAC Maintained Independently of Blood Monocytes.

(A) 3.5-month-old homozygous CD45.1 and CD45.2 (KPC or wild-type C57BL/6) mice were surgically joined to create parabiotic pairs. Tissues were analyzed after 2 or 6 weeks of parabiosis. Representative plots (6 weeks) of chimerism in indicated cell types are shown.

(B) Quantification of chimerism in (A); (n=6-16/group).

(C) $MHCII^{Hi}$ and $MHCII^{Low}$ composition of $CD45.1^{+}CD45.2^{(-)}$-derived TAMs in (B).

(D) C57BL/6J mice were lethally irradiated and adoptively transferred with bone marrow cells from homozygous CD45.1 mice. Analysis of chimerism in several tissues after 6 weeks is depicted.

(E) Quantification of chimerism in $MHCII^{Hi}$ and $MHCII^{Low}$ macrophage subsets in normal pancreas in (D).

(F) Representative plots of (E).

(G) Autochthonous KPC mice bearing premalignant disease (3.5-month-old) were lethally irradiated and adoptively transferred with bone marrow cells from CD45.1 mice. Tissues were analyzed for chimerism after 6 weeks, when disease had progressed to full PDAC. Relative CD45.1 and CD45.2 percentages analyzed by flow cytometry are depicted.

(H) Quantification of chimerism in $MHCII^{Hi}$ and $MHCII^{Low}$ TAMs in (G).

(I) Tumor-naïve mice and orthotopic KPC tumor-bearing mice were treated with clodronate-loaded liposomes followed by i.v. injection of FITC-labeled beads. Tissue macrophages were analyzed for FITC signal by flow cytometry after 24 hours.

(J) Representative flow cytometry plots of $beads^{+}$ TAMs in orthotopic PDAC from (I).

(K) $MHCII^{Hi}$ and $MHCII^{Low}$ composition of $beads^{+}$ TAMs from (I).

Data are shown as mean ± SEM and * denotes $p<0.05$ by t-test.

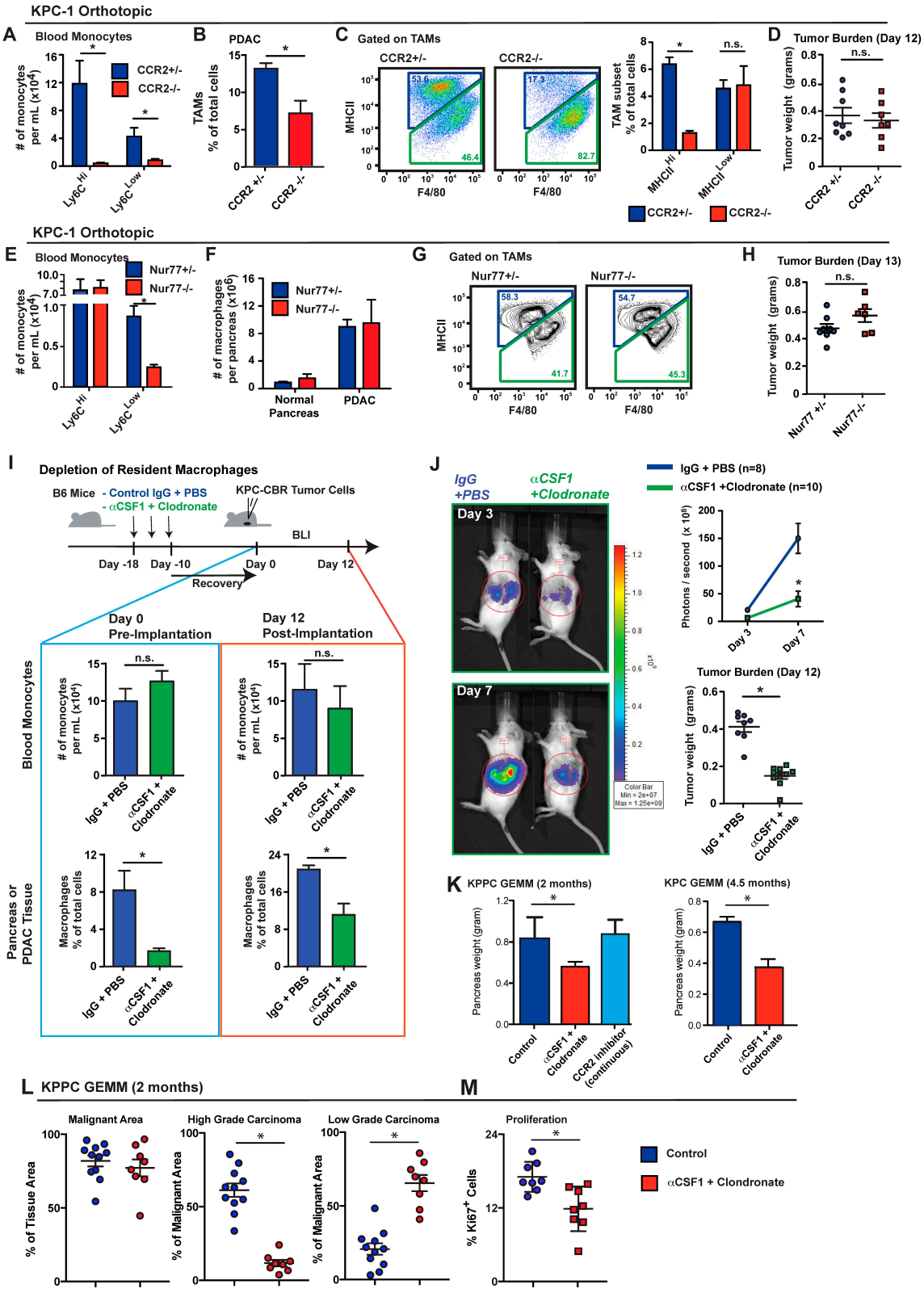
KPC-1 Orthotopic
A
Blood Monocytes
# of monocytes per mL (x10⁴)
CCR2+/-
CCR2-/-
Ly6C Hi
Ly6C Low
B
PDAC
TAMs % of total cells
CCR2 +/-
CCR2 -/-
C
Gated on TAMs
CCR2+/-
CCR2-/-
MHCII
F4/80
53.6
46.4
17.3
82.7
TAM subset % of total cells
MHCII Hi
MHCII Low
n.s.
D
Tumor Burden (Day 12)
Tumor weight (grams)
KPC-1 Orthotopic
E
Blood Monocytes
Nur77+/-
Nur77-/-
F
# of macrophages per pancreas (x10⁶)
Normal Pancreas
PDAC
G
Gated on TAMs
58.3
41.7
54.7
45.3
H
Tumor Burden (Day 13)
Nur77 +/-
Nur77 -/-
I
Depletion of Resident Macrophages
B6 Mice
- Control IgG + PBS
- αCSF1 + Clodronate
KPC-CBR Tumor Cells
BLI
Day -18
Day -10
Day 0
Day 12
Recovery
Day 0
Pre-Implantation
Day 12
Post-Implantation
Blood Monocytes
Pancreas or PDAC Tissue
Macrophages % of total cells
IgG + PBS
αCSF1 + Clodronate
J
IgG +PBS
αCSF1 +Clodronate
IgG + PBS (n=8)
αCSF1 +Clodronate (n=10)
Day 3
Day 7
Photons / second (x 10⁶)
Tumor Burden (Day 12)
Tumor weight (grams)
K
KPPC GEMM (2 months)
KPC GEMM (4.5 months)
Pancreas weight (gram)
Control
αCSF1 + Clodronate
CCR2 inhibitor (continuous)
L
KPPC GEMM (2 months)
Malignant Area
High Grade Carcinoma
Low Grade Carcinoma
% of Tissue Area
% of Malignant Area
M
Proliferation
% Ki67+ Cells
Control
αCSF1 + Clondronate

Figure 3.3. Tissue-Resident Macrophages Promote PDAC Progression.

(A-D) KPC cells were orthotopically implanted into $CCR2^{+/-}$ and $CCR2^{-/-}$ mice. Tumors were processed on Day 12 for flow cytometry analysis.

(A) Blood was drawn from orthotopic KPC-2-bearing mice via intracardiac puncture. Monocytes were assessed by flow cytometry (n=3-4/group).

(B) Frequency of macrophages orthotopic KPC-2 tissues of $CCR2^{+/-}$ and $CCR2^{-/-}$ mice.

(C) Frequency of $MHCII^{Hi}$ and ^{Low} TAM subsets assessed by flow cytometry in orthotopic KPC-2 tumors. Representative plots of TAM subsets are shown (n=3-4/group).

(D) Wet weights of KPC-2 tumors in (B).

(E-H) KPC-2 cells were orthotopically implanted into $Nur77^{+/-}$ and $Nur77^{-/-}$ mice. Tumors were processed on Day 13 for flow cytometry analysis (n=4/group normal, n=6-8/group of tumor bearing).

(E) Blood was drawn from orthotopic PDAC-bearing mice via intracardiac puncture. Monocytes were quantified.

(F) Quantity of macrophages in normal pancreas and orthotopic PDAC in $Nur77^{+/-}$ and $Nur77^{-/-}$ mice.

(G) Representative plots of $MHCII^{Hi}$ and ^{Low} TAM subsets.

(H) Wet weights of KPC-2 tumors in (F).

(I-J) KPC-2-$CBRLuc^{+}$ cells were orthotopically implanted into IgG/PBS- or αCSF1/clodronate-treated mice. Bioluminescence imaging (BLI) was used to measure tumor progression. Tumors were processed on Day 12 for flow cytometry and tumor burden analyses.

(I) Scheme of pancreas-resident macrophage depletion followed by orthotopic PDAC of KPC-2-CBRLuc^{+} cells. Blood monocytes and pancreatic macrophage numbers before and after PDAC implantation are shown.

(J) Tumor burden based on BLI and wet weight measurement.

(K) 2.5-month-old KPC or 1.0-month-old KPPC mice were treated with αCSF1/clodronate. Tumor burden was analyzed at 4.5 or 2.0 month of age.

Data are shown as mean ± SEM and * denotes $p<0.05$ by t-test or Mann-Whitney test.

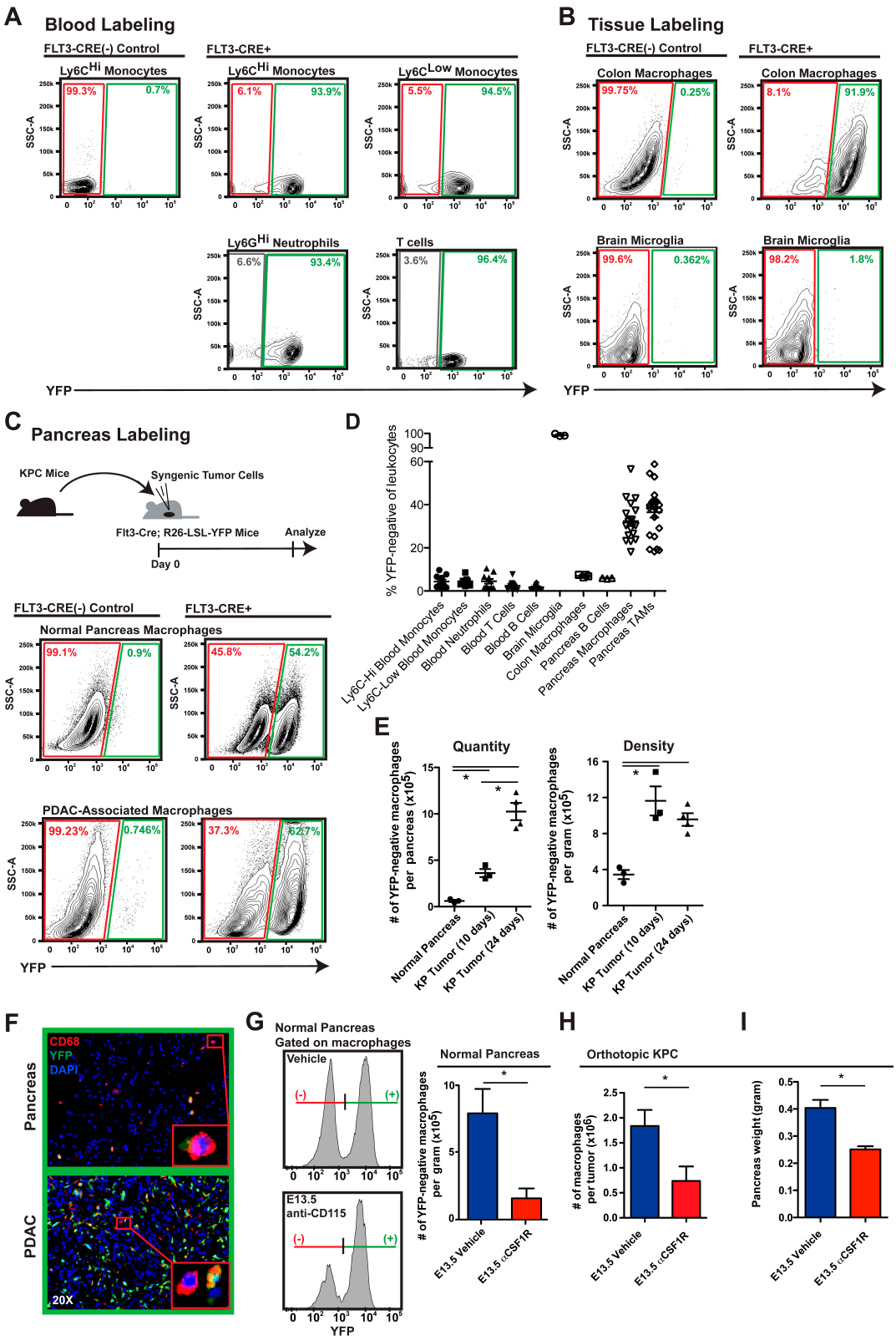
A
Blood Labeling
FLT3-CRE(-) Control
FLT3-CRE+
Ly6C^Hi Monocytes
99.3%
0.7%
Ly6C^Hi Monocytes
6.1%
93.9%
Ly6C^Low Monocytes
5.5%
94.5%
Ly6G^Hi Neutrophils
6.6%
93.4%
T cells
3.6%
96.4%
SSC-A
YFP
B
Tissue Labeling
FLT3-CRE(-) Control
FLT3-CRE+
Colon Macrophages
99.75%
0.25%
Colon Macrophages
8.1%
91.9%
Brain Microglia
99.6%
0.362%
Brain Microglia
98.2%
1.8%
SSC-A
YFP
C
Pancreas Labeling
KPC Mice
Syngenic Tumor Cells
Flt3-Cre; R26-LSL-YFP Mice
Analyze
Day 0
FLT3-CRE(-) Control
FLT3-CRE+
Normal Pancreas Macrophages
99.1%
0.9%
45.8%
54.2%
PDAC-Associated Macrophages
99.23%
0.746%
37.3%
62.7%
SSC-A
YFP
D
% YFP-negative of leukocytes
Ly6C-Hi Blood Monocytes
Ly6C-Low Blood Monocytes
Blood Neutrophils
Blood T Cells
Blood B Cells
Brain Microglia
Colon Macrophages
Pancreas B Cells
Pancreas Macrophages
Pancreas TAMs
E
Quantity
Density
# of YFP-negative macrophages per pancreas (x10^5)
# of YFP-negative macrophages per gram (x10^5)
Normal Pancreas
KP Tumor (10 days)
KP Tumor (24 days)
F
CD68
YFP
DAPI
Pancreas
PDAC
20X
G
Normal Pancreas
Gated on macrophages
Vehicle
E13.5
anti-CD115
(-)
(+)
YFP
Normal Pancreas
# of YFP-negative macrophages per gram (x10^5)
E13.5 Vehicle
E13.5 αCSF1R
H
Orthotopic KPC
# of macrophages per tumor (x10^6)
E13.5 Vehicle
E13.5 αCSF1R
I
Pancreas weight (gram)
E13.5 Vehicle
E13.5 αCSF1R

Figure 3.4. Embryonically Derived Macrophages are Significant Components of Tissue-Resident TAMs and Expand During PDAC Progression.

(A-C) KPC-1 cells were orthotopically implanted into Flt3-Cre^{YFP} mice. Indicated tissues were analyzed by flow cytometry for YFP expression. Representative flow cytometry plots of YFP signal in leukocytes from blood (A), macrophages from colon and brain (B), and macrophages in normal pancreas and end stage PDAC tissues (C) are depicted.

(D) Quantifications of percentage of YFP-negativity in leukocytes from (A-C; n=7-22/group).

(E) Kinetics of YFP-negative macrophages quantity and density in orthotopic KPC-1 tumors.

(F) Representative immunofluorescence images of CD68 and YFP from (C). Inlets identify YFP-positive and YFP-negative macrophages.

(G) Flt3-Cre^{YFP} reporter mice were treated with αCSF1R on E13.5. Pancreas was isolated at 6 weeks of age. Density of YFP-negative macrophages was quantified (n=3-5/group).

(H) C57BL/6 mice were treated with αCSF1R or vehicle on E13.5. Orthotopic PDAC was established at 6 weeks of age. TAMs were quantified after 12 days (n=5-6/group).

(I) Tumor burden from (H) was analyzed (n=6-9/group).

Data are shown as mean ± SEM and * denotes $p<0.05$ by t-test.

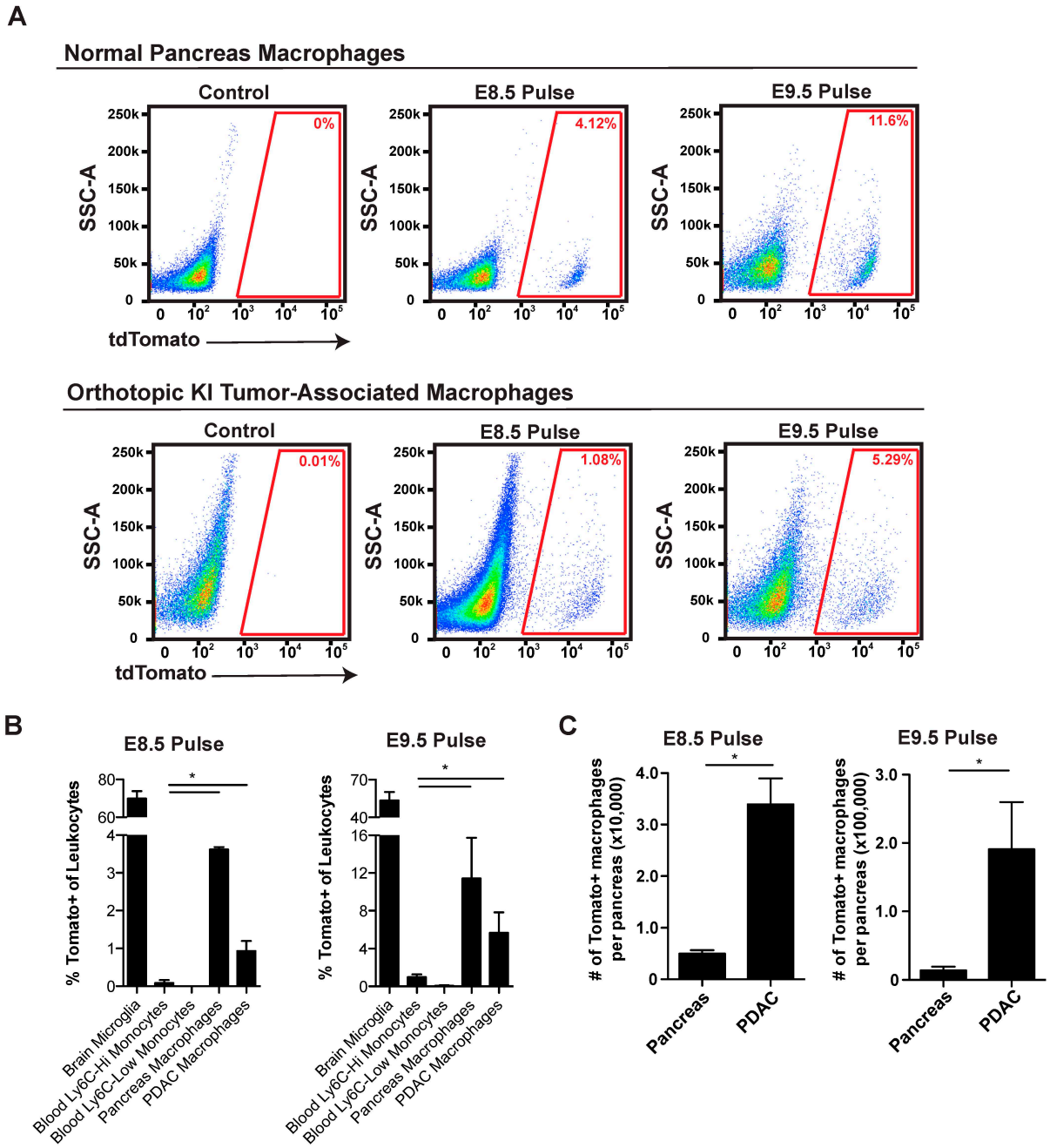
A
Normal Pancreas Macrophages
Control
E8.5 Pulse
E9.5 Pulse
0%
4.12%
11.6%
SSC-A
tdTomato
Orthotopic KI Tumor-Associated Macrophages
0.01%
1.08%
5.29%
B
E8.5 Pulse
E9.5 Pulse
% Tomato+ of Leukocytes
Brain Microglia
Blood Ly6C-Hi Monocytes
Blood Ly6C-Low Monocytes
Pancreas Macrophages
PDAC Macrophages
C
# of Tomato+ macrophages per pancreas (x10,000)
# of Tomato+ macrophages per pancreas (x100,000)
Pancreas
PDAC

Figure 3.5. Yolk Sac-Derived Macrophages Expand during PDAC Progression.

(A) Representative flow cytometry plot of tdTomato signals in the normal pancreas and orthotopic KI tumors of adult mice upon E8.5 or E9.5 tamoxifen pulse.

(B) Percentage of indicated leukocytes that were labeled upon E8.5 or E9.5 tamoxifen pulse (n=3-7/group).

(C) Absolute numbers of tdTomato+ macrophages in the normal pancreas and orthotopic KI tumors (n=3-4/group).

Data are shown as mean ± SEM and * denotes $p<0.05$ by t-test.

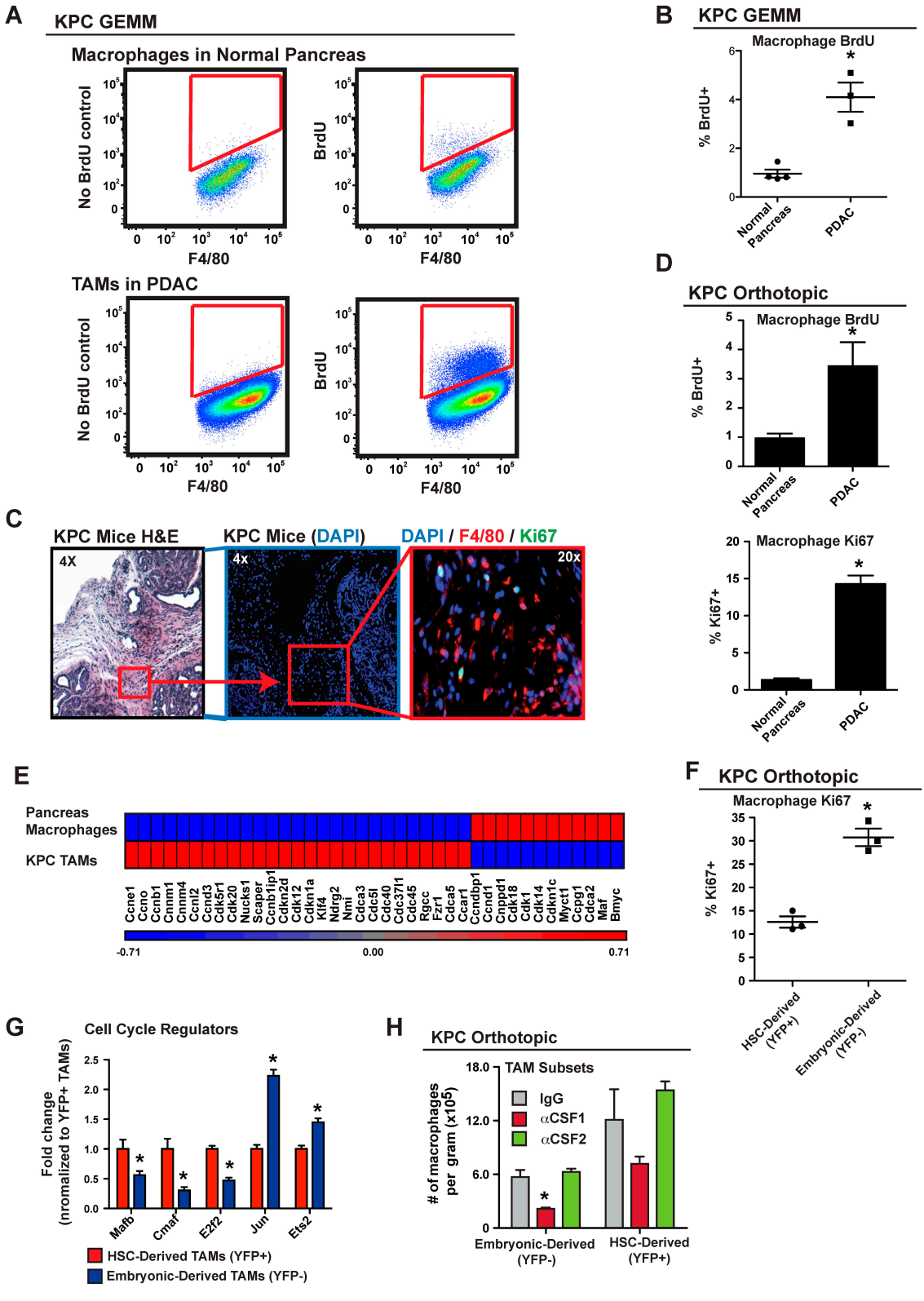
A
KPC GEMM
Macrophages in Normal Pancreas
No BrdU control
BrdU
F4/80
TAMs in PDAC
B
KPC GEMM
Macrophage BrdU
% BrdU+
Normal Pancreas
PDAC
C
KPC Mice H&E
KPC Mice (DAPI)
DAPI / F4/80 / Ki67
4X
4x
20x
D
KPC Orthotopic
Macrophage BrdU
Macrophage Ki67
% Ki67+
E
Pancreas Macrophages
KPC TAMs
Ccne1 Ccno Ccnb1 Cnnm1 Cnnm4 Ccnl2 Ccnd3 Cdk5r1 Cdk20 Nucks1 Scaper Ccnb1ip1 Cdkn2d Cdk12 Cdkn1a Klf4 Ndrg2 Nmi Cdca3 Cdc5l Cdc40 Cdc37l1 Cdc45 Rgcc Fzr1 Cdca5 Ccar1 Ccndbp1 Ccnd1 Cnppd1 Cdk18 Cdk1 Cdk14 Cdkn1c Myct1 Ccpg1 Cdca2 Maf Bmyc
-0.71
0.00
0.71
F
KPC Orthotopic
Macrophage Ki67
% Ki67+
HSC-Derived (YFP+)
Embryonic-Derived (YFP-)
G
Cell Cycle Regulators
Fold change (nromalized to YFP+ TAMs)
Mafb
Cmaf
E2f2
Jun
Ets2
HSC-Derived TAMs (YFP+)
Embryonic-Derived TAMs (YFP-)
H
KPC Orthotopic
TAM Subsets
IgG
αCSF1
αCSF2
# of macrophages per gram (x10^5)
Embryonic-Derived (YFP-)
HSC-Derived (YFP+)

Figure 3.6. Embryonically Derived Macrophages in PDAC Expand through *in situ* Proliferation.

(A) Analysis of autochthonous KPC PDAC and normal pancreas tissues for BrdU+ macrophages. Animals were injected with BrdU 3 hours prior to sacrifice. Representative plots are shown.

(B) Quantification of BrdU incorporation in (A).

(C) Representative immunofluorescence images of Ki67 and F4/80 staining in autochthonous KPC tumors.

(D) Quantification of flow cytometry data for Ki67 and BrdU positivity in macrophages in normal pancreas and orthotopic KPC-1 tumors (n=4-5/group).

(E) Heat map of cell cycle regulation genes assessed by array on RNA in macrophages isolated from normal pancreas and autochthonous KPC PDAC tissues (n=6/group).

(F) Orthotopic KPC-1 tumors were established in Flt3-Cre^{YFP} reporter mice. Proliferation of TAM subsets was analyzed by flow cytometry for Ki67.

(G) TAM subsets were sorted from orthotopic KPC-1 tumors in Flt3-Cre^{YFP} mice. Q-PCR analyses were performed to quantify transcripts of proliferation regulation genes.

(H) Orthotopic KPC-1-bearing Flt3-Cre^{YFP} reporter mice were treated with three doses of aCSF1 or αCSF2 on Days 7, 11, and 14. TAM subsets were quantified on Day 15.

Data are shown as mean ± SEM and * denotes $p<0.05$ by t-test.

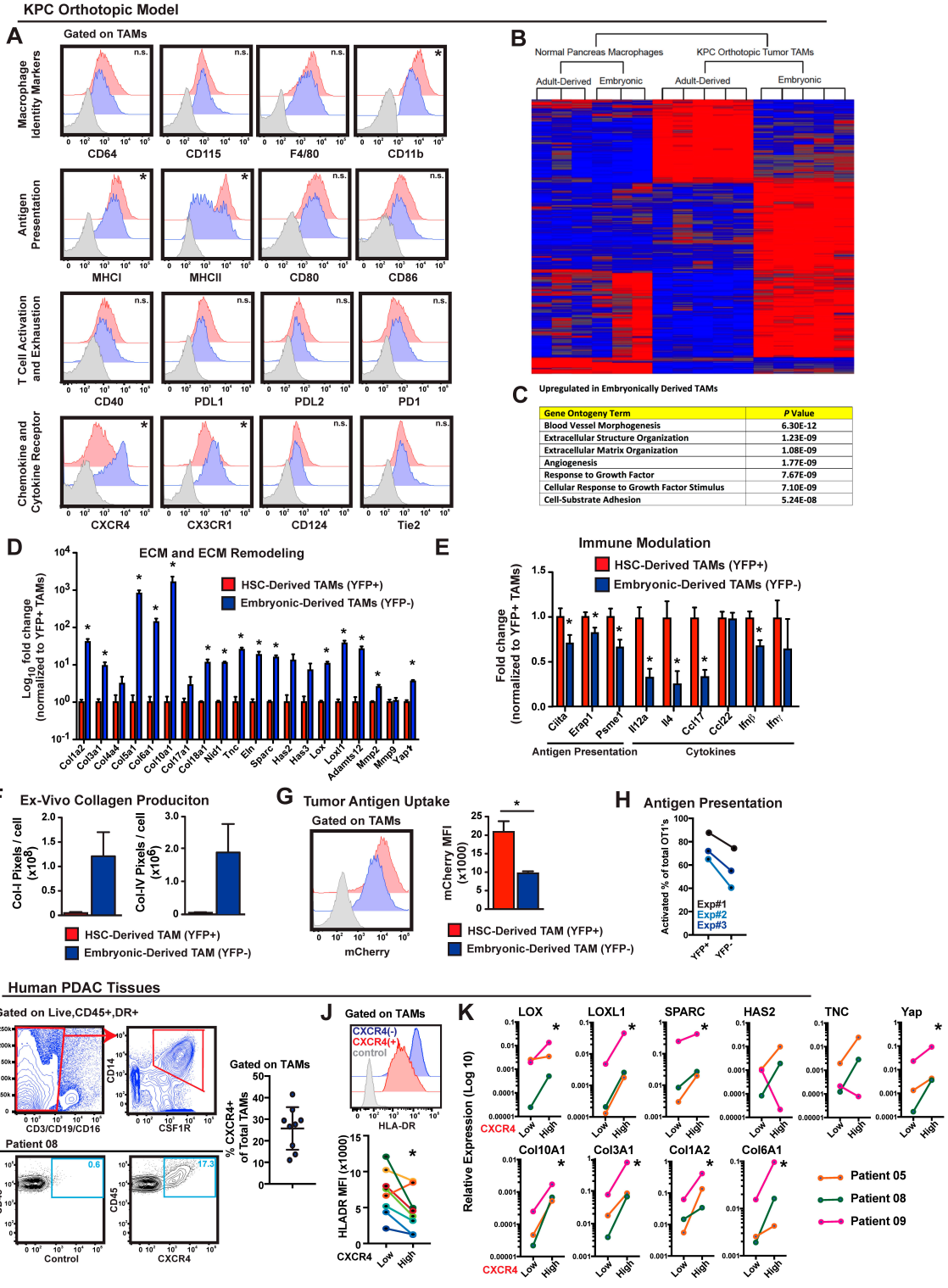
KPC Orthotopic Model
A
Gated on TAMs
Macrophage Identity Markers
CD64
CD115
F4/80
CD11b
Antigen Presentation
MHCI
MHCII
CD80
CD86
T Cell Activation and Exhaustion
CD40
PDL1
PDL2
PD1
Chemokine and Cytokine Receptor
CXCR4
CX3CR1
CD124
Tie2
n.s.
B
Normal Pancreas Macrophages
KPC Orthotopic Tumor TAMs
Adult-Derived
Embryonic
Adult-Derived
Embryonic
C
Upregulated in Embryonically Derived TAMs
Gene Ontogeny Term | P Value
Blood Vessel Morphogenesis | 6.30E-12
Extracellular Structure Organization | 1.23E-09
Extracellular Matrix Organization | 1.08E-09
Angiogenesis | 1.77E-09
Response to Growth Factor | 7.67E-09
Cellular Response to Growth Factor Stimulus | 7.10E-09
Cell-Substrate Adhesion | 5.24E-08
D
ECM and ECM Remodeling
HSC-Derived TAMs (YFP+)
Embryonic-Derived TAMs (YFP-)
Log10 fold change (normalized to YFP+ TAMs)
Col1a2
Col3a1
Col4a4
Col5a1
Col6a1
Col10a1
Col17a1
Col18a1
Nid1
Tnc
Eln
Sparc
Has2
Has3
Lox
Loxl1
Adamts12
Mmp2
Mmp9
Yap*
E
Immune Modulation
HSC-Derived TAMs (YFP+)
Embryonic-Derived TAMs (YFP-)
Fold change (normalized to YFP+ TAMs)
Ciita
Erap1
Psme1
Il12a
Il4
Ccl17
Ccl22
Ifnβ
Ifnγ
Antigen Presentation
Cytokines
F
Ex-Vivo Collagen Produciton
Col-I Pixels / cell (x10^8)
Col-IV Pixels / cell (x10^6)
HSC-Derived TAM (YFP+)
Embryonic-Derived TAM (YFP-)
G
Tumor Antigen Uptake
Gated on TAMs
mCherry
mCherry MFI (x1000)
HSC-Derived TAM (YFP+)
Embryonic-Derived TAM (YFP-)
H
Antigen Presentation
Activated % of total OT1's
Exp#1
Exp#2
Exp#3
YFP+
YFP-
Human PDAC Tissues
I
Gated on Live,CD45+,DR+
SSC-A
CD3/CD19/CD16
CD14
CSF1R
Patient 08
CD45
Control
CXCR4
0.6
17.3
Gated on TAMs
% CXCR4+ of Total TAMs
J
Gated on TAMs
CXCR4(-)
CXCR4(+)
control
HLA-DR
HLADR MFI (x1000)
CXCR4
Low
High
K
LOX
LOXL1
SPARC
HAS2
TNC
Yap
Col10A1
Col3A1
Col1A2
Col6A1
Relative Expression (Log 10)
CXCR4
Low
High
Patient 05
Patient 08
Patient 09

Figure 3.7. Embryonically Derived TAMs Have Distinct Phenotypes and Functions that are Recapitulated by Subsets of TAMs in Human PDAC.

(A) Flow cytometry analysis of orthotopic KPC-1 PDAC tissues in Flt3-Cre^{YFP} mice stained with indicated antibodies and gated on TAMs (gray, isotype control; blue, YFP-negative TAMs; red YFP-positive TAMs).

(B) YFP-positive and YFP-negative macrophages were sorted from normal pancreas or late-stage orthotopic KPC-1 tumors of Flt3-Cre^{YFP} mice. RNA was extracted for microarray analyses. Hierarchical clustering of genes that were differentially expressed between macrophage subsets either in normal pancreas or PDAC is shown.

(C) Gene ontogeny analyses of molecules expressed at higher levels in YFP-negative TAMs.

(D-E) Q-PCR analyses of gene expression for molecules involved in ECM modification (D) or immune modulation (E). Analysis was performed on RNA from sorted YFP+ and (-) TAMs from Flt3-Cre^{YFP} mice bearing KCP-1 tumors (n=5/group). Genes were selected from the top candidates in (B).

(F) Analysis of collagen production *ex vivo* by YFP+ and (-) TAMs sorted from orthotopic KPC-1 PDAC tissues in Flt3-Cre^{YFP} mice. Collagen laydown was assessed after 36 hours by immunofluorescence intensity. Experiments are representative of three independent repeats.

(G) Orthotopic tumors were established in Flt3-Cre^{YFP} reporter mice using KPC-1-mCherry^{+} tumor cells. TAMs were analyzed for mCherry positivity. Representative flow plots and mean fluorescence intensity (MFI) are depicted (n=4/group).

(H) Analysis of antigen presentation to CD8^{+} T cells by YFP+ and (-) TAMs sorted from Flt3-Cre^{YFP} mice bearing KPC-1 tumors. Antigen presentation was assessed by the ability of TAMs to activate OT1 cells after SIINFEKL loading and measured by CFSE-dilution and/or

$CD44^+/CD69^+/CD62L^-$ expression on T cells. Three independent sorting experiments are depicted as paired analyses.

(I) Flow cytometry analysis of human PDAC tissues from surgical resections is depicted. The percentage of $CXCR4^+$ TAMs of total is shown for nine patients.

(J) Analysis of HLA-DR expression in CXCR4-positive and negative TAMs using data from (I). A representative flow plot and MFI analysis in paired samples are depicted.

(K) Q-PCR analysis of mRNA from CXCR4-positive and negative TAMs sorted from human PDAC tissues. Pro-fibrotic genes assessed were identified in (B), and analysis of paired isolates from three patients is depicted. All graphs depict mean values +/- SEM and * denotes $p<0.05$ by t-test, Mann-Whitney test, or Wilcoxon matched pairs rank test as appropriate for the data set.

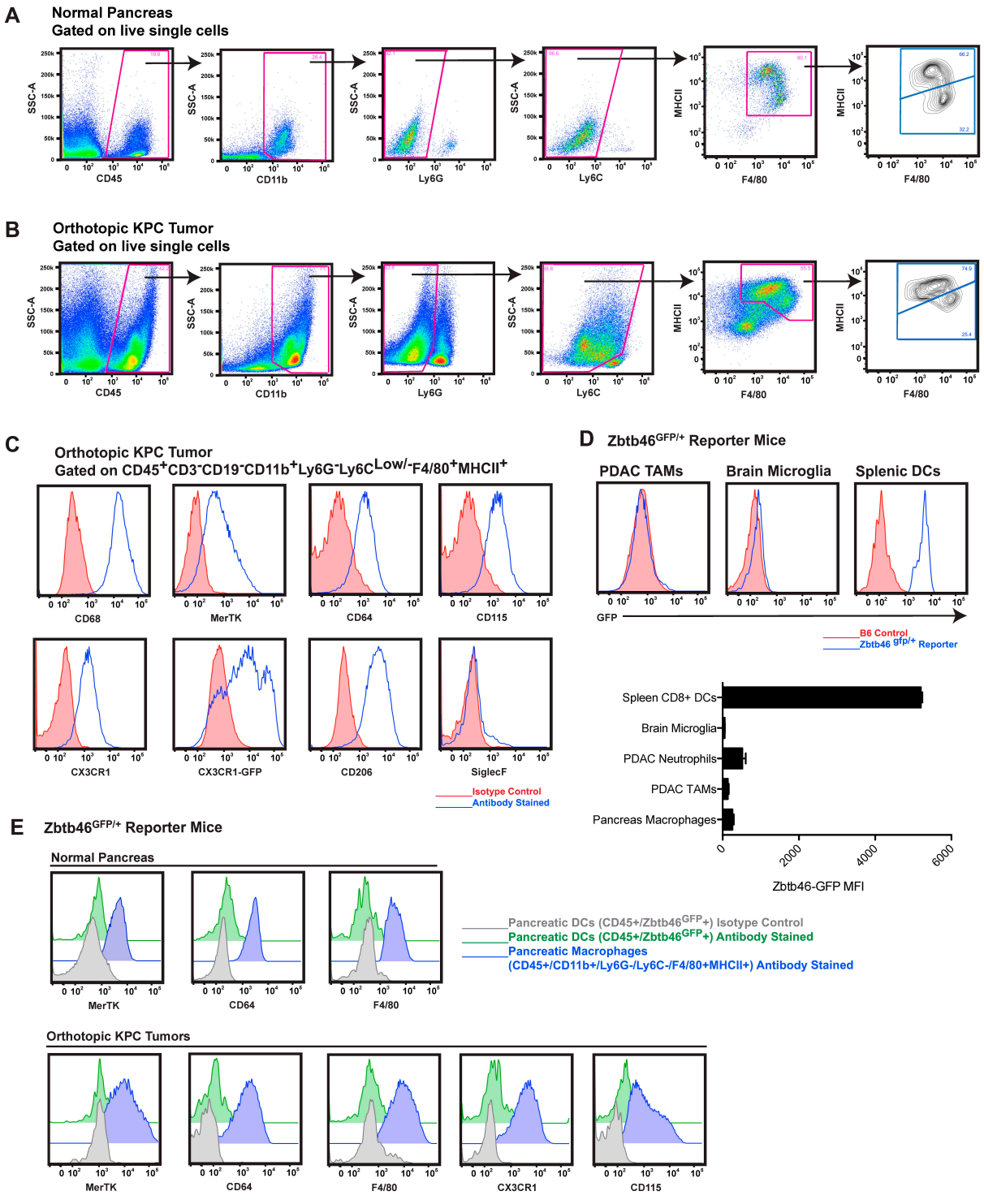
A
Normal Pancreas
Gated on live single cells
SSC-A
CD45
CD11b
Ly6G
Ly6C
MHCII
F4/80
B
Orthotopic KPC Tumor
Gated on live single cells
C
Orthotopic KPC Tumor
Gated on CD45+CD3-CD19-CD11b+Ly6G-Ly6CLow/-F4/80+MHCII+
CD68
MerTK
CD64
CD115
CX3CR1
CX3CR1-GFP
CD206
SiglecF
Isotype Control
Antibody Stained
D
Zbtb46GFP/+ Reporter Mice
PDAC TAMs
Brain Microglia
Splenic DCs
GFP
B6 Control
Zbtb46 gfp/+ Reporter
Spleen CD8+ DCs
Brain Microglia
PDAC Neutrophils
PDAC TAMs
Pancreas Macrophages
0
2000
4000
6000
Zbtb46-GFP MFI
E
Zbtb46GFP/+ Reporter Mice
Normal Pancreas
MerTK
CD64
F4/80
Pancreatic DCs (CD45+/Zbtb46GFP+) Isotype Control
Pancreatic DCs (CD45+/Zbtb46GFP+) Antibody Stained
Pancreatic Macrophages
(CD45+/CD11b+/Ly6G-/Ly6C-/F4/80+MHCII+) Antibody Stained
Orthotopic KPC Tumors
MerTK
CD64
F4/80
CX3CR1
CD115

Figure 3.8, related to Figure 3.1. Macrophage Gating Strategy in Normal Pancreas and Orthotopic Tumors.

(A) Representative flow cytometry plots showing gating strategy to identify macrophages in normal pancreas.

(B) Representative flow cytometry plots showing gating strategy to identify macrophages in orthotopic tumors established using KPC-1 cells.

(C) Measurement of listed surface markers analyzed by flow cytometry and pre-gated on macrophages in orthotopic KPC-1 tumors as shown in (B). To confirm CX3CR1 antibody staining, orthotopic KPC-1 tumors were established in $CX3CR1^{gfp/gfp}$ mice; Representative flow cytometry plot of GFP signals in TAMs is shown. (representative of n=15).

(D) Representative flow cytometry plots of Zbtb46-GFP fluorescence in TAMs of orthotopic KPC-1 tumors, brain microglia ($CD45^{Low}/CD11b^{Hi}/F4/80^{+}$), and splenic dendritic cells (DCs) ($CD45^{+}/CD11c^{+}/MHCII^{+}/B220^{-}/CD8^{+}$ or $CD11b^{+}$). Mean fluorescence intensity (MFI) for each cell population is calculated by deducting baseline MFI of isotype staining control from the MFI of stained samples. (n=4-5/group, mean ± SEM).

(E) Measurement of listed surface markers in pancreatic dendritic cells (DCs) and macrophages by flow cytometry.

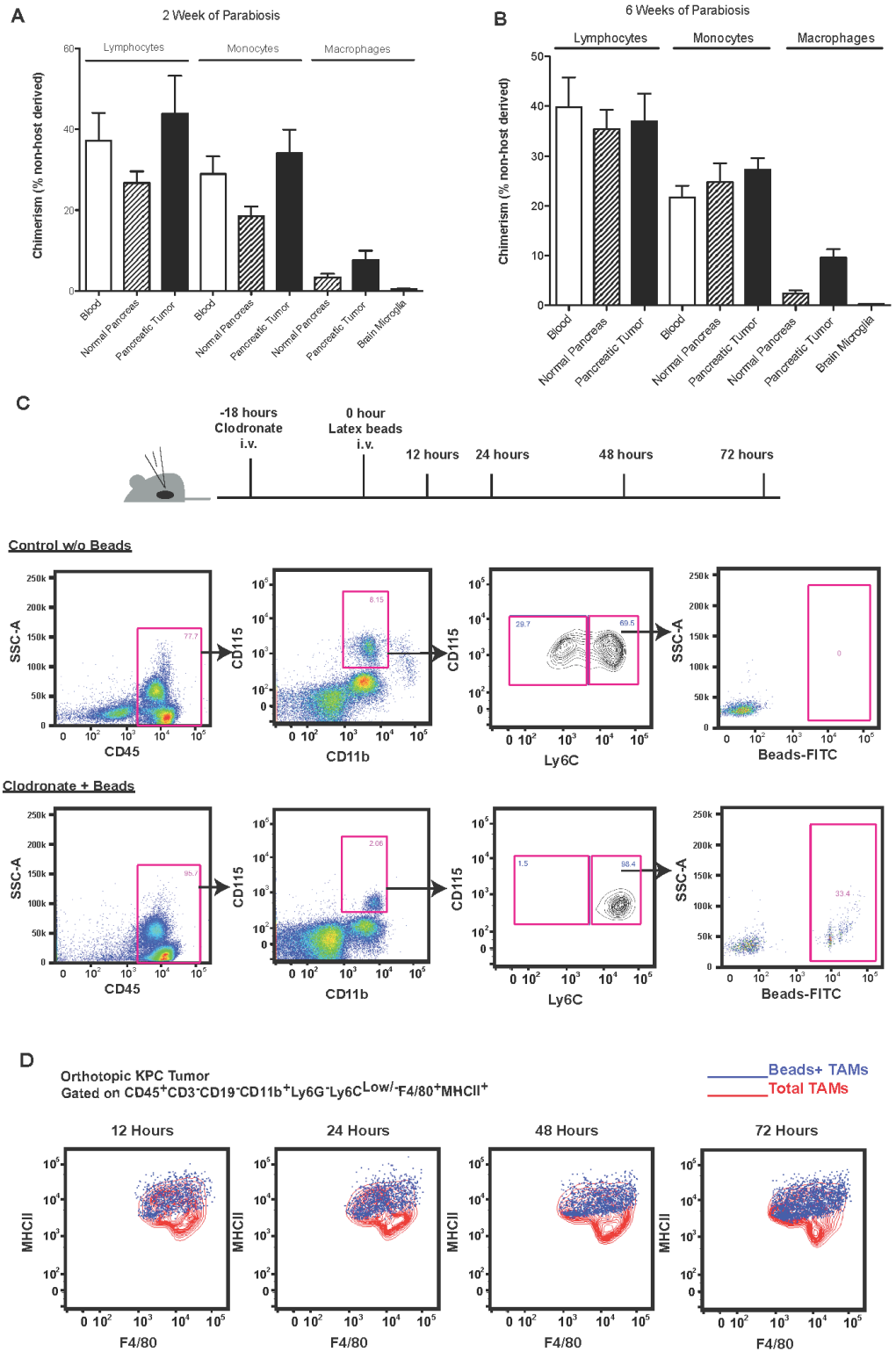
A
2 Week of Parabiosis
Lymphocytes
Monocytes
Macrophages
Chimerism (% non-host derived)
Blood
Normal Pancreas
Pancreatic Tumor
Brain Microglia
B
6 Weeks of Parabiosis
C
-18 hours
Clodronate
i.v.
0 hour
Latex beads
i.v.
12 hours
24 hours
48 hours
72 hours
Control w/o Beads
Clodronate + Beads
SSC-A
CD45
CD11b
CD115
Ly6C
Beads-FITC
D
Orthotopic KPC Tumor
Gated on CD45+CD3-CD19-CD11b+Ly6G-Ly6CLow/-F4/80+MHCII+
Beads+ TAMs
Total TAMs
12 Hours
24 Hours
48 Hours
72 Hours
MHCII
F4/80

Figure 3.9, related to Figure 3.2. Substantial Portions of Macrophages in Normal Pancreas and PDAC Self-Maintain Independently of Blood Monocytes.

(A-B) 3.5-month-old homozygous CD45.1 and CD45.2 (KPC or wild-type C57BL/6) mice were surgically joined to create parabiotic pairs. Chimerism of indicated leukocytes were analyzed 2 weeks (A) or 6 weeks (B) after the establishment of parabiosis. (n=6-16/group, mean ± SEM).

(C) KPC-1 orthotopic tumor-bearing mice were treated with clodronate i.v. to deplete circulating $Ly6C^{Low}$ monocytes, followed by retro-orbital injection of FITC-labeled latex beads. Representative flow cytometry plots showing FITC signals in blood $Ly6C^{Hi}$ monocytes 24 hours after bead injection.

(D) Representative flow cytometry plots of $beads^{+}$ TAMs in orthotopic KPC-1 tumors at indicated time points (n=3/time point).

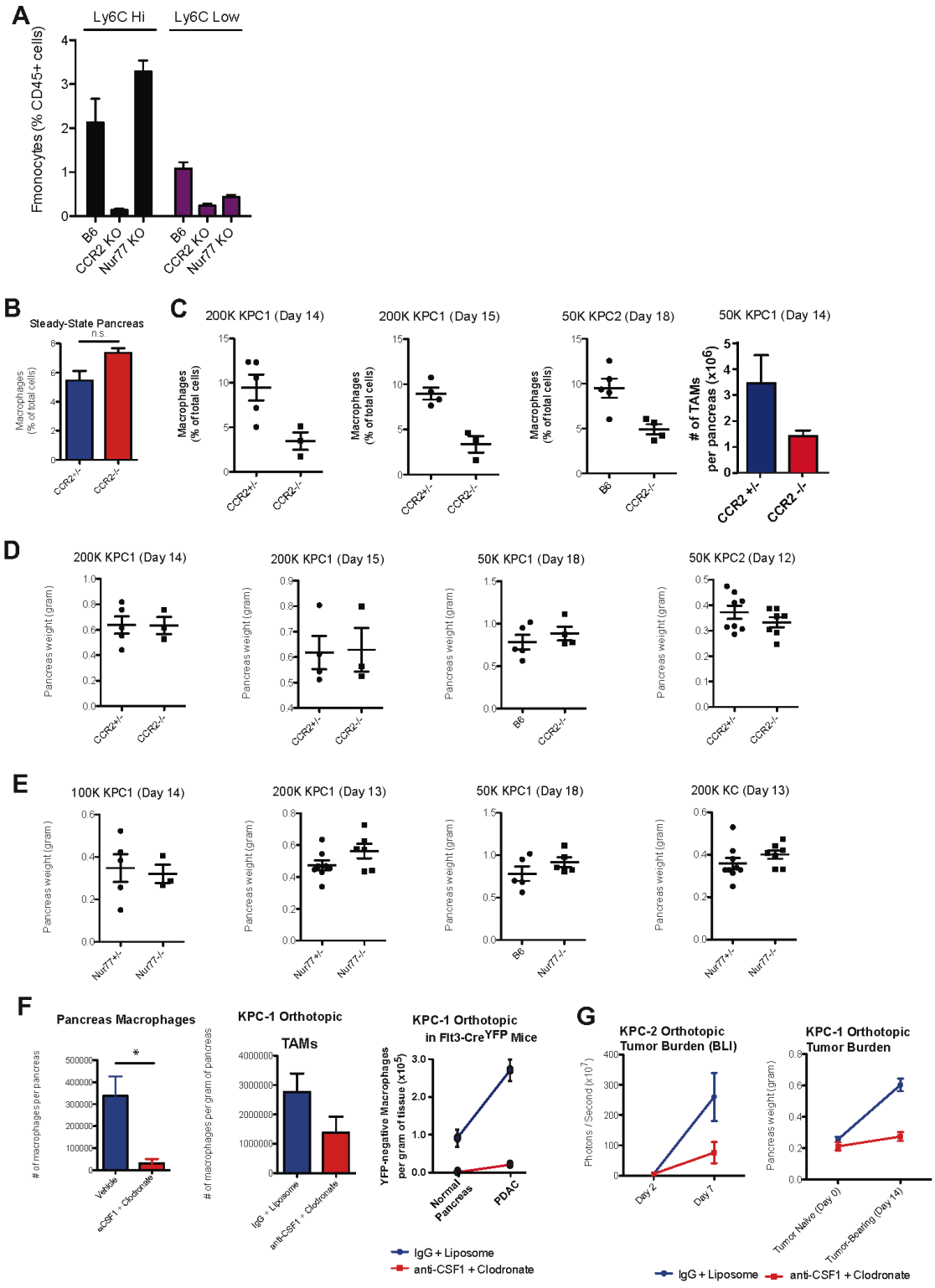
A
Ly6C Hi
Ly6C Low
Fmonocytes (% CD45+ cells)
B6
CCR2 KO
Nur77 KO
B6
CCR2 KO
Nur77 KO
B
Steady-State Pancreas
n.s.
Macrophages (% of total cells)
CCR2+/-
CCR2-/-
C
200K KPC1 (Day 14)
200K KPC1 (Day 15)
50K KPC2 (Day 18)
50K KPC1 (Day 14)
Macrophages (% of total cells)
# of TAMs per pancreas (x10^6)
CCR2+/-
CCR2-/-
B6
CCR2 +/-
CCR2 -/-
D
200K KPC1 (Day 14)
200K KPC1 (Day 15)
50K KPC1 (Day 18)
50K KPC2 (Day 12)
Pancreas weight (gram)
CCR2+/-
CCR2-/-
B6
E
100K KPC1 (Day 14)
200K KPC1 (Day 13)
50K KPC1 (Day 18)
200K KC (Day 13)
Pancreas weight (gram)
Nur77+/-
Nur77-/-
B6
F
Pancreas Macrophages
# of macrophages per pancreas
*
Vehicle
aCSF1 + Clodronate
KPC-1 Orthotopic
TAMs
# of macrophages per gram of pancreas
IgG + Liposome
anti-CSF1 + Clodronate
KPC-1 Orthotopic in Flt3-Cre^YFP Mice
YFP-negative Macrophages per gram of tissue (x10^5)
Normal Pancreas
PDAC
IgG + Liposome
anti-CSF1 + Clodronate
G
KPC-2 Orthotopic Tumor Burden (BLI)
Photons / Second (x10^7)
Day 2
Day 7
KPC-1 Orthotopic Tumor Burden
Pancreas weight (gram)
Tumor Naïve (Day 0)
Tumor-Bearing (Day 14)
IgG + Liposome
anti-CSF1 + Clodronate

Figure 3.10, related to Figure 3.3. Deficiencies in Tissue Resident Macrophages but Not in Blood Monocytes Impact PDAC Tumor Burden.

(A) Representative quantification of blood monocyte frequency in tumor-bearing B6, $CCR2^{-/-}$ and $Nur77^{-/-}$ mice. (n=3-5/group).

(B) Representative quantification of pancreatic macrophage frequency in tumor-free $CCR2^{+/-}$ and $CCR2^{-/-}$ mice. (n=3/group).

(C) Orthotopic tumors were established in B6, $CCR2^{+/-}$ or $CCR2^{-/-}$ mice with 200,000 or 50,000 KPC-1 or KPC-2 cells. Frequencies or quantities of TAMs from 4 independent experiments were analyzed at indicated time points after tumor implantation. Each bar graph represents an independent experiment.

(D) Tumor burden analysis from (C).

(E) Orthotopic tumors were established in B6, $Nur77^{+/-}$, or $Nur77^{-/-}$ mice (numbers and cell types indicated). Tumor weights were measured at indicated time points. Each bar graph represents an independent experiment.

(F) 8-week old C57BL/6 (left and middle) or Flt3-Cre^{YFP} (right) mice were treated with αCSF1 combined with clodronate as described in **Experimental Approach**. Orthotopic tumors were subsequently established using KPC-2 or KPC-1 cells. Quantities of macrophages prior to or after tumor establishment were assessed by flow cytometry. (n=3-4/data point)

(G) Tumor burden from (F) were analyzed by bioluminescence imaging (BLI) or wet tumor weight. (n=4-5/data point/group)

Data are shown as mean ± SEM and ∗ denotes $p<0.05$ by t-test.

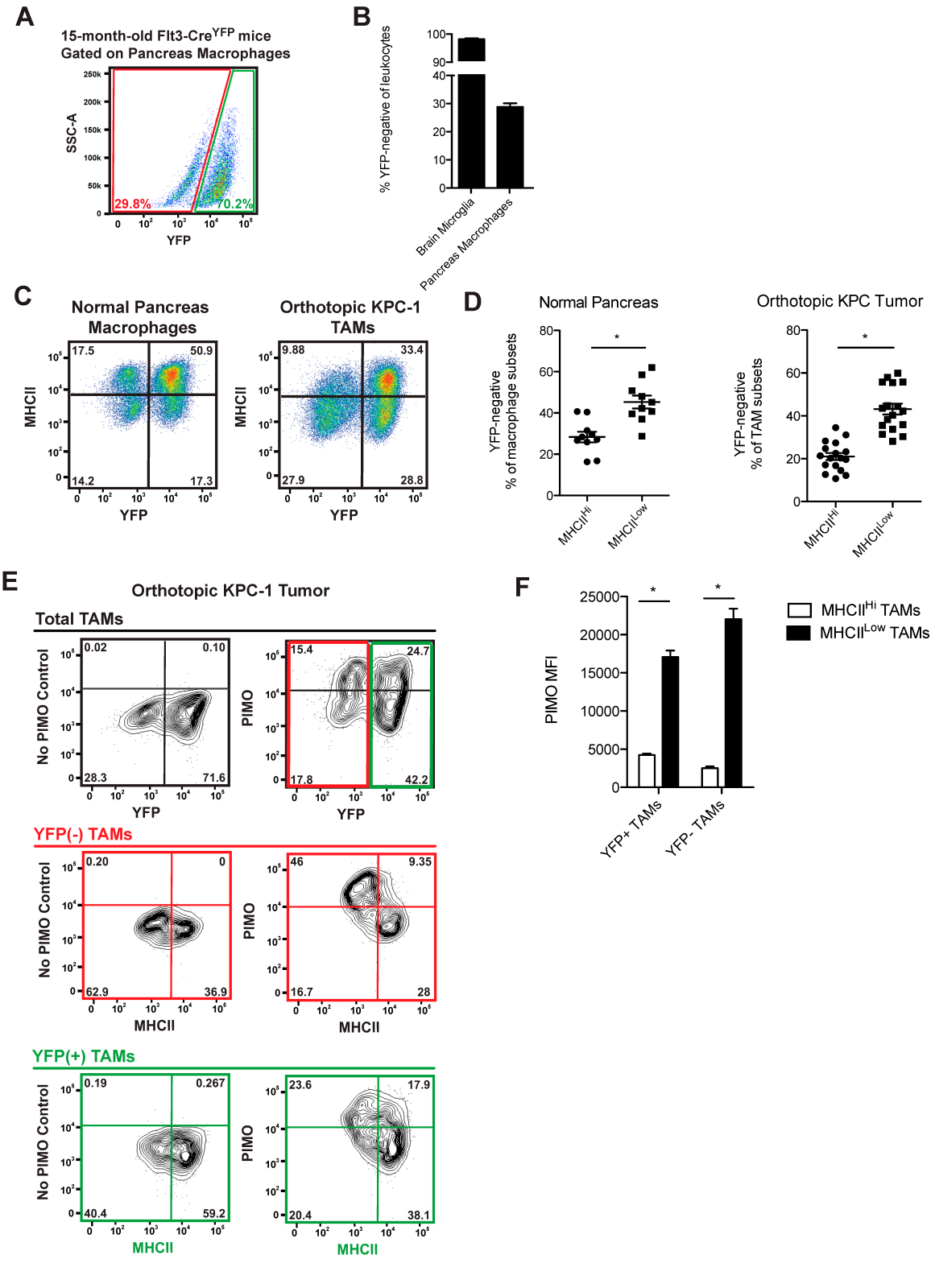
A
15-month-old Flt3-Cre^YFP mice
Gated on Pancreas Macrophages
SSC-A
YFP
29.8%
70.2%
B
% YFP-negative of leukocytes
Brain Microglia
Pancreas Macrophages
C
Normal Pancreas Macrophages
Orthotopic KPC-1 TAMs
MHCII
YFP
17.5
50.9
14.2
17.3
9.88
33.4
27.9
28.8
D
Normal Pancreas
Orthotopic KPC Tumor
YFP-negative % of macrophage subsets
YFP-negative % of TAM subsets
MHCII^Hi
MHCII^Low
E
Orthotopic KPC-1 Tumor
Total TAMs
YFP(-) TAMs
YFP(+) TAMs
No PIMO Control
PIMO
0.02
0.10
28.3
71.6
15.4
24.7
17.8
42.2
0.20
0
62.9
36.9
46
9.35
16.7
28
0.19
0.267
40.4
59.2
23.6
17.9
20.4
38.1
F
PIMO MFI
MHCII^Hi TAMs
MHCII^Low TAMs
YFP+ TAMs
YFP- TAMs

Figure 3.11, related to Figure 3.4. Embryonically Derived Macrophages are Present in the Pancreas and PDAC of Adult Mice and are Enriched in the MHCII^{Low} Subset.

(A) Representative flow cytometry plots of YFP signals in pancreatic macrophages of 15-month-old tumor-free Flt3-Cre^{YFP} mice.

(B) Percentage of YFP-negativity in indicated leukocytes from 15-month-old tumor-free Flt3-Cre^{YFP} mice. (n=3).

(C) Representative flow cytometry plots showing YFP and MHCII signals in macrophages from normal pancreas of orthotopic KPC-1 tumors.

(D) Percentage of YFP-negativity in MHCII^{Hi} and MHCII^{Low} macrophage subsets in normal pancreas and orthotopic KPC-1 tumors.

(E) Representative flow cytometry plots of pimonidazole (PIMO) signals in indicated TAM subsets.

(F) MFI of PIMO signals in indicated TAM subsets from (E).

Data are shown as mean ± SEM and ∗ denotes $p<0.05$ by t-test.

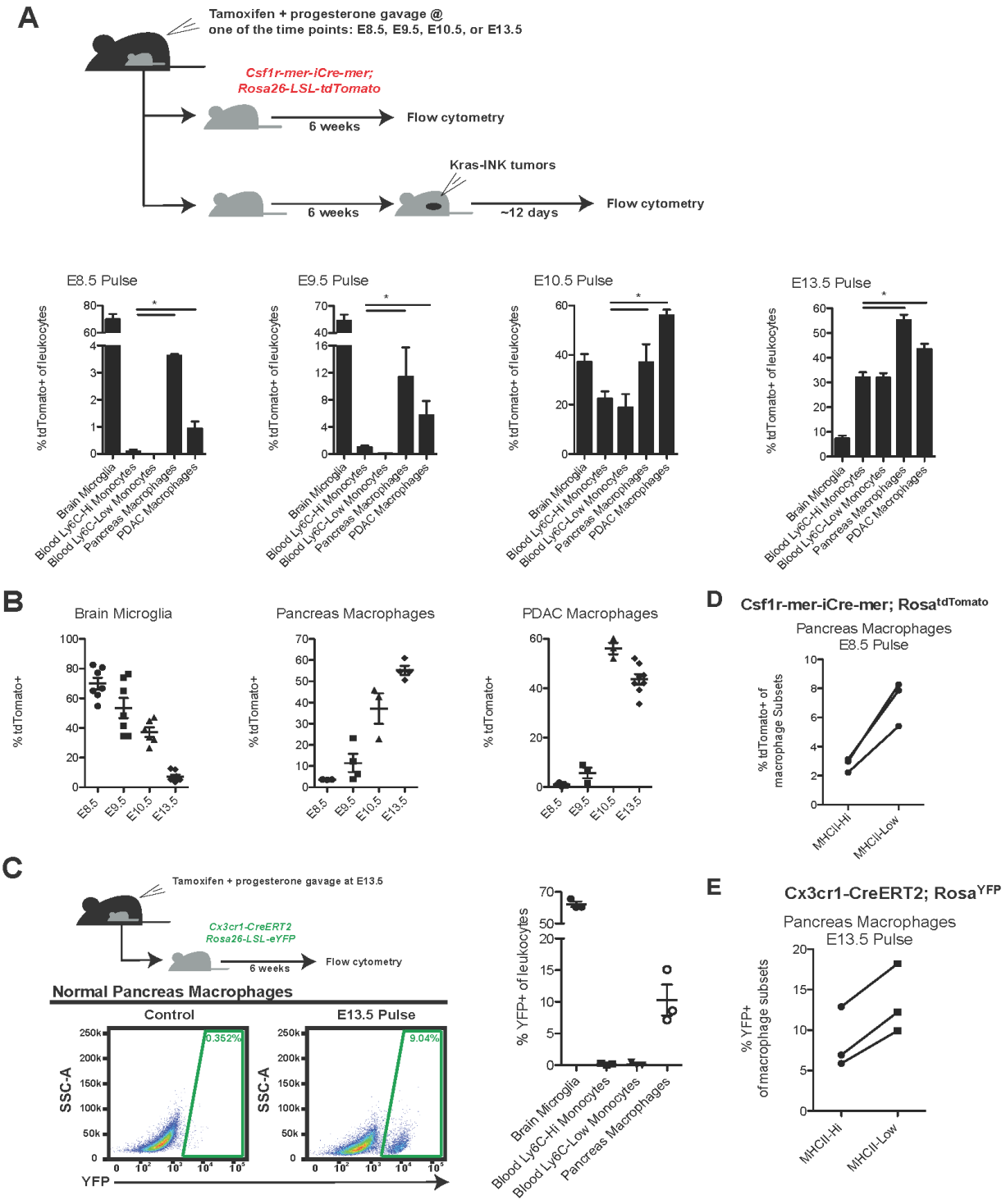
A
Tamoxifen + progesterone gavage @
one of the time points: E8.5, E9.5, E10.5, or E13.5
Csf1r-mer-iCre-mer;
Rosa26-LSL-tdTomato
6 weeks
Flow cytometry
Kras-INK tumors
6 weeks
~12 days
Flow cytometry
E8.5 Pulse
E9.5 Pulse
E10.5 Pulse
E13.5 Pulse
% tdTomato+ of leukocytes
Brain Microglia
Blood Ly6C-Hi Monocytes
Blood Ly6C-Low Monocytes
Pancreas Macrophages
PDAC Macrophages
B
Brain Microglia
Pancreas Macrophages
PDAC Macrophages
% tdTomato+
E8.5
E9.5
E10.5
E13.5
C
Tamoxifen + progesterone gavage at E13.5
Cx3cr1-CreERT2
Rosa26-LSL-eYFP
6 weeks
Flow cytometry
Normal Pancreas Macrophages
Control
E13.5 Pulse
0.352%
9.04%
SSC-A
YFP
% YFP+ of leukocytes
D
Csf1r-mer-iCre-mer; Rosa tdTomato
Pancreas Macrophages
E8.5 Pulse
% tdTomato+ of macrophage Subsets
MHCII-Hi
MHCII-Low
E
Cx3cr1-CreERT2; Rosa YFP
Pancreas Macrophages
E13.5 Pulse
% YFP+ of macrophage subsets
MHCII-Hi
MHCII-Low

Figure 3.12, related to Figure 3.5. Yolk Sac and Fetal Liver Derived Pancreatic Macrophages are Present in the Pancreas and PDAC of Adult Mice and are Enriched in the MHCII^{Low} Subset.

(A) Csf1r-Mer-iCre-Mer; Rosa26-LSL-tdTomato mice were treated with tamoxifen at indicated time points. Labeling efficiency in indicated leukocyte populations was analyzed by flow cytometry. (n=3-7/group)

(B) Kinetics of labeling efficiency in brain microglia, pancreas macrophages, and PDAC TAMs from (A).

(C) Cx3cr1-CreERT2; Rosa26-LSL-eYFP mice were treated with tamoxifen at E13.5. Labeling efficiency in indicated leukocyte populations was analyzed by flow cytometry. Representative flow cytometry plots of YFP signals in pancreatic macrophages are shown.

(D) Labeling efficiency of CSF1R^{+} cells in pancreatic macrophage subsets from (A-B).

(E) Labeling efficiency of CX3CR1^{+} cells in pancreatic macrophage subsets from (C).

Data are shown as mean ± SEM and ∗ denotes $p<0.05$ by t-test.

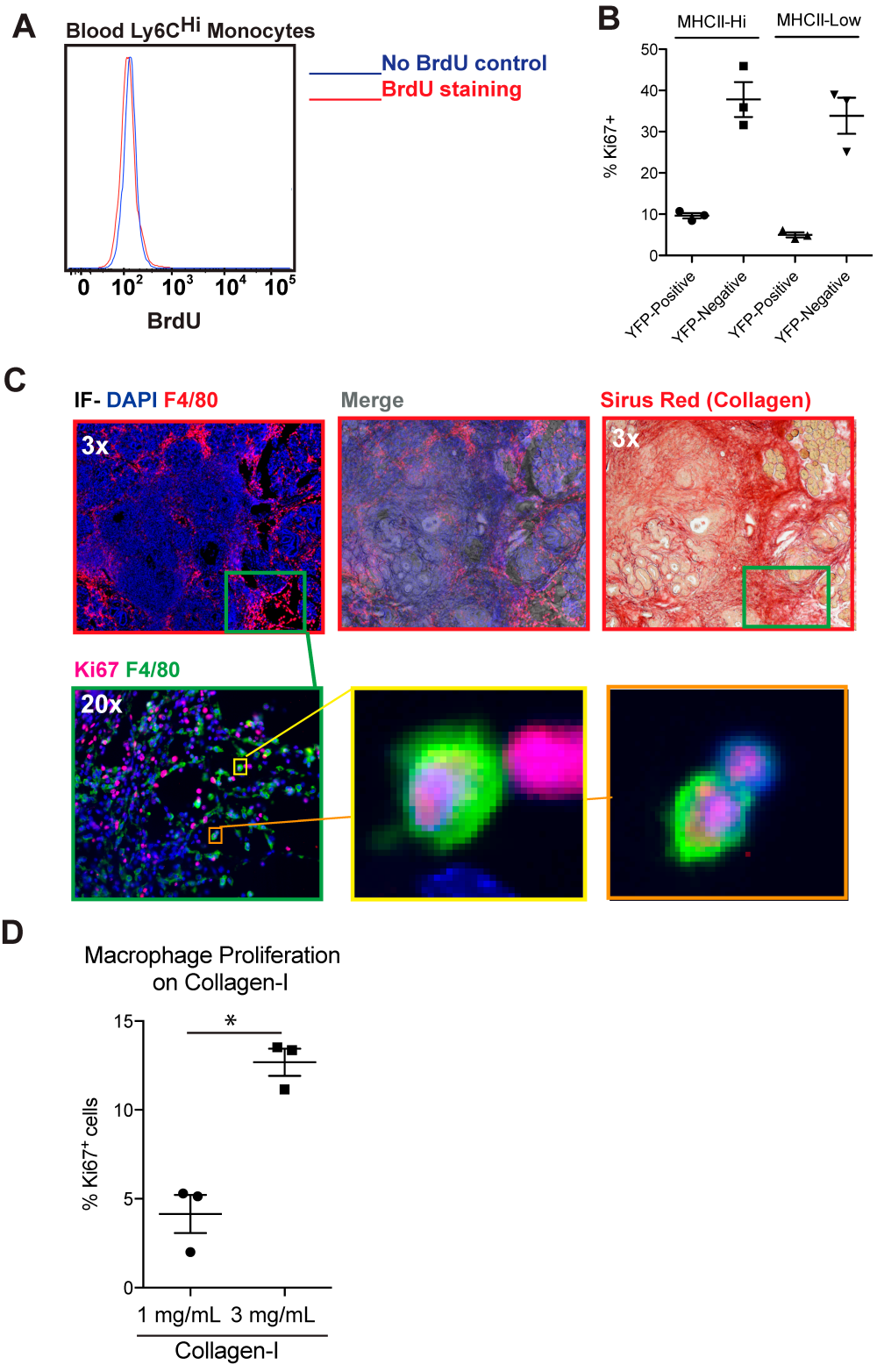
A
Blood Ly6C^Hi Monocytes
No BrdU control
BrdU staining
0
10^2
10^3
10^4
10^5
BrdU
B
MHCII-Hi
MHCII-Low
% Ki67+
50
40
30
20
10
0
YFP-Positive
YFP-Negative
YFP-Positive
YFP-Negative
C
IF- DAPI F4/80
Merge
Sirus Red (Collagen)
3x
3x
Ki67 F4/80
20x
D
Macrophage Proliferation
on Collagen-I
% Ki67+ cells
15
10
5
0
*
1 mg/mL
3 mg/mL
Collagen-I

Figure 3.13, related to Figure 3.6. *In Situ* Proliferating Macrophages Localize in Proximity to Fibrotic Tumor Areas.

(A) Representative flow cytometry plot showing 3-hour BrdU incorporation in blood Ly6C^{Hi} monocytes.

(B) Percentage of Ki67 positivity in indicated TAM subsets of KPC-1 tumor-bearing Flt3-Cre^{YFP} mice.

(C) Serial sections from autochthonous KPC tumors were stained for macrophages (F4/80) and proliferation marker Ki67. Inlets demonstrate double positive cells. Fibrosis was assessed in the adjacent section by Sirius Red staining.

(D) Bone marrow-derived macrophages were cultured on collagen I at different densities. Percent of Ki67 positivity were quantified by immunofluorescence staining.

Data are shown as mean ± SEM and ∗ denotes $p<0.05$ by t-test.

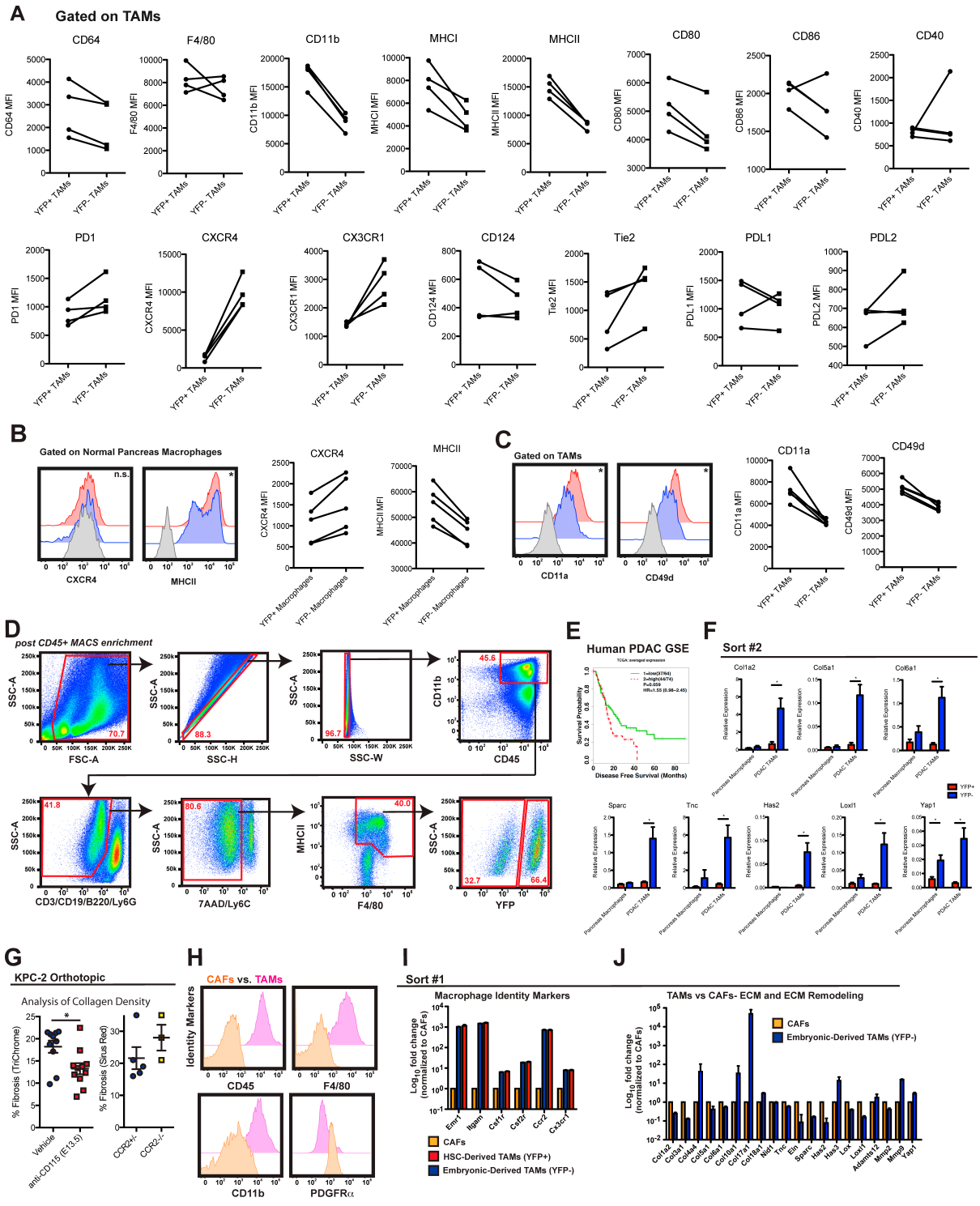
A
Gated on TAMs
CD64
F4/80
CD11b
MHCI
MHCII
CD80
CD86
CD40
PD1
CXCR4
CX3CR1
CD124
Tie2
PDL1
PDL2
YFP+ TAMs
YFP- TAMs
B
Gated on Normal Pancreas Macrophages
n.s.
CXCR4
MHCII
YFP+ Macrophages
YFP- Macrophages
C
Gated on TAMs
CD11a
CD49d
D
post CD45+ MACS enrichment
FSC-A
SSC-H
SSC-W
CD45
CD3/CD19/B220/Ly6G
7AAD/Ly6C
F4/80
YFP
E
Human PDAC GSE
Survival Probability
Disease Free Survival (Months)
F
Sort #2
Col1a2
Col5a1
Col6a1
Sparc
Tnc
Has2
Loxl1
Yap1
Pancreas Macrophages
PDAC-TAMs
YFP+
YFP-
G
KPC-2 Orthotopic
Analysis of Collagen Density
% Fibrosis (TriChrome)
% Fibrosis (Sirius Red)
Vehicle
anti-CD115 (E13.5)
CCR2+/-
CCR2-/-
H
CAFs vs. TAMs
Identity Markers
CD45
F4/80
CD11b
PDGFRα
I
Sort #1
Macrophage Identity Markers
Log10 fold change (normalized to CAFs)
Emr1
Itgam
Csf1r
Csf2r
Ccr2
Cx3cr1
CAFs
HSC-Derived TAMs (YFP+)
Embryonic-Derived TAMs (YFP-)
J
TAMs vs CAFs- ECM and ECM Remodeling
CAFs
Embryonic-Derived TAMs (YFP-)
Col1a1
Col3a1
Col4a1
Col5a1
Col6a1
Col10a1
Col17a1
Col18a1
Mdt1
Tnc
Ein
Sparc
Has2
Has3
Lox
Loxl1
Adamts12
Mmp2
Mmp9
Yap1

Figure 3.14, related to Figure 3.7. Embryonically Derived TAMs Have Distinct Surface Marker Expression and Unique Pro-fibrotic Transcriptional Profile.

(A) MFI of indicated markers in TAMs from orthotopic KPC-1 tumors in Flt3-Cre^{YFP} mice. Value is calculated by deducting baseline MFI of isotype staining control from the MFI of stained samples.

(B) MFI of CXCR4 and MHCII in normal pancreatic macrophages. Representative histograms are shown.

(C) MFI of CD11a and CD49d in TAMs from orthotopic KPC-1 tumors in Flt3-Cre^{YFP} mice. Representative histograms are shown.

(D) Representative flow cytometry plots showing gating strategies used to sort YFP-positive and -negative TAMs from Flt3-Cre^{YFP} mice.

(E) Kaplan-Meier analysis of patient cohorts stratified by expression level of genes that are higher in Flt3-Cre$^{YFP\text{-}negative}$ TAMs based on analysis in **Figure 3.7B**.

(F) Q-PCR analyses of indicated genes in Flt3-Cre$^{YFP\text{-}positive}$ (red) and Flt3-Cre$^{YFP\text{-}negative}$ (blue) TAMs in a second repeat of sorting. (n=5/group for normal pancreas macrophages, n=6/group for TAMs).

(G) Quantification of PDAC collagen density by image analysis of Trichrome or Sirus Red staining on orthotopic KPC-2 tumors implanted in mice treated with anti-CD115 at E13.5 or CCR2$^{-/-}$ mice or control mice.

(H) Expression of listed surface markers in cancer-associated fibroblasts (CAFs) (orange) and TAMs (pink).

(I) Q-PCR analyses of indicated genes coding for macrophage surface identity markers in cancer-associated fibroblasts (CAFs) (orange), Flt3-Cre$^{YFP\text{-}positive}$ (red) and Flt3-Cre$^{YFP\text{-}negative}$ (blue) TAMs. (n=6/group for TAMs)

(J) Q-PCR analyses of indicated genes coding for ECM production and modification molecules in cancer-associated fibroblasts (CAFs) (orange) and Flt3-Cre$^{YFP\text{-}negative}$ TAMs (blue). (n=6/group for TAMs)

Data are shown as mean ± SEM and ∗ denotes $p<0.05$ by t-test.

Table 3.1, Top 40 Genes Higher in the Flt3-Cre$^{YFP\text{-}Negative}$ TAM subset on Microarray

Entrez Gene ID	Gene Symbol	Fold Change (YFP-Negative vs. -Positive)	Adjusted p-Value
16949	*Loxl1*	63.289225	0.000875412
20319	*Sfrp2*	49.434489	0.002976931
14125	*Fcer1a*	47.168637	0.001479908
13078	*Cyp1b1*	46.682438	0.000577909
12833	*Col6a1*	44.095025	0.005380821
14107	*Fat1*	43.982448	0.00067664
17022	*Lum*	43.106335	0.002411298
20716	*Serpina3n*	42.226946	2.36575E-06
107449	*Unc5b*	37.411451	6.02918E-05
21923	*Tnc*	36.737766	1.75967E-05
12834	*Col6a2*	33.948455	0.0107914
13179	*Dcn*	32.864451	0.000918713
109624	*Cald1*	32.081952	0.009871551
20692	*Sparc*	30.158108	0.002911626
12945	*Dmbt1*	29.555895	0.002827771
71228	*Dlg5*	28.841214	0.000450364
218952	*Fermt2*	28.552239	0.000900703
12873	*Cpa3*	28.488505	0.009611972
50781	*Dkk3*	28.452825	0.000765057
16948	*Lox*	28.392067	2.20501E-05
18073	*Nid1*	26.763409	0.006042784
13602	*Sparcl1*	26.16561	0.02195566
18028	*Nfib*	24.737366	0.0450516
242608	*Podn*	23.756922	0.001129132
16948	*Lox*	23.563272	0.000163479
170643	*Kirrel*	23.48621	0.004143432
19662	*Rbp4*	23.361095	0.000281845
22601	*Yap1*	22.207021	0.001841186
67701	*Wfdc2*	22.1382	0.001520571
12111	*Bgn*	22.120345	0.004549826
69675	*Pxdn*	22.116972	0.003057716
12831	*Col5a1*	22.061485	0.004469495
17534	*Mrc2*	21.234791	0.001029897
18596	*Pdgfrb*	21.193765	0.003426061
17153	*Mal*	21.021883	0.000893123
15228	*Foxg1*	21.009472	0.000115044
239337	*Adamts12*	20.932199	0.008746559
12842	*Col1a1*	20.290887	0.000281845
17112	*Tm4sf1*	19.497997	0.00545794
66773	*Gm17019*	19.069459	0.000785569

Table 3.2, Mouse Antibodies for Flow Cytometry and FACS

Antigen	Clone	Fluorophore	Source
B220	RA3-6B2	APC	BioLegend
BrdU	3D4	FITC	BD Bioscience
CD3	145-2C11	APC, PerCP-Cy5.5	eBioscience
CD11a	M17/4	PE	BioLegend
CD11b	M1/70	Alexa700, PE-Cy7	eBioscience
CD16/CD32	93	Unconjugated	eBioscience
CD19	eBio1D3	APC	eBioscience
CD40	1C10	PE-Cy5	eBioscience
CD45	30-F11	PE-Cy7, APC-Cy7	eBioscience
CD45.1	A20	APC	eBioscience
CD45.2	104	FITC	eBioscience
CD49d	R1-2	PE	BioLegend
CD64	X54-5/7.1	PE	eBioscience
CD68	FA-11	FITC	eBioscience
CD80	16-10A1	PE-Cy5	eBioscience
CD86	GL1	PE-Cy5	eBioscience
CD115	AFS98	PE	eBioscience
		BV605	BioLegend
CD124	mIL4R-M1	PE	BD Biosciences
CD206	MR5D3	FITC	AbD Serotec
	C068C2	PE-Cy7	BioLegend
CX3CR1	SA011F11	PE	BioLegend
CXCR4	2B11	PerCP-eFluor710	eBioscience
F4/80	BM8	PE-Cy5, PE	eBioscience
Keratin	C11	Alexa488	Cell Signaling
Ki67	SolA15	FITC	eBioscience
	16A8	BV605	BioLegend
Ly6C	HK1.4	PerCP-Cy5.5, Alexa488	eBioscience
Ly6G	1A8	PE	eBioscience
		APC	BioLegend
MerTK	108928	PE	R&D
	DS5MMER	PE-Cy7	eBioscience
MHCI	34-1-2S	PE	eBioscience
MHCII	M5/114.15.2	eFluor450, APC-Cy7	eBioscience
PD1	J43	PE	eBioscience
PDGFRα	APA5	PE	eBioscience
PDL1	MIH5	PE	eBioscience
PDL2	122	PE	eBioscience
SiglecF	ES22-10D8	APC, PE-Vio770	Miltenyi
	E50-2440	PE	BD Biosciences
Tie2	TEK4	PE	BioLegend

Table 3.3, Antibodies for Immunofluorescence Staining

Antigen	Clone	Species	Source
CD68	KP-1	Mouse anti-human	NeoMarkers
	Polyclonal Ab125212	Rabbit anti-mouse	Abcam
CD163	EPR19518	Rabbit anti-human	Abcam
CD206	Polyclonal Ab64693	Rabbit anti-human	Abcam
Collagen I	3G3	Rabbit anti-mouse	Abcam
Collagen IV	Polyclonal Ab6586	Mouse anti-mouse	Abcam
CXCR4	D4Z7W	Rabbit anti-human/mouse	Cell Signaling
F4/80	BM8	Rat anti-mouse	eBioscience
Ki67	MIB-1	Mouse anti-human	DaKo
	Polyclonal Ab15580	Rabbit anti-mouse	Abcam
Pan-Keratin	C11	Anti-Human/Mouse	Cell Signaling

Table 3.4. Human Antibodies for Flow Cytometry and FACS

Antigen	Clone	Fluorophores	Source
CD3	HIT3a	PE	BD Biosciences
CD11b	ICRF44	Alexa488	BioLegend
CD14	61D3	Qdot605	eBioscience
CD16	3G8	PE	BD Biosciences
CD19	HIB19	PE	BD Biosciences
CD45	2D1	APC-Cy7	BD Biosciences
CD115	12-3A3-1B10	PE-Cy7	eBioscience
CXCR4	12G5	Alexa488	R&D Systems
		PerCP-Cy5.5	eBioscience
HLA-DR	L243	eFluor450	eBioscience

Chapter 4: Future Directions

4.1 Reprogramming myeloid responses to improve cancer immunotherapies

Therapeutics that activates anti-tumor immune responses has demonstrated significant potential for the treatment of solid tumors. One of the most promising strategies targets immune checkpoint molecules, such as programmed death 1 (PD1) or cytotoxic T lymphocyte-associated antigen 4 (CTLA4) (Simpson et al., 2013). These immune checkpoint molecules counteract pro-inflammatory signals and block anti-tumor T cell activities. The potential of this type of strategies was demonstrated by the efficacy of CTLA4 antagonistic antibody, ipilimumab, in the treatment of subsets of metastatic melanoma (Hodi et al., 2010), as well as recent FDA approval of PD1 for the same indication. Another category of immunotherapies involves tumor vaccination through adoptive transfer of tumor antigen-specific T cells or dendritic cells (Rosenberg et al., 2008). An example is Sipuleucel-T, an autologous dendritic cell-based vaccination designed to activate T cells targeting a prostate cancer antigen, which significantly improved patient overall survival in a phase III trial (Kantoff et al., 2010). Despite clear efficacy in subsets of human cancer, these approaches are not effective in all patients or all cancer types. For example, although ipilimumab achieved impressive response rates in melanoma patients, it failed as a monotherapy to improve clinical outcome of patients with pancreatic cancer (Royal et al., 2010).

One possible explanation for the lack of responses in many patients to immunotherapy is the presence of a suppressive immune microenvironment. While tumor antigen-specific T cells may be present in many cancers, the immune infiltrate is often dominated by various subsets of myeloid cells. Tumor-infiltrating suppressive myeloid cells include macrophages, immature

dendritic cells, and monocytic or granulocytic myeloid-derived suppressor cells (MDSCs). These suppressive cells can silence adaptive immune responses by blocking the recruitment of cytotoxic T lymphocytes (CTLs) to the tumor tissue, metabolically inhibiting CTL functions, chemically modifying T cell receptors to hinder the recognition of tumor antigens, and/or amplifying immune suppression via the expansion of regulatory T cells (Gabrilovich and Nagaraj, 2009; Qian and Pollard, 2010). Altogether, these myeloid cell activities can allow tumor cells to evade endogenous and treatment-elicited immune surveillance. Therefore, these subsets of suppressive myeloid cells could impose significant limitations on efficient immunotherapies (**Figure 4.1**). Correspondingly, strategies to manipulate suppressive myeloid cells may also provide opportunities to improve the efficacy of immunotherapy. Several recent studies demonstrated that combining therapeutics that alleviates immune suppression by targeting myeloid cell activities could improve the outcome of immunotherapy in mouse models.

Work from our own group assessed if targeting tumor-associated macrophages (TAMs) could mitigate immune suppression and improve immunotherapy in pancreatic ductal adenocarcinoma (PDAC) models (Zhu et al., 2014). We targeted TAMs through the inhibition of macrophage colony-stimulating factor receptor (CSF1R) signaling, which plays an essential role in macrophage differentiation, trafficking, and survival. Blockade of CSF1R signaling not only reduced the total number of suppressive macrophages in the tumor tissue, but also reprogrammed the remaining TAMs to support anti-tumor T cell responses, as shown by elevated interferon expression, reduced immunosuppressive activities, and improved antigen presentation capacity in the remaining TAMs. One unwanted consequence of CSF1R signal blockade is the upregulation of programmed death ligand 1 (PDL1) in tumor cells and CTLA4 in T cells, which potentially poses a significant limitation on the efficacy of CSF1R blockade. However, this may

also provide an opportunity to convert tumors that are unresponsive to PD1/CTLA4 antagonists to be more sensitive to checkpoint-based immunotherapeutics. Based on this rationale, we designed a combination therapy by coupling CSF1/CSF1R signal blockade with immune checkpoint antagonists in murine PDAC models. While checkpoint inhibitors alone achieved limited efficacy in restraining tumor growth, the addition of CSF1R blockade markedly improved the efficacy of PD1 and CTLA4 antagonists and led to regression of well-established tumors (Zhu et al., 2014). These data demonstrated that CSF1R signal blockade could render tumors more responsive to checkpoint antagonist-based therapies. Similarly, work by Mok *et al.* showed that targeting TAMs through CSF1R blockade could also enhance the efficacy of adoptive cell transfer (ACT)-based immunotherapy to reduce tumor burden in a mouse melanoma model (Mok et al., 2014). Interestingly, these tumor restraining effects correlated with increased expansion of adoptively transferred T cells both in the tumor and in peripheral lymphoid tissues, suggesting that reprograming myeloid responses could lead to increased anti-tumor T cell function systemically. Taken together, these studies indicate that mitigation of immune suppression through depletion or reprogramming of TAMs could enhance the clinical outcomes of checkpoint-based therapeutics and adoptive cell transfer-based immunotherapies.

It is important to note that innate immune cells other than macrophages are also promising targets. Examples include neutrophils, which are similarly abundant in many types of cancers. In a syngeneic murine rhabdomyosarcoma model, Highfill *et al.* demonstrated that an immunosuppressive microenvironment driven by granulocytic MDSC populations suppresses the efficacy of anti-PD1 treatment (Highfill et al., 2014). In human sarcoma patients and mouse models, tumor cells often overexpress a family of C-X-C motif chemokines, including CXCL1, 2, and 8. Their predominant receptor, CXCR2, is expressed on granulocytes and promotes

granulocytic MDSC trafficking into tumor sites. Inhibition of CXCR2 signaling blocked the recruitment of granulocytic MDSCs to the tumor site and significantly enhanced the efficacy of PD1 blockade. These data suggest that responses to immune checkpoint blockade are limited by the suppressive microenvironment driven by granulocytes, and that alleviation of this suppression could improve the efficacy of checkpoint-based therapies.

In conclusion, the suppressive tumor microenvironment driven by myeloid cells may pose a major limitation on the efficiency of immunotherapy. Therefore, combining immunotherapy with strategies that reprogram the suppressive tumor microenvironment holds significant promises in cancer treatment (**Figure 4.1**). Development of such strategies will require careful evaluation, as tumor cells, immune responses, and chosen therapeutic strategies all interact in a complex and dynamic manner. Future work is needed to determine which myeloid populations mediate suppression in specific tumor types, and what immunotherapeutic strategies are optimal for combination.

4.2 Regulation of tissue resident macrophages

Having identified the contribution of pancreas resident macrophages to TAM populations in PDAC, the logical next question is how we can target these cells to improve cancer treatment. Solution to this question relies on better understanding of the basic biological activities of tissue resident macrophages.

Tissue resident macrophages face two major challenges throughout the life of an organism. First, they need to self-maintain long-term both during homeostatic conditions and during aging. Second, they need to be able to expand to meet the proliferative demands upon pathological challenges, exemplified by the case of tumor development. To persist with aging,

tissue resident macrophages could be replenished through self-renewal. However, based on propidium iodine staining and BrdU incorporation assays, we saw very minimal level of apoptosis and proliferation in pancreas resident macrophages under homeostatic conditions. While low level of "tonic" proliferation could sustain long-term self-renewal, this could also suggest a second possibility that tissue resident macrophages persist through longevity. Further experiments are needed to distinguish between these two possibilities. One approach would be to perform a pulse chase experiment, such as BrdU or doxycycline-inducible H2B-GFP pulse. During the extended pulse period in young adult mice, tissue resident cells will be labeled as BrdU-or GFP-positive. The dilution or retention of the BrdU/GFP signals would tell us whether proliferation or longevity is responsible for the maintenance of tissue resident macrophages during aging.

On the other hand, embryonically derived macrophages dramatically enhance their proliferative activities during tumor challenge. Concomitantly, molecules involved in both extrinsic and intrinsic apoptosis pathways are upregulated, leading to elevated level of apoptosis. This suggests that as embryonically derived macrophages expand through in situ proliferation, these cells achieve high turnover rates at the expense of the longevity machinery. It is important to note that we only observed proliferation in a small fraction of tumor-associated macrophages. This leads us to ask: during tumor progression, is the proliferative activity restricted to a small subset of macrophages with progenitor-like properties, or is the macrophage pool simply a uniform collection of terminally differentiated cells that undergo proliferation in a stochastic manner? The current paradigm supports the latter, despite the lack of sufficient number of studies to support these claims. Hashimoto *et al.* attempted to address this question using a combination of a diphtheria toxin (DT)-mediated macrophage double depletion model with BrdU

pulse-chase experiment. They treated CD169-DTR (diphtheria toxin receptor) with DT to deplete lung resident macrophages, and treated mice with daily doses of BrdU for 11 days, at the end of which the lung macrophage numbers recovered to pre-treatment level. Following a BrdU-free chase period, they treated mice again with one dose of DT, and analyzed cell cycle status 2 days later based on Ki67 staining. The prediction was that if there were progenitor-like cells within the macrophage population, the Ki67 positive cells, which indicate cell repopulation during the second recovery, would be restricted to the BrdU-labeled subset, i.e. cells that have proliferated during the first recovery. On contrary, if macrophages stochastically proliferate to repopulate, a fraction of Ki67-positive cells could be observed in both the BrdU-labeled and BrdU-negative cells. Indeed, the latter is what they observed, suggesting that lung macrophages proliferate in a stochastic model to repopulate, at least in this model (Hashimoto et al., 2013). Similarly, in a CX3CR1-CreER-based pulse-chase experiment, Bruttger *et al.* demonstrated that upon depletion using the DTR system, microglia repopulate possibly in a stochastic manner from a pre-existing population labeled by tamoxifen (Bruttger et al., 2015). On the contrary, in a different depletion experiment using CSF1R blockade, Elmore *et al.* showed that $CX3CR1^{+}$ microglia repopulate through in situ proliferation of a $CX3CR1^{-}$ progenitor population (Elmore et al., 2014). Further characterization showed the expression of Nestin and IB4 in these population, which are markers not associated with microglia. Despite being positive for IBA1, which indicates microglia identity, these progenitor-like cells also express c-Kit and CD34, which are expressed in hematopoietic stem and progenitor cells. This study showed the possible existence of a progenitor subset that is capable of sustaining tissue macrophages, at least during the recovery of these cells.

In murine pancreatic ductal adenocarcinoma models, not all macrophages seem to expand during tumor progression. In the CSF1R-mer-iCre-mer; Rosa26-LSL-tdTomato lineage tracing model, yolk sac-derived macrophages can be labeled upon tamoxifen induction on E8.5 or E9.5. Labeled cells persist in adult mice and further expand numerically in established tumors **(Figures 3.5 and 3.12)**. However, in the CX3CR1-CreER; Rosa26-LSL-eYFP model, E13.5 tamoxifen treatment led to the labeling of a significant percentage of macrophages in normal pancreas of adult mice. However, the labeled population was dramatically decreased. Similarly, if we treat mice of this genotype in adulthood with 30 days of tamoxifen labeling followed by tumor implantation, the number of tamoxifen labeled macrophages was decreased in established tumors. This suggests the possibility that a population of $CX3CR1^{Low/Neg}$ macrophages residing the pancreas actively proliferated during tumor progression and replaced the $CX3CR1^{Hi}$ subset. Further experiments are needed to address the possibility that a macrophage progenitor subset is responsible for the expansion of tissue resident macrophages during PDAC progression.

In order to target tissue resident macrophages, we need to understand what signals regulate their proliferation, and what stromal components produce these signals. These signals require tight regulation for several reasons. First, these signals need to be inhibited at steady state, so that the cells do not prematurely exhaust their proliferative potential that precludes their persistence with aging. Second, these signals need to be recognized to activate division cycles before the proliferative demands are overwhelmed. Preliminary data demonstrate that loss of microbiota induces the expansion of macrophage numbers in normal pancreas (not shown), suggesting that signaling pathways downstream of certain pattern recognition receptors could mediate the quiescence of tissue resident macrophages. Alternatively, microbiota could educate some other circulating leukocytes, which then suppress the proliferative activities of pancreas

resident macrophages. It would be interesting to see if microbiota is altered in PDAC-bearing mice to change the *in situ* proliferation of embryonically derived TAMs.

Microarray analyses of embryonically derived and hematopoietic stem cell-derived macrophages in normal pancreas and PDAC also demonstrated potential signaling pathways that mediate macrophage proliferation. A number of receptors are upregulated in the embryonically derived macrophages, including I-7 receptor, Frizzled B, cKit, CD44, CXCR4, CXCR7, CCR2, Endothelin receptor A, Ephrin A2, TGF beta receptor 1, nuclear hormone receptors (NR4A1, NR4A3, Retinoic acid receptor alpha 2), and GPR132. Comparison between embryonically derived and HSC-derived TAMs demonstrated that embryonically derived TAMs have higher level of TGF beta-receptor 3, FGF receptor like-1, Frizzled 1, and N-cadherin genes. Interestingly, among the genes in the embryonic macrophages that are upregulated by the tumor, three genes remained higher than their monocyte-derived TAM counterparts: PDGF receptor beta, Frizzled 4, and secreted Frizzled-related protein 2 (Sfrp2). Both Frizzled 4 and Sfrp2 are involved in Wnt signaling pathways. The identification of interesting targets suggests that we could explore the potential relevance of PDGF and Wnt signaling pathways in the regulation of TAM proliferation.

Lastly, it is important to note that the pathways that mediate TAM proliferation and functionality may be uncoupled. CXCR4 is a unique marker of embryonically derived macrophages, and its specificity is only manifested in PDAC but not normal pancreas. Treatment of orthotopic PDAC-bearing mice did not alter TAM numbers or proliferation (data not shown). However, it would be interesting to see if CXCR4 signaling is involved in shaping the functions of the embryonically derived TAM subset.

4.3 Targeting the cancer cell-macrophage-fibrosis triad

As we develop therapeutic strategies to target the cancer microenvironment, it is important to note that not all tumor types are created equal. Each tumor has its unique stromal structure that needs to be considered.

Two hallmarks of pancreatic ductal adenocarcinoma are the extensive myeloid infiltration and dense desmoplastic reactions characterized by high level of fibrosis. High levels of macrophage infiltration predict worse survival duration for PDAC patients (DeNardo et al., 2011; Ino et al., 2013), making them a good therapeutic target. Indeed, depletion of TAMs in murine models of PDAC decreased tumor infiltrating cells, relieved immunosuppression, and improved responses to both chemotherapies and checkpoint-based immune therapies (Mitchem et al., 2013; Zhu et al., 2014). On the other hand, fibrosis is considered to be another major barrier of PDAC treatment. While fibrosis was originally considered to provide a mechanical encapsulation that contains the primary tumor and prevents its spread, high level of fibrosis was later found to negatively correlate with patient outcome. Excessive amount of fibrosis increases interstitial fluid pressures, induces collapses of vasculature, and presents major physical barriers to perfusion and diffusion of small molecule-based therapeutics (Provenzano et al., 2012). Therefore, alleviation of fibrotic elements in the stroma, by targeting hyaluronan acid for example, enhances the delivery of chemotherapies and improves overall survival in preclinical mouse models. Alternatively, targeting tumor cell-intrinsic pathways, such as the focal adhesion kinase pathway, to reduce fibrosis also improves chemotherapy and checkpoint-based and adoptive cell transfer-based immunotherapies (Jiang et al., 2016). It is important to note that while fibroblast cells are the major source of fibrosis, simply stripping fibroblasts may not generate favorable outcome (Ozdemir et al., 2014). This could be due to the heterogeneity in the

quality of fibrosis: certain configurations of extracellular matrix structure could be necessary for anti-tumor activities. Therefore, it may be more favorable to reprogram tumor cells or fibroblasts to alleviate fibrosis, or alter the qualities of the ECM components. It would be interesting to see if macrophages could serve as a target during these processes. Our study demonstrated that myeloid cells, in particular tissue resident macrophages of embryonic origin, are involved in the modulation of fibrosis. Fibrosis, in turn, could serve as a positive feedback loop to enhance the *in situ* proliferation of tissue resident macrophages. Therefore, it is possible to foresee a combination treatment option that combines the reprogramming of macrophages with the alleviation of desmoplasia.

4.4 Targeting the hematopoietic system to optimize tumor immunity

As we expand our knowledge of the tumor immune microenvironment, it is important to remind ourselves that the local immune microenvironment likely results from a systemic level of immune responses. Immune cells are not generated in isolation, but are provided by the hematopoietic system at different stages in various lymphoid organs, such as bone marrow, spleen, and embryonic organs including yolk sac and fetal liver. This is not only true in mouse models but also observed in human patients: patients not only show enhanced level of immune infiltration in the tumor tissue, but also have elevated level of circulating immune cells and increased production in the bone marrow. Change in the qualities of systemic immune cell production is also seen in the hematopoietic system, as shown by the expansion of myeloid progenitors at the expense of lymphoid production (Casbon et al., 2015), which leads to increased myeloid-mediated immunosuppression coupled with impaired adaptive T cell cytotoxicity. Therefore, it is important to study how the hematopoietic differentiation pathways

are skewed in tumors, and how we can target these processes to combat cancer. Interestingly, bias towards myeloid expansion at the cost of lymphopoiesis is also seen during aging, suggesting the possibility that this skewed hematopoiesis during aging could contribute to cancer initiation by promoting chronic inflammation (Akunuru and Geiger, 2016; Geiger et al., 2013). In addition, knowledge of how tumors communicate with distant sites such as the bone marrow to modulate the immune system on an organismal level is still lacking. Such studies could provide insights into whether we can engineer an immune system from the source, i.e. hematopoietic stem and progenitor cells, and provide novel options that can further improve current immunotherapeutics.

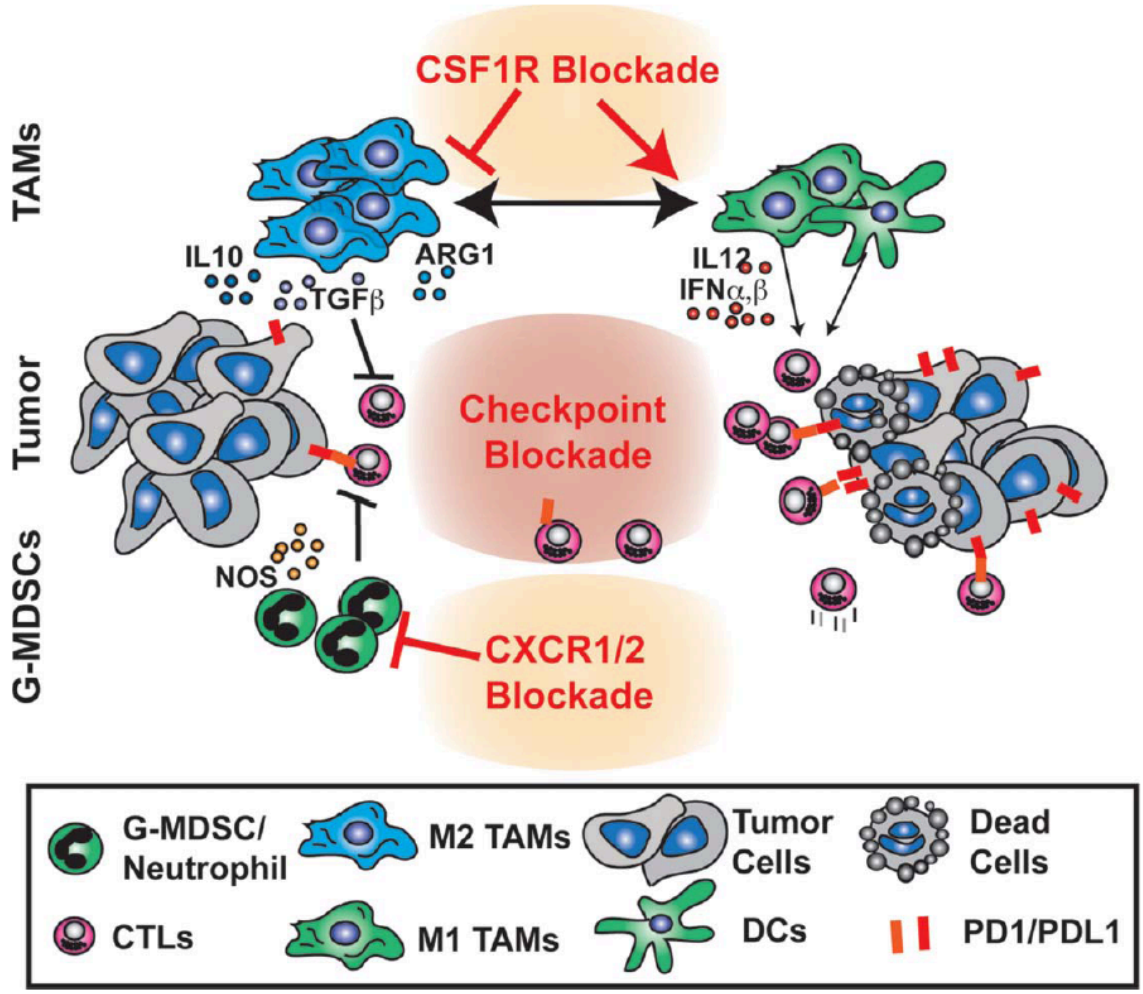

Figure 4.1. Reprogramming of the myeloid responses to enhance anti-tumor immunity.

Tumor tissues contain extensive infiltration of suppressive myeloid cells, such as tumor-associated macrophages (TAMs), immature dendritic cells (DCs), and granulocytic myeloid-derived suppressor cells (G-MDSCs), which inhibit anti-tumor activities of cytotoxic T lymphocytes (CTLs). Strategies to alleviate immune suppression mediated by these myeloid cells, such as using CSF1R inhibition or CXCR1/2 signal blockade, could reprogram these myeloid cells to activate the adaptive immune system and enhance the efficacy of immunotherapeutics to eliminate tumor cells.

References

Aaltonen, T., Adelman, J., Akimoto, T., Albrow, M.G., Alvarez Gonzalez, B., Amerio, S., Amidei, D., Anastassov, A., Annovi, A., Antos, J.*, et al.* (2009). Search for the associated production of the standard-model Higgs Boson in the all-hadronic channel. Phys Rev Lett *103*, 221801.

Afik, R., Zigmond, E., Vugman, M., Klepfish, M., Shimshoni, E., Pasmanik-Chor, M., Shenoy, A., Bassat, E., Halpern, Z., Geiger, T.*, et al.* (2016). Tumor macrophages are pivotal constructors of tumor collagenous matrix. The Journal of experimental medicine *213*, 2315-2331.

Ajami, B., Bennett, J.L., Krieger, C., Tetzlaff, W., and Rossi, F.M. (2007). Local self-renewal can sustain CNS microglia maintenance and function throughout adult life. Nature neuroscience *10*, 1538-1543.

Akunuru, S., and Geiger, H. (2016). Aging, Clonality, and Rejuvenation of Hematopoietic Stem Cells. Trends in molecular medicine *22*, 701-712.

Amano, S.U., Cohen, J.L., Vangala, P., Tencerova, M., Nicoloro, S.M., Yawe, J.C., Shen, Y., Czech, M.P., and Aouadi, M. (2014). Local proliferation of macrophages contributes to obesity-associated adipose tissue inflammation. Cell metabolism *19*, 162-171.

Arandjelovic, S., and Ravichandran, K.S. (2015). Phagocytosis of apoptotic cells in homeostasis. Nature immunology *16*, 907-917.

Artis, D.R., Bremer, R., Gillette, S., Hurt, C.R., Ibrahim, P.L., and Zuckerman, R.L. (2005). Molecular Scaffolds for Kinase Ligand Development (United States: Plexxikon, Inc.).

Aurora, A.B., Porrello, E.R., Tan, W., Mahmoud, A.I., Hill, J.A., Bassel-Duby, R., Sadek, H.A., and Olson, E.N. (2014). Macrophages are required for neonatal heart regeneration. The Journal of clinical investigation *124*, 1382-1392.

Bain, C.C., Bravo-Blas, A., Scott, C.L., Gomez Perdiguero, E., Geissmann, F., Henri, S., Malissen, B., Osborne, L.C., Artis, D., and Mowat, A.M. (2014). Constant replenishment from circulating monocytes maintains the macrophage pool in the intestine of adult mice. Nature immunology *15*, 929-937.

Bain, C.C., Hawley, C.A., Garner, H., Scott, C.L., Schridde, A., Steers, N.J., Mack, M., Joshi, A., Guilliams, M., Mowat, A.M.*, et al.* (2016). Long-lived self-renewing bone marrow-derived macrophages displace embryo-derived cells to inhabit adult serous cavities. Nature communications *7*, ncomms11852.

Balaz, P., Friess, H., Kondo, Y., Zhu, Z., Zimmermann, A., and Buchler, M.W. (2002). Human macrophage metalloelastase worsens the prognosis of pancreatic cancer. Ann Surg *235*, 519-527.

Bayne, L.J., Beatty, G.L., Jhala, N., Clark, C.E., Rhim, A.D., Stanger, B.Z., and Vonderheide, R.H. (2012). Tumor-derived granulocyte-macrophage colony-stimulating factor regulates myeloid inflammation and T cell immunity in pancreatic cancer. Cancer cell *21*, 822-835.

Beatty, G.L., Chiorean, E.G., Fishman, M.P., Saboury, B., Teitelbaum, U.R., Sun, W., Huhn, R.D., Song, W., Li, D., Sharp, L.L.*, et al.* (2011). CD40 agonists alter tumor stroma and show efficacy against pancreatic carcinoma in mice and humans. Science *331*, 1612-1616.

Beatty, G.L., Winograd, R., Evans, R.A., Long, K.B., Luque, S.L., Lee, J.W., Clendenin, C., Gladney, W.L., Knoblock, D.M., Guirnalda, P.D.*, et al.* (2015). Exclusion of T Cells From Pancreatic Carcinomas in Mice Is Regulated by Ly6C(low) F4/80(+) Extratumoral Macrophages. Gastroenterology *149*, 201-210.

Ben-Mordechai, T., Holbova, R., Landa-Rouben, N., Harel-Adar, T., Feinberg, M.S., Abd Elrahman, I., Blum, G., Epstein, F.H., Silman, Z., Cohen, S.*, et al.* (2013). Macrophage subpopulations are essential for infarct repair with and without stem cell therapy. Journal of the American College of Cardiology *62*, 1890-1901.

Biswas, S.K., and Mantovani, A. (2010). Macrophage plasticity and interaction with lymphocyte subsets: cancer as a paradigm. Nature immunology *11*, 889-896.

Bleriot, C., Dupuis, T., Jouvion, G., Eberl, G., Disson, O., and Lecuit, M. (2015). Liver-resident macrophage necroptosis orchestrates type 1 microbicidal inflammation and type-2-mediated tissue repair during bacterial infection. Immunity *42*, 145-158.

Border, W.A., Okuda, S., Languino, L.R., and Ruoslahti, E. (1990). Transforming growth factor-beta regulates production of proteoglycans by mesangial cells. Kidney international *37*, 689-695.

Boulter, L., Govaere, O., Bird, T.G., Radulescu, S., Ramachandran, P., Pellicoro, A., Ridgway, R.A., Seo, S.S., Spee, B., Van Rooijen, N.*, et al.* (2012). Macrophage-derived Wnt opposes Notch signaling to specify hepatic progenitor cell fate in chronic liver disease. Nature medicine *18*, 572-579.

Bowman, R.L., Klemm, F., Akkari, L., Pyonteck, S.M., Sevenich, L., Quail, D.F., Dhara, S., Simpson, K., Gardner, E.E., Iacobuzio-Donahue, C.A.*, et al.* (2016). Macrophage Ontogeny Underlies Differences in Tumor-Specific Education in Brain Malignancies. Cell reports *17*, 2445-2459.

Boyer, S.W., Schroeder, A.V., Smith-Berdan, S., and Forsberg, E.C. (2011). All hematopoietic cells develop from hematopoietic stem cells through Flk2/Flt3-positive progenitor cells. Cell stem cell *9*, 64-73.

Brestoff, J.R., Kim, B.S., Saenz, S.A., Stine, R.R., Monticelli, L.A., Sonnenberg, G.F., Thome, J.J., Farber, D.L., Lutfy, K., Seale, P.*, et al.* (2015). Group 2 innate lymphoid cells promote beiging of white adipose tissue and limit obesity. Nature *519*, 242-246.

Bruttger, J., Karram, K., Wortge, S., Regen, T., Marini, F., Hoppmann, N., Klein, M., Blank, T., Yona, S., Wolf, Y.*, et al.* (2015). Genetic Cell Ablation Reveals Clusters of Local Self-Renewing Microglia in the Mammalian Central Nervous System. Immunity *43*, 92-106.

Calderon, B., Carrero, J.A., Ferris, S.T., Sojka, D.K., Moore, L., Epelman, S., Murphy, K.M., Yokoyama, W.M., Randolph, G.J., and Unanue, E.R. (2015). The pancreas anatomy conditions the origin and properties of resident macrophages. The Journal of experimental medicine *212*, 1497-1512.

Campbell, M.J., Tonlaar, N.Y., Garwood, E.R., Huo, D., Moore, D.H., Khramtsov, A.I., Au, A., Baehner, F., Chen, Y., Malaka, D.O.*, et al.* (2010). Proliferating macrophages associated with high grade, hormone receptor negative breast cancer and poor clinical outcome. Breast Cancer Res Treat.

Casbon, A.J., Reynaud, D., Park, C., Khuc, E., Gan, D.D., Schepers, K., Passegue, E., and Werb, Z. (2015). Invasive breast cancer reprograms early myeloid differentiation in the bone marrow to generate immunosuppressive neutrophils. Proceedings of the National Academy of Sciences of the United States of America *112*, E566-575.

Castellana, D., Paus, R., and Perez-Moreno, M. (2014). Macrophages contribute to the cyclic activation of adult hair follicle stem cells. PLoS biology *12*, e1002002.

Cattin, A.L., Burden, J.J., Van Emmenis, L., Mackenzie, F.E., Hoving, J.J., Garcia Calavia, N., Guo, Y., McLaughlin, M., Rosenberg, L.H., Quereda, V.*, et al.* (2015). Macrophage-Induced

Blood Vessels Guide Schwann Cell-Mediated Regeneration of Peripheral Nerves. Cell *162*, 1127-1139.

Chen, J., Feng, Y., Lu, L., Wang, H., Dai, L., Li, Y., and Zhang, P. (2012). Interferon-gamma-induced PD-L1 surface expression on human oral squamous carcinoma via PKD2 signal pathway. Immunobiology *217*, 385-393.

Chen, Z., Feng, X., Herting, C.J., Alvarez Garcia, V., Nie, K., Pong, W.W., Rasmussen, R., Dwivedi, B., Seby, S., Wolf, S.A.*, et al.* (2017). Cellular and molecular identity of tumor-associated macrophages in glioblastoma. Cancer research.

Chow, A., Huggins, M., Ahmed, J., Hashimoto, D., Lucas, D., Kunisaki, Y., Pinho, S., Leboeuf, M., Noizat, C., van Rooijen, N.*, et al.* (2013). CD169(+) macrophages provide a niche promoting erythropoiesis under homeostasis and stress. Nature medicine *19*, 429-436.

Coffelt, S.B., Hughes, R., and Lewis, C.E. (2009). Tumor-associated macrophages: effectors of angiogenesis and tumor progression. Biochimica et biophysica acta *1796*, 11-18.

Collin, M.P., Hart, D.N., Jackson, G.H., Cook, G., Cavet, J., Mackinnon, S., Middleton, P.G., and Dickinson, A.M. (2006). The fate of human Langerhans cells in hematopoietic stem cell transplantation. The Journal of experimental medicine *203*, 27-33.

Collisson, E.A., Sadanandam, A., Olson, P., Gibb, W.J., Truitt, M., Gu, S., Cooc, J., Weinkle, J., Kim, G.E., Jakkula, L.*, et al.* (2011). Subtypes of pancreatic ductal adenocarcinoma and their differing responses to therapy. Nature medicine *17*, 500-503.

Conway, J.G., McDonald, B., Parham, J., Keith, B., Rusnak, D.W., Shaw, E., Jansen, M., Lin, P., Payne, A., Crosby, R.M.*, et al.* (2005). Inhibition of colony-stimulating-factor-1 signaling in vivo with the orally bioavailable cFMS kinase inhibitor GW2580. Proceedings of the National Academy of Sciences of the United States of America *102*, 16078-16083.

Cortez-Retamozo, V., Etzrodt, M., Newton, A., Ryan, R., Pucci, F., Sio, S.W., Kuswanto, W., Rauch, P.J., Chudnovskiy, A., Iwamoto, Y.*, et al.* (2013). Angiotensin II drives the production of tumor-promoting macrophages. Immunity *38*, 296-308.

Coussens, L.M., Fingleton, B., and Matrisian, L.M. (2002). Matrix metalloproteinase inhibitors and cancer: trials and tribulations. Science *295*, 2387-2392.

Cumano, A., and Godin, I. (2007). Ontogeny of the hematopoietic system. Annual review of immunology *25*, 745-785.

De Palma, M., Venneri, M.A., Galli, R., Sergi Sergi, L., Politi, L.S., Sampaolesi, M., and Naldini, L. (2005). Tie2 identifies a hematopoietic lineage of proangiogenic monocytes required for tumor vessel formation and a mesenchymal population of pericyte progenitors. Cancer cell *8*, 211-226.

de Souza, L.F., Jardim, F.R., Sauter, I.P., de Souza, M.M., and Bernard, E.A. (2008). High glucose increases RAW 264.7 macrophages activation by lipoteichoic acid from Staphylococcus aureus. Clinica chimica acta; international journal of clinical chemistry *398*, 130-133.

DeNardo, D.G., Barreto, J.B., Andreu, P., Vasquez, L., Tawfik, D., Kolhatkar, N., and Coussens, L.M. (2009). CD4(+) T cells regulate pulmonary metastasis of mammary carcinomas by enhancing protumor properties of macrophages. Cancer cell *16*, 91-102.

DeNardo, D.G., Brennan, D.J., Rexhepaj, E., Ruffell, B., Shiao, S.L., Madden, S.F., Gallagher, W.M., Wadhwani, N., Keil, S.D., Junaid, S.A.*, et al.* (2011). Leukocyte complexity predicts breast cancer survival and functionally regulates response to chemotherapy. Cancer discovery *1*, 54-67.

Dunkelberger, J.R., and Song, W.C. (2010). Complement and its role in innate and adaptive immune responses. Cell research *20*, 34-50.

Dunn, G.P., Bruce, A.T., Sheehan, K.C., Shankaran, V., Uppaluri, R., Bui, J.D., Diamond, M.S., Koebel, C.M., Arthur, C., White, J.M.*, et al.* (2005). A critical function for type I interferons in cancer immunoediting. Nature immunology *6*, 722-729.

Dutta, P., Hoyer, F.F., Grigoryeva, L.S., Sager, H.B., Leuschner, F., Courties, G., Borodovsky, A., Novobrantseva, T., Ruda, V.M., Fitzgerald, K.*, et al.* (2015). Macrophages retain hematopoietic stem cells in the spleen via VCAM-1. The Journal of experimental medicine *212*, 497-512.

Elmore, M.R., Najafi, A.R., Koike, M.A., Dagher, N.N., Spangenberg, E.E., Rice, R.A., Kitazawa, M., Matusow, B., Nguyen, H., West, B.L.*, et al.* (2014). Colony-stimulating factor 1 receptor signaling is necessary for microglia viability, unmasking a microglia progenitor cell in the adult brain. Neuron *82*, 380-397.

Engelhardt, J.J., Boldajipour, B., Beemiller, P., Pandurangi, P., Sorensen, C., Werb, Z., Egeblad, M., and Krummel, M.F. (2012). Marginating dendritic cells of the tumor microenvironment cross-present tumor antigens and stably engage tumor-specific T cells. Cancer cell *21*, 402-417.

Ensan, S., Li, A., Besla, R., Degousee, N., Cosme, J., Roufaiel, M., Shikatani, E.A., El-Maklizi, M., Williams, J.W., Robins, L.*, et al.* (2016). Self-renewing resident arterial macrophages arise from embryonic CX3CR1(+) precursors and circulating monocytes immediately after birth. Nature immunology *17*, 159-168.

Epelman, S., Lavine, K.J., Beaudin, A.E., Sojka, D.K., Carrero, J.A., Calderon, B., Brija, T., Gautier, E.L., Ivanov, S., Satpathy, A.T.*, et al.* (2014). Embryonic and adult-derived resident cardiac macrophages are maintained through distinct mechanisms at steady state and during inflammation. Immunity *40*, 91-104.

Erblich, B., Zhu, L., Etgen, A.M., Dobrenis, K., and Pollard, J.W. (2011). Absence of colony stimulation factor-1 receptor results in loss of microglia, disrupted brain development and olfactory deficits. PloS one *6*, e26317.

Eyles, J., Puaux, A.L., Wang, X., Toh, B., Prakash, C., Hong, M., Tan, T.G., Zheng, L., Ong, L.C., Jin, Y.*, et al.* (2010). Tumor cells disseminate early, but immunosurveillance limits metastatic outgrowth, in a mouse model of melanoma. The Journal of clinical investigation *120*, 2030-2039.

Fleetwood, A.J., Lawrence, T., Hamilton, J.A., and Cook, A.D. (2007). Granulocyte-macrophage colony-stimulating factor (CSF) and macrophage CSF-dependent macrophage phenotypes display differences in cytokine profiles and transcription factor activities: implications for CSF blockade in inflammation. Journal of immunology *178*, 5245-5252.

Franklin, R.A., and Li, M.O. (2016). Ontogeny of Tumor-associated Macrophages and Its Implication in Cancer Regulation. Trends Cancer *2*, 20-34.

Franklin, R.A., Liao, W., Sarkar, A., Kim, M.V., Bivona, M.R., Liu, K., Pamer, E.G., and Li, M.O. (2014). The cellular and molecular origin of tumor-associated macrophages. Science *344*, 921-925.

Gabrilovich, D.I., and Nagaraj, S. (2009). Myeloid-derived suppressor cells as regulators of the immune system. Nature reviews Immunology *9*, 162-174.

Gautier, E.L., Shay, T., Miller, J., Greter, M., Jakubzick, C., Ivanov, S., Helft, J., Chow, A., Elpek, K.G., Gordonov, S.*, et al.* (2012). Gene-expression profiles and transcriptional regulatory pathways that underlie the identity and diversity of mouse tissue macrophages. Nature immunology *13*, 1118-1128.

Geiger, H., de Haan, G., and Florian, M.C. (2013). The ageing haematopoietic stem cell compartment. Nature reviews Immunology *13*, 376-389.

Gibbings, S.L., Goyal, R., Desch, A.N., Leach, S.M., Prabagar, M., Atif, S.M., Bratton, D.L., Janssen, W., and Jakubzick, C.V. (2015). Transcriptome analysis highlights the conserved difference between embryonic and postnatal-derived alveolar macrophages. Blood *126*, 1357-1366.

Ginhoux, F., Greter, M., Leboeuf, M., Nandi, S., See, P., Gokhan, S., Mehler, M.F., Conway, S.J., Ng, L.G., Stanley, E.R.*, et al.* (2010). Fate mapping analysis reveals that adult microglia derive from primitive macrophages. Science *330*, 841-845.

Ginhoux, F., and Guilliams, M. (2016). Tissue-Resident Macrophage Ontogeny and Homeostasis. Immunity *44*, 439-449.

Gomez Perdiguero, E., Klapproth, K., Schulz, C., Busch, K., Azzoni, E., Crozet, L., Garner, H., Trouillet, C., de Bruijn, M.F., Geissmann, F.*, et al.* (2015). Tissue-resident macrophages originate from yolk-sac-derived erythro-myeloid progenitors. Nature *518*, 547-551.

Gosselin, D., Link, V.M., Romanoski, C.E., Fonseca, G.J., Eichenfield, D.Z., Spann, N.J., Stender, J.D., Chun, H.B., Garner, H., Geissmann, F.*, et al.* (2014). Environment drives selection and function of enhancers controlling tissue-specific macrophage identities. Cell *159*, 1327-1340.

Goswami, S., Sahai, E., Wyckoff, J.B., Cammer, M., Cox, D., Pixley, F.J., Stanley, E.R., Segall, J.E., and Condeelis, J.S. (2005). Macrophages promote the invasion of breast carcinoma cells via a colony-stimulating factor-1/epidermal growth factor paracrine loop. Cancer research *65*, 5278-5283.

Gregory, C.D., and Devitt, A. (2004). The macrophage and the apoptotic cell: an innate immune interaction viewed simplistically? Immunology *113*, 1-14.

Grivennikov, S.I., and Karin, M. (2010). Inflammation and oncogenesis: a vicious connection. Current opinion in genetics & development *20*, 65-71.

Gundra, U.M., Girgis, N.M., Ruckerl, D., Jenkins, S., Ward, L.N., Kurtz, Z.D., Wiens, K.E., Tang, M.S., Basu-Roy, U., Mansukhani, A.*, et al.* (2014). Alternatively activated macrophages derived from monocytes and tissue macrophages are phenotypically and functionally distinct. Blood *123*, e110-122.

Gyorki, D.E., Asselin-Labat, M.L., van Rooijen, N., Lindeman, G.J., and Visvader, J.E. (2009). Resident macrophages influence stem cell activity in the mammary gland. Breast cancer research : BCR *11*, R62.

Haberstroh, U., Zahner, G., Disser, M., Thaiss, F., Wolf, G., and Stahl, R.A. (1993). TGF-beta stimulates rat mesangial cell proliferation in culture: role of PDGF beta-receptor expression. The American journal of physiology *264*, F199-205.

Hambardzumyan, D., Gutmann, D.H., and Kettenmann, H. (2016). The role of microglia and macrophages in glioma maintenance and progression. Nature neuroscience *19*, 20-27.

Hamid, O., Robert, C., Daud, A., Hodi, F.S., Hwu, W.J., Kefford, R., Wolchok, J.D., Hersey, P., Joseph, R.W., Weber, J.S.*, et al.* (2013). Safety and tumor responses with lambrolizumab (anti-PD-1) in melanoma. N Engl J Med *369*, 134-144.

Hanna, R.N., Carlin, L.M., Hubbeling, H.G., Nackiewicz, D., Green, A.M., Punt, J.A., Geissmann, F., and Hedrick, C.C. (2011). The transcription factor NR4A1 (Nur77) controls bone marrow differentiation and the survival of Ly6C- monocytes. Nature immunology *12*, 778-785.

Hashimoto, D., Chow, A., Noizat, C., Teo, P., Beasley, M.B., Leboeuf, M., Becker, C.D., See, P., Price, J., Lucas, D.*, et al.* (2013). Tissue-resident macrophages self-maintain locally throughout adult life with minimal contribution from circulating monocytes. Immunity *38*, 792-804.

Highfill, S.L., Cui, Y., Giles, A.J., Smith, J.P., Zhang, H., Morse, E., Kaplan, R.N., and Mackall, C.L. (2014). Disruption of CXCR2-mediated MDSC tumor trafficking enhances anti-PD1 efficacy. Sci Transl Med *6*, 237ra267.

Hingorani, S.R., Wang, L., Multani, A.S., Combs, C., Deramaudt, T.B., Hruban, R.H., Rustgi, A.K., Chang, S., and Tuveson, D.A. (2005). Trp53R172H and KrasG12D cooperate to promote chromosomal instability and widely metastatic pancreatic ductal adenocarcinoma in mice. Cancer cell *7*, 469-483.

Hodi, F.S., O'Day, S.J., McDermott, D.F., Weber, R.W., Sosman, J.A., Haanen, J.B., Gonzalez, R., Robert, C., Schadendorf, D., Hassel, J.C.*, et al.* (2010). Improved survival with ipilimumab in patients with metastatic melanoma. N Engl J Med *363*, 711-723.

Hoeffel, G., Chen, J., Lavin, Y., Low, D., Almeida, F.F., See, P., Beaudin, A.E., Lum, J., Low, I., Forsberg, E.C.*, et al.* (2015). C-Myb(+) erythro-myeloid progenitor-derived fetal monocytes give rise to adult tissue-resident macrophages. Immunity *42*, 665-678.

Hruban, R.H., Maitra, A., Kern, S.E., and Goggins, M. (2007). Precursors to pancreatic cancer. Gastroenterology clinics of North America *36*, 831-849, vi.

Hussain, S.P., and Harris, C.C. (2007). Inflammation and cancer: an ancient link with novel potentials. International journal of cancer *121*, 2373-2380.

Ino, Y., Yamazaki-Itoh, R., Shimada, K., Iwasaki, M., Kosuge, T., Kanai, Y., and Hiraoka, N. (2013). Immune cell infiltration as an indicator of the immune microenvironment of pancreatic cancer. Br J Cancer *108*, 914-923.

Ip, W.K., and Medzhitov, R. (2015). Macrophages monitor tissue osmolarity and induce inflammatory response through NLRP3 and NLRC4 inflammasome activation. Nature communications *6*, 6931.

Jakubzick, C., Gautier, E.L., Gibbings, S.L., Sojka, D.K., Schlitzer, A., Johnson, T.E., Ivanov, S., Duan, Q., Bala, S., Condon, T.*, et al.* (2013). Minimal differentiation of classical monocytes as they survey steady-state tissues and transport antigen to lymph nodes. Immunity *39*, 599-610.

Jantsch, J., Binger, K.J., Muller, D.N., and Titze, J. (2014). Macrophages in homeostatic immune function. Frontiers in physiology *5*, 146.

Jenkins, S.J., Ruckerl, D., Cook, P.C., Jones, L.H., Finkelman, F.D., van Rooijen, N., MacDonald, A.S., and Allen, J.E. (2011). Local macrophage proliferation, rather than recruitment from the blood, is a signature of TH2 inflammation. Science *332*, 1284-1288.

Jiang, H., Hegde, S., Knolhoff, B.L., Zhu, Y., Herndon, J.M., Meyer, M.A., Nywening, T.M., Hawkins, W.G., Shapiro, I.M., Weaver, D.T.*, et al.* (2016). Targeting focal adhesion kinase renders pancreatic cancers responsive to checkpoint immunotherapy. Nature medicine *22*, 851-860.

Jiao, X., Sherman, B.T., Huang da, W., Stephens, R., Baseler, M.W., Lane, H.C., and Lempicki, R.A. (2012). DAVID-WS: a stateful web service to facilitate gene/protein list analysis. Bioinformatics *28*, 1805-1806.

Jonuleit, H., Schmitt, E., Schuler, G., Knop, J., and Enk, A.H. (2000). Induction of interleukin 10-producing, nonproliferating CD4(+) T cells with regulatory properties by repetitive stimulation with allogeneic immature human dendritic cells. The Journal of experimental medicine *192*, 1213-1222.

Kang, K., Reilly, S.M., Karabacak, V., Gangl, M.R., Fitzgerald, K., Hatano, B., and Lee, C.H. (2008). Adipocyte-derived Th2 cytokines and myeloid PPARdelta regulate macrophage polarization and insulin sensitivity. Cell metabolism *7*, 485-495.

Kantoff, P.W., Higano, C.S., Shore, N.D., Berger, E.R., Small, E.J., Penson, D.F., Redfern, C.H., Ferrari, A.C., Dreicer, R., Sims, R.B.*, et al.* (2010). Sipuleucel-T immunotherapy for castration-resistant prostate cancer. N Engl J Med *363*, 411-422.

Kaplan, D.H., Shankaran, V., Dighe, A.S., Stockert, E., Aguet, M., Old, L.J., and Schreiber, R.D. (1998). Demonstration of an interferon gamma-dependent tumor surveillance system in immunocompetent mice. Proceedings of the National Academy of Sciences of the United States of America *95*, 7556-7561.

Khorana, A.A., Ryan, C.K., Cox, C., Eberly, S., and Sahasrabudhe, D.M. (2003). Vascular endothelial growth factor, CD68, and epidermal growth factor receptor expression and survival in patients with Stage II and Stage III colon carcinoma: a role for the host response in prognosis. Cancer *97*, 960-968.

Kim, K.W., Williams, J.W., Wang, Y.T., Ivanov, S., Gilfillan, S., Colonna, M., Virgin, H.W., Gautier, E.L., and Randolph, G.J. (2016). MHC II+ resident peritoneal and pleural macrophages rely on IRF4 for development from circulating monocytes. The Journal of experimental medicine *213*, 1951-1959.

Kim, M.P., Evans, D.B., Wang, H., Abbruzzese, J.L., Fleming, J.B., and Gallick, G.E. (2009). Generation of orthotopic and heterotopic human pancreatic cancer xenografts in immunodeficient mice. Nat Protoc *4*, 1670-1680.

Kim, R., Emi, M., and Tanabe, K. (2006). Functional roles of immature dendritic cells in impaired immunity of solid tumour and their targeted strategies for provoking tumour immunity. Clinical and experimental immunology *146*, 189-196.

Kitamura, T., Qian, B.Z., Soong, D., Cassetta, L., Noy, R., Sugano, G., Kato, Y., Li, J., and Pollard, J.W. (2015). CCL2-induced chemokine cascade promotes breast cancer metastasis by

enhancing retention of metastasis-associated macrophages. The Journal of experimental medicine *212*, 1043-1059.

Klose, C.S., and Artis, D. (2016). Innate lymphoid cells as regulators of immunity, inflammation and tissue homeostasis. Nature immunology *17*, 765-774.

Koebel, C.M., Vermi, W., Swann, J.B., Zerafa, N., Rodig, S.J., Old, L.J., Smyth, M.J., and Schreiber, R.D. (2007). Adaptive immunity maintains occult cancer in an equilibrium state. Nature *450*, 903-907.

Kohyama, M., Ise, W., Edelson, B.T., Wilker, P.R., Hildner, K., Mejia, C., Frazier, W.A., Murphy, T.L., and Murphy, K.M. (2009). Role for Spi-C in the development of red pulp macrophages and splenic iron homeostasis. Nature *457*, 318-321.

Kopp, J.L., von Figura, G., Mayes, E., Liu, F.F., Dubois, C.L., Morris, J.P.t., Pan, F.C., Akiyama, H., Wright, C.V., Jensen, K.*, et al.* (2012). Identification of Sox9-dependent acinar-to-ductal reprogramming as the principal mechanism for initiation of pancreatic ductal adenocarcinoma. Cancer cell *22*, 737-750.

Kurahara, H., Shinchi, H., Mataki, Y., Maemura, K., Noma, H., Kubo, F., Sakoda, M., Ueno, S., Natsugoe, S., and Takao, S. (2011). Significance of M2-polarized tumor-associated macrophage in pancreatic cancer. J Surg Res *167*, e211-219.

Lackner, C., Jukic, Z., Tsybrovskyy, O., Jatzko, G., Wette, V., Hoefler, G., Klimpfinger, M., Denk, H., and Zatloukal, K. (2004). Prognostic relevance of tumour-associated macrophages and von Willebrand factor-positive microvessels in colorectal cancer. Virchows Archiv : an international journal of pathology *445*, 160-167.

Langowski, J.L., Zhang, X., Wu, L., Mattson, J.D., Chen, T., Smith, K., Basham, B., McClanahan, T., Kastelein, R.A., and Oft, M. (2006). IL-23 promotes tumour incidence and growth. Nature *442*, 461-465.

Laoui, D., Van Overmeire, E., Di Conza, G., Aldeni, C., Keirsse, J., Morias, Y., Movahedi, K., Houbracken, I., Schouppe, E., Elkrim, Y.*, et al.* (2014). Tumor hypoxia does not drive differentiation of tumor-associated macrophages but rather fine-tunes the M2-like macrophage population. Cancer research *74*, 24-30.

Lavin, Y., Winter, D., Blecher-Gonen, R., David, E., Keren-Shaul, H., Merad, M., Jung, S., and Amit, I. (2014). Tissue-resident macrophage enhancer landscapes are shaped by the local microenvironment. Cell *159*, 1312-1326.

Le, D.T., Lutz, E., Uram, J.N., Sugar, E.A., Onners, B., Solt, S., Zheng, L., Diaz, L.A., Jr., Donehower, R.C., Jaffee, E.M.*, et al.* (2013). Evaluation of ipilimumab in combination with allogeneic pancreatic tumor cells transfected with a GM-CSF gene in previously treated pancreatic cancer. J Immunother *36*, 382-389.

Lee, J.J., Takei, M., Hori, S., Inoue, Y., Harada, Y., Tanosaki, R., Kanda, Y., Kami, M., Makimoto, A., Mineishi, S.*, et al.* (2002). The role of PGE(2) in the differentiation of dendritic cells: how do dendritic cells influence T-cell polarization and chemokine receptor expression? Stem cells *20*, 448-459.

Lewis, C.E., De Palma, M., and Naldini, L. (2007). Tie2-expressing monocytes and tumor angiogenesis: regulation by hypoxia and angiopoietin-2. Cancer research *67*, 8429-8432.

Liu, J., Xiang, Z., and Ma, X. (2004). Role of IFN regulatory factor-1 and IL-12 in immunological resistance to pathogenesis of N-methyl-N-nitrosourea-induced T lymphoma. Journal of immunology *173*, 1184-1193.

Lobov, I.B., Rao, S., Carroll, T.J., Vallance, J.E., Ito, M., Ondr, J.K., Kurup, S., Glass, D.A., Patel, M.S., Shu, W., *et al.* (2005). WNT7b mediates macrophage-induced programmed cell death in patterning of the vasculature. Nature *437*, 417-421.

Loser, K., Scherer, A., Krummen, M.B., Varga, G., Higuchi, T., Schwarz, T., Sharpe, A.H., Grabbe, S., Bluestone, J.A., and Beissert, S. (2005). An important role of CD80/CD86-CTLA-4 signaling during photocarcinogenesis in mice. Journal of immunology *174*, 5298-5305.

Lumeng, C.N., Bodzin, J.L., and Saltiel, A.R. (2007). Obesity induces a phenotypic switch in adipose tissue macrophage polarization. The Journal of clinical investigation *117*, 175-184.

Ma, Y., Shurin, G.V., Peiyuan, Z., and Shurin, M.R. (2013). Dendritic cells in the cancer microenvironment. Journal of Cancer *4*, 36-44.

Mahnke, K., Schmitt, E., Bonifaz, L., Enk, A.H., and Jonuleit, H. (2002). Immature, but not inactive: the tolerogenic function of immature dendritic cells. Immunology and cell biology *80*, 477-483.

Mantovani, A. (2008). From phagocyte diversity and activation to probiotics: back to Metchnikoff. Eur J Immunol *38*, 3269-3273.

Mantovani, A., Allavena, P., Sica, A., and Balkwill, F. (2008). Cancer-related inflammation. Nature *454*, 436-444.

Mantovani, A., and Sica, A. (2010). Macrophages, innate immunity and cancer: balance, tolerance, and diversity. Curr Opin Immunol *22*, 231-237.

Mantovani, A., Vecchi, A., and Allavena, P. (2014). Pharmacological modulation of monocytes and macrophages. Current opinion in pharmacology *17*, 38-44.

Martinez, F.O., Helming, L., and Gordon, S. (2009). Alternative activation of macrophages: an immunologic functional perspective. Annual review of immunology *27*, 451-483.

Martinez, F.O., Sica, A., Mantovani, A., and Locati, M. (2008). Macrophage activation and polarization. Front Biosci *13*, 453-461.

Mass, E., Ballesteros, I., Farlik, M., Halbritter, F., Gunther, P., Crozet, L., Jacome-Galarza, C.E., Handler, K., Klughammer, J., Kobayashi, Y.*, et al.* (2016). Specification of tissue-resident macrophages during organogenesis. Science *353*.

Meng, X.M., Nikolic-Paterson, D.J., and Lan, H.Y. (2016). TGF-beta: the master regulator of fibrosis. Nature reviews Nephrology *12*, 325-338.

Merad, M., Manz, M.G., Karsunky, H., Wagers, A., Peters, W., Charo, I., Weissman, I.L., Cyster, J.G., and Engleman, E.G. (2002). Langerhans cells renew in the skin throughout life under steady-state conditions. Nature immunology *3*, 1135-1141.

Mitchem, J.B., Brennan, D.J., Knolhoff, B.L., Belt, B.A., Zhu, Y., Sanford, D.E., Belaygorod, L., Carpenter, D., Collins, L., Piwnica-Worms, D.*, et al.* (2013). Targeting tumor-infiltrating macrophages decreases tumor-initiating cells, relieves immunosuppression, and improves chemotherapeutic responses. Cancer research *73*, 1128-1141.

Miyake, Y., Kaise, H., Isono, K., Koseki, H., Kohno, K., and Tanaka, M. (2007). Protective role of macrophages in noninflammatory lung injury caused by selective ablation of alveolar epithelial type II Cells. Journal of immunology *178*, 5001-5009.

Mok, S., Koya, R.C., Tsui, C., Xu, J., Robert, L., Wu, L., Graeber, T.G., West, B.L., Bollag, G., and Ribas, A. (2013). Inhibition of CSF-1 Receptor Improves the Antitumor Efficacy of Adoptive Cell Transfer Immunotherapy. Cancer research.

Mok, S., Koya, R.C., Tsui, C., Xu, J., Robert, L., Wu, L., Graeber, T.G., West, B.L., Bollag, G., and Ribas, A. (2014). Inhibition of CSF-1 receptor improves the antitumor efficacy of adoptive cell transfer immunotherapy. Cancer research *74*, 153-161.

Molawi, K., Wolf, Y., Kandalla, P.K., Favret, J., Hagemeyer, N., Frenzel, K., Pinto, A.R., Klapproth, K., Henri, S., Malissen, B., *et al.* (2014). Progressive replacement of embryo-derived cardiac macrophages with age. The Journal of experimental medicine *211*, 2151-2158.

Monticelli, L.A., Sonnenberg, G.F., Abt, M.C., Alenghat, T., Ziegler, C.G., Doering, T.A., Angelosanto, J.M., Laidlaw, B.J., Yang, C.Y., Sathaliyawala, T., *et al.* (2011). Innate lymphoid cells promote lung-tissue homeostasis after infection with influenza virus. Nature immunology *12*, 1045-1054.

Mosser, D.M., and Edwards, J.P. (2008). Exploring the full spectrum of macrophage activation. Nature reviews Immunology *8*, 958-969.

Movahedi, K., Laoui, D., Gysemans, C., Baeten, M., Stange, G., Van den Bossche, J., Mack, M., Pipeleers, D., In't Veld, P., De Baetselier, P., *et al.* (2010). Different tumor microenvironments contain functionally distinct subsets of macrophages derived from Ly6C(high) monocytes. Cancer research *70*, 5728-5739.

Muller, S., Quast, T., Schroder, A., Hucke, S., Klotz, L., Jantsch, J., Gerzer, R., Hemmersbach, R., and Kolanus, W. (2013). Salt-dependent chemotaxis of macrophages. PloS one *8*, e73439.

Multhoff, G., Molls, M., and Radons, J. (2011). Chronic inflammation in cancer development. Frontiers in immunology *2*, 98.

Murray, P.J., Allen, J.E., Biswas, S.K., Fisher, E.A., Gilroy, D.W., Goerdt, S., Gordon, S., Hamilton, J.A., Ivashkiv, L.B., Lawrence, T., *et al.* (2014). Macrophage activation and polarization: nomenclature and experimental guidelines. Immunity *41*, 14-20.

Nandi, S., Gokhan, S., Dai, X.M., Wei, S., Enikolopov, G., Lin, H., Mehler, M.F., and Stanley, E.R. (2012). The CSF-1 receptor ligands IL-34 and CSF-1 exhibit distinct developmental brain

expression patterns and regulate neural progenitor cell maintenance and maturation. Developmental biology *367*, 100-113.

Nascimento, M., Huang, S.C., Smith, A., Everts, B., Lam, W., Bassity, E., Gautier, E.L., Randolph, G.J., and Pearce, E.J. (2014). Ly6Chi monocyte recruitment is responsible for Th2 associated host-protective macrophage accumulation in liver inflammation due to schistosomiasis. PLoS pathogens *10*, e1004282.

Nausch, N., and Cerwenka, A. (2008). NKG2D ligands in tumor immunity. Oncogene *27*, 5944-5958.

Nguyen, K.D., Qiu, Y., Cui, X., Goh, Y.P., Mwangi, J., David, T., Mukundan, L., Brombacher, F., Locksley, R.M., and Chawla, A. (2011). Alternatively activated macrophages produce catecholamines to sustain adaptive thermogenesis. Nature *480*, 104-108.

Nielsen, S.R., Quaranta, V., Linford, A., Emeagi, P., Rainer, C., Santos, A., Ireland, L., Sakai, T., Sakai, K., Kim, Y.S.*, et al.* (2016). Macrophage-secreted granulin supports pancreatic cancer metastasis by inducing liver fibrosis. Nature cell biology *18*, 549-560.

Novitskiy, S.V., Ryzhov, S., Zaynagetdinov, R., Goldstein, A.E., Huang, Y., Tikhomirov, O.Y., Blackburn, M.R., Biaggioni, I., Carbone, D.P., Feoktistov, I.*, et al.* (2008). Adenosine receptors in regulation of dendritic cell differentiation and function. Blood *112*, 1822-1831.

Noy, R., and Pollard, J.W. (2014). Tumor-associated macrophages: from mechanisms to therapy. Immunity *41*, 49-61.

Nywening, T.M., Wang-Gillam, A., Sanford, D.E., Belt, B.A., Panni, R.Z., Cusworth, B.M., Toriola, A.T., Nieman, R.K., Worley, L.A., Yano, M.*, et al.* (2016). Targeting tumour-associated macrophages with CCR2 inhibition in combination with FOLFIRINOX in patients with

borderline resectable and locally advanced pancreatic cancer: a single-centre, open-label, dose-finding, non-randomised, phase 1b trial. Lancet Oncol.

O'Sullivan, T., Saddawi-Konefka, R., Vermi, W., Koebel, C.M., Arthur, C., White, J.M., Uppaluri, R., Andrews, D.M., Ngiow, S.F., Teng, M.W.*, et al.* (2012). Cancer immunoediting by the innate immune system in the absence of adaptive immunity. The Journal of experimental medicine *209*, 1869-1882.

Odegaard, J.I., and Chawla, A. (2013). Pleiotropic actions of insulin resistance and inflammation in metabolic homeostasis. Science *339*, 172-177.

Ojalvo, L.S., King, W., Cox, D., and Pollard, J.W. (2009). High-density gene expression analysis of tumor-associated macrophages from mouse mammary tumors. The American journal of pathology *174*, 1048-1064.

Orkin, S.H., and Zon, L.I. (2008). Hematopoiesis: an evolving paradigm for stem cell biology. Cell *132*, 631-644.

Ortega-Gomez, A., Perretti, M., and Soehnlein, O. (2013). Resolution of inflammation: an integrated view. EMBO molecular medicine *5*, 661-674.

Ozdemir, B.C., Pentcheva-Hoang, T., Carstens, J.L., Zheng, X., Wu, C.C., Simpson, T.R., Laklai, H., Sugimoto, H., Kahlert, C., Novitskiy, S.V.*, et al.* (2014). Depletion of carcinoma-associated fibroblasts and fibrosis induces immunosuppression and accelerates pancreas cancer with reduced survival. Cancer cell *25*, 719-734.

Palucka, K., and Banchereau, J. (2012). Cancer immunotherapy via dendritic cells. Nature reviews Cancer *12*, 265-277.

Patsialou, A., Wyckoff, J., Wang, Y., Goswami, S., Stanley, E.R., and Condeelis, J.S. (2009). Invasion of human breast cancer cells in vivo requires both paracrine and autocrine loops involving the colony-stimulating factor-1 receptor. Cancer research *69*, 9498-9506.

Peng, H., Jiang, X., Chen, Y., Sojka, D.K., Wei, H., Gao, X., Sun, R., Yokoyama, W.M., and Tian, Z. (2013). Liver-resident NK cells confer adaptive immunity in skin-contact inflammation. The Journal of clinical investigation *123*, 1444-1456.

Perdiguero, E.G., and Geissmann, F. (2016). The development and maintenance of resident macrophages. Nature immunology *17*, 2-8.

Pierce, J.H., Di Marco, E., Cox, G.W., Lombardi, D., Ruggiero, M., Varesio, L., Wang, L.M., Choudhury, G.G., Sakaguchi, A.Y., Di Fiore, P.P.*, et al.* (1990). Macrophage-colony-stimulating factor (CSF-1) induces proliferation, chemotaxis, and reversible monocytic differentiation in myeloid progenitor cells transfected with the human c-fms/CSF-1 receptor cDNA. Proceedings of the National Academy of Sciences of the United States of America *87*, 5613-5617.

Pinto, A.R., Godwin, J.W., and Rosenthal, N.A. (2014). Macrophages in cardiac homeostasis, injury responses and progenitor cell mobilisation. Stem cell research *13*, 705-714.

Pollard, J.W. (2009). Trophic macrophages in development and disease. Nature reviews Immunology *9*, 259-270.

Pradere, J.P., Kluwe, J., De Minicis, S., Jiao, J.J., Gwak, G.Y., Dapito, D.H., Jang, M.K., Guenther, N.D., Mederacke, I., Friedman, R.*, et al.* (2013). Hepatic macrophages but not dendritic cells contribute to liver fibrosis by promoting the survival of activated hepatic stellate cells in mice. Hepatology *58*, 1461-1473.

Priceman, S.J., Sung, J.L., Shaposhnik, Z., Burton, J.B., Torres-Collado, A.X., Moughon, D.L., Johnson, M., Lusis, A.J., Cohen, D.A., Iruela-Arispe, M.L.*, et al.* (2010). Targeting distinct

tumor-infiltrating myeloid cells by inhibiting CSF-1 receptor: combating tumor evasion of antiangiogenic therapy. Blood *115*, 1461-1471.

Provenzano, P.P., Cuevas, C., Chang, A.E., Goel, V.K., Von Hoff, D.D., and Hingorani, S.R. (2012). Enzymatic targeting of the stroma ablates physical barriers to treatment of pancreatic ductal adenocarcinoma. Cancer cell *21*, 418-429.

Pucci, F., Venneri, M.A., Biziato, D., Nonis, A., Moi, D., Sica, A., Di Serio, C., Naldini, L., and De Palma, M. (2009). A distinguishing gene signature shared by tumor-infiltrating Tie2-expressing monocytes, blood "resident" monocytes, and embryonic macrophages suggests common functions and developmental relationships. Blood *114*, 901-914.

Pull, S.L., Doherty, J.M., Mills, J.C., Gordon, J.I., and Stappenbeck, T.S. (2005). Activated macrophages are an adaptive element of the colonic epithelial progenitor niche necessary for regenerative responses to injury. Proceedings of the National Academy of Sciences of the United States of America *102*, 99-104.

Pylayeva-Gupta, Y., Lee, K.E., Hajdu, C.H., Miller, G., and Bar-Sagi, D. (2012). Oncogenic Kras-Induced GM-CSF Production Promotes the Development of Pancreatic Neoplasia. Cancer cell *21*, 836-847.

Pyonteck, S.M., Akkari, L., Schuhmacher, A.J., Bowman, R.L., Sevenich, L., Quail, D.F., Olson, O.C., Quick, M.L., Huse, J.T., Teijeiro, V.*, et al.* (2013). CSF-1R inhibition alters macrophage polarization and blocks glioma progression. Nature medicine *19*, 1264-1272.

Pyonteck, S.M., Gadea, B.B., Wang, H.W., Gocheva, V., Hunter, K.E., Tang, L.H., and Joyce, J.A. (2011). Deficiency of the macrophage growth factor CSF-1 disrupts pancreatic neuroendocrine tumor development. Oncogene.

Qian, B.Z., Li, J., Zhang, H., Kitamura, T., Zhang, J., Campion, L.R., Kaiser, E.A., Snyder, L.A., and Pollard, J.W. (2011). CCL2 recruits inflammatory monocytes to facilitate breast-tumour metastasis. Nature *475*, 222-225.

Qian, B.Z., and Pollard, J.W. (2010). Macrophage diversity enhances tumor progression and metastasis. Cell *141*, 39-51.

Robinette, M.L., Fuchs, A., Cortez, V.S., Lee, J.S., Wang, Y., Durum, S.K., Gilfillan, S., Colonna, M., and Immunological Genome, C. (2015). Transcriptional programs define molecular characteristics of innate lymphoid cell classes and subsets. Nature immunology *16*, 306-317.

Rosenberg, S.A., Restifo, N.P., Yang, J.C., Morgan, R.A., and Dudley, M.E. (2008). Adoptive cell transfer: a clinical path to effective cancer immunotherapy. Nature reviews Cancer *8*, 299-308.

Rowe, J.H., Ertelt, J.M., and Way, S.S. (2012). Innate IFN-gamma is essential for programmed death ligand-1-mediated T cell stimulation following Listeria monocytogenes infection. Journal of immunology *189*, 876-884.

Roy, L.D., Sahraei, M., Subramani, D.B., Besmer, D., Nath, S., Tinder, T.L., Bajaj, E., Shanmugam, K., Lee, Y.Y., Hwang, S.I.*, et al.* (2011). MUC1 enhances invasiveness of pancreatic cancer cells by inducing epithelial to mesenchymal transition. Oncogene *30*, 1449-1459.

Royal, R.E., Levy, C., Turner, K., Mathur, A., Hughes, M., Kammula, U.S., Sherry, R.M., Topalian, S.L., Yang, J.C., Lowy, I.*, et al.* (2010). Phase 2 trial of single agent Ipilimumab (anti-CTLA-4) for locally advanced or metastatic pancreatic adenocarcinoma. J Immunother *33*, 828-833.

Ruffell, B., Chang-Strachan, D., Chan, V., Rosenbusch, A., Ho, C.M., Pryer, N., Daniel, D., Hwang, E.S., Rugo, H.S., and Coussens, L.M. (2014). Macrophage IL-10 blocks CD8+ T cell-dependent responses to chemotherapy by suppressing IL-12 expression in intratumoral dendritic cells. Cancer cell *26*, 623-637.

Ruffell, B., and Coussens, L.M. (2015). Macrophages and therapeutic resistance in cancer. Cancer cell *27*, 462-472.

Saha, S., Aranda, E., Hayakawa, Y., Bhanja, P., Atay, S., Brodin, N.P., Li, J., Asfaha, S., Liu, L., Tailor, Y.*, et al.* (2016). Macrophage-derived extracellular vesicle-packaged WNTs rescue intestinal stem cells and enhance survival after radiation injury. Nature communications *7*, 13096.

Sandberg, M.L., Sutton, S.E., Pletcher, M.T., Wiltshire, T., Tarantino, L.M., Hogenesch, J.B., and Cooke, M.P. (2005). c-Myb and p300 regulate hematopoietic stem cell proliferation and differentiation. Developmental cell *8*, 153-166.

Sanford, D.E., Belt, B.A., Panni, R.Z., Mayer, A.B., Deshpande, A.D., Carpenter, D., Mitchem, J.B., Plambeck-Suess, S., Worley, L.A., Goetz, B.D.*, et al.* (2013). Inflammatory Monocyte Mobilization Decreases Patient Survival in Pancreatic Cancer: a Role for Targeting the CCL2/CCR2 Axis. Clin Cancer Res.

Satoh, T., Nakagawa, K., Sugihara, F., Kuwahara, R., Ashihara, M., Yamane, F., Minowa, Y., Fukushima, K., Ebina, I., Yoshioka, Y.*, et al.* (2017). Identification of an atypical monocyte and committed progenitor involved in fibrosis. Nature *541*, 96-101.

Satpathy, A.T., Kc, W., Albring, J.C., Edelson, B.T., Kretzer, N.M., Bhattacharya, D., Murphy, T.L., and Murphy, K.M. (2012). Zbtb46 expression distinguishes classical dendritic cells and their committed progenitors from other immune lineages. The Journal of experimental medicine *209*, 1135-1152.

Schmid, R.M. (2002). Acinar-to-ductal metaplasia in pancreatic cancer development. The Journal of clinical investigation *109*, 1403-1404.

Schubert, C., Schalk-Hihi, C., Struble, G.T., Ma, H.C., Petrounia, I.P., Brandt, B., Deckman, I.C., Patch, R.J., Player, M.R., Spurlino, J.C.*, et al.* (2007). Crystal structure of the tyrosine kinase domain of colony-stimulating factor-1 receptor (cFMS) in complex with two inhibitors. J Biol Chem *282*, 4094-4101.

Schulz, C., Gomez Perdiguero, E., Chorro, L., Szabo-Rogers, H., Cagnard, N., Kierdorf, K., Prinz, M., Wu, B., Jacobsen, S.E., Pollard, J.W.*, et al.* (2012). A lineage of myeloid cells independent of Myb and hematopoietic stem cells. Science *336*, 86-90.

Scott, C.L., Zheng, F., De Baetselier, P., Martens, L., Saeys, Y., De Prijck, S., Lippens, S., Abels, C., Schoonooghe, S., Raes, G.*, et al.* (2016). Bone marrow-derived monocytes give rise to self-renewing and fully differentiated Kupffer cells. Nature communications *7*, 10321.

Serbina, N.V., Jia, T., Hohl, T.M., and Pamer, E.G. (2008). Monocyte-mediated defense against microbial pathogens. Annual review of immunology *26*, 421-452.

Shankaran, V., Ikeda, H., Bruce, A.T., White, J.M., Swanson, P.E., Old, L.J., and Schreiber, R.D. (2001). IFNgamma and lymphocytes prevent primary tumour development and shape tumour immunogenicity. Nature *410*, 1107-1111.

Sharma, S.K., Chintala, N.K., Vadrevu, S.K., Patel, J., Karbowniczek, M., and Markiewski, M.M. (2015). Pulmonary alveolar macrophages contribute to the premetastatic niche by suppressing antitumor T cell responses in the lungs. Journal of immunology *194*, 5529-5538.

Sheng, J., Ruedl, C., and Karjalainen, K. (2015). Most Tissue-Resident Macrophages Except Microglia Are Derived from Fetal Hematopoietic Stem Cells. Immunity *43*, 382-393.

Shi, C., and Pamer, E.G. (2011). Monocyte recruitment during infection and inflammation. Nature reviews Immunology *11*, 762-774.

Simpson, T.R., Li, F., Montalvo-Ortiz, W., Sepulveda, M.A., Bergerhoff, K., Arce, F., Roddie, C., Henry, J.Y., Yagita, H., Wolchok, J.D.*, et al.* (2013). Fc-dependent depletion of tumor-infiltrating regulatory T cells co-defines the efficacy of anti-CTLA-4 therapy against melanoma. The Journal of experimental medicine *210*, 1695-1710.

Spranger, S., Spaapen, R.M., Zha, Y., Williams, J., Meng, Y., Ha, T.T., and Gajewski, T.F. (2013). Up-regulation of PD-L1, IDO, and T(regs) in the melanoma tumor microenvironment is driven by CD8(+) T cells. Sci Transl Med *5*, 200ra116.

Strachan, D.C., Ruffell, B., Oei, Y., Bissell, M.J., Coussens, L.M., Pryer, N., and Daniel, D. (2013). CSF1R inhibition delays cervical and mammary tumor growth in murine models by attenuating the turnover of tumor-associated macrophages and enhancing infiltration by CD8 T cells. Oncoimmunology *2*, e26968.

Stratford, J.K., Bentrem, D.J., Anderson, J.M., Fan, C., Volmar, K.A., Marron, J.S., Routh, E.D., Caskey, L.S., Samuel, J.C., Der, C.J.*, et al.* (2010). A six-gene signature predicts survival of patients with localized pancreatic ductal adenocarcinoma. PLoS Med *7*, e1000307.

Tacke, F., Ginhoux, F., Jakubzick, C., van Rooijen, N., Merad, M., and Randolph, G.J. (2006). Immature monocytes acquire antigens from other cells in the bone marrow and present them to T cells after maturing in the periphery. The Journal of experimental medicine *203*, 583-597.

Takeuchi, O., and Akira, S. (2010). Pattern recognition receptors and inflammation. Cell *140*, 805-820.

Tamoutounour, S., Guilliams, M., Montanana Sanchis, F., Liu, H., Terhorst, D., Malosse, C., Pollet, E., Ardouin, L., Luche, H., Sanchez, C.*, et al.* (2013). Origins and functional

specialization of macrophages and of conventional and monocyte-derived dendritic cells in mouse skin. Immunity *39*, 925-938.

Terawaki, S., Chikuma, S., Shibayama, S., Hayashi, T., Yoshida, T., Okazaki, T., and Honjo, T. (2011). IFN-alpha directly promotes programmed cell death-1 transcription and limits the duration of T cell-mediated immunity. Journal of immunology *186*, 2772-2779.

Titze, J. (2014). Sodium balance is not just a renal affair. Current opinion in nephrology and hypertension *23*, 101-105.

Tsai, J., Lee, J.T., Wang, W., Zhang, J., Cho, H., Mamo, S., Bremer, R., Gillette, S., Kong, J., Haass, N.K.*, et al.* (2008). Discovery of a selective inhibitor of oncogenic B-Raf kinase with potent antimelanoma activity. Proceedings of the National Academy of Sciences of the United States of America *105*, 3041-3046.

Usunier, B., Benderitter, M., Tamarat, R., and Chapel, A. (2014). Management of fibrosis: the mesenchymal stromal cells breakthrough. Stem cells international *2014*, 340257.

van de Laar, L., Saelens, W., De Prijck, S., Martens, L., Scott, C.L., Van Isterdael, G., Hoffmann, E., Beyaert, R., Saeys, Y., Lambrecht, B.N.*, et al.* (2016). Yolk Sac Macrophages, Fetal Liver, and Adult Monocytes Can Colonize an Empty Niche and Develop into Functional Tissue-Resident Macrophages. Immunity *44*, 755-768.

Van Dyken, S.J., and Locksley, R.M. (2013). Interleukin-4- and interleukin-13-mediated alternatively activated macrophages: roles in homeostasis and disease. Annual review of immunology *31*, 317-343.

van Netten, J.P., Ashmead, B.J., Parker, R.L., Thornton, I.G., Fletcher, C., Cavers, D., Coy, P., and Brigden, M.L. (1993). Macrophage-tumor cell associations: a factor in metastasis of breast cancer? Journal of leukocyte biology *54*, 360-362.

Varol, C., Mildner, A., and Jung, S. (2015). Macrophages: development and tissue specialization. Annual review of immunology *33*, 643-675.

Wang, J., and Kubes, P. (2016). A Reservoir of Mature Cavity Macrophages that Can Rapidly Invade Visceral Organs to Affect Tissue Repair. Cell *165*, 668-678.

Wolchok, J.D., Kluger, H., Callahan, M.K., Postow, M.A., Rizvi, N.A., Lesokhin, A.M., Segal, N.H., Ariyan, C.E., Gordon, R.A., Reed, K.*, et al.* (2013). Nivolumab plus ipilimumab in advanced melanoma. N Engl J Med *369*, 122-133.

Wynn, T.A., and Vannella, K.M. (2016). Macrophages in Tissue Repair, Regeneration, and Fibrosis. Immunity *44*, 450-462.

Xue, J., Schmidt, S.V., Sander, J., Draffehn, A., Krebs, W., Quester, I., De Nardo, D., Gohel, T.D., Emde, M., Schmidleithner, L.*, et al.* (2014). Transcriptome-based network analysis reveals a spectrum model of human macrophage activation. Immunity *40*, 274-288.

Yang, J., Liao, D., Chen, C., Liu, Y., Chuang, T.H., Xiang, R., Markowitz, D., Reisfeld, R.A., and Luo, Y. (2013). Tumor-associated macrophages regulate murine breast cancer stem cells through a novel paracrine EGFR/Stat3/Sox-2 signaling pathway. Stem cells *31*, 248-258.

Yona, S., Kim, K.W., Wolf, Y., Mildner, A., Varol, D., Breker, M., Strauss-Ayali, D., Viukov, S., Guilliams, M., Misharin, A.*, et al.* (2013). Fate mapping reveals origins and dynamics of monocytes and tissue macrophages under homeostasis. Immunity *38*, 79-91.

Yun, M.H., Davaapil, H., and Brockes, J.P. (2015). Recurrent turnover of senescent cells during regeneration of a complex structure. eLife *4*.

Zhang, L., and Wang, C.C. (2014). Inflammatory response of macrophages in infection. Hepatobiliary & pancreatic diseases international : HBPD INT *13*, 138-152.

Zhu, Y., Knolhoff, B.L., Meyer, M.A., Nywening, T.M., West, B.L., Luo, J., Wang-Gillam, A., Goedegebuure, S.P., Linehan, D.C., and DeNardo, D.G. (2014). CSF1/CSF1R blockade reprograms tumor-infiltrating macrophages and improves response to T-cell checkpoint immunotherapy in pancreatic cancer models. Cancer research *74*, 5057-5069.